x-ray computed tomography (CT)

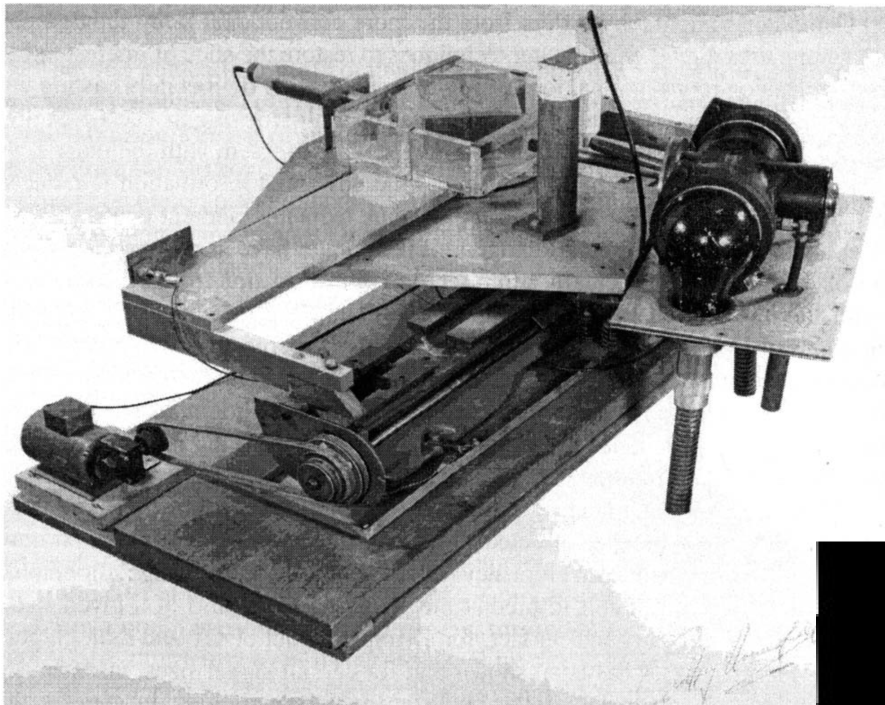

Hounsfield, 1969

additional literature:
W.A. Kalender: Computertomographie
Publicis MCD Verlag, 2000

x-ray computed tomography (CT)

brief historical overview of CT development

1895 W.C. Röntgen discovers a ‘new kind of radiation’, later termed “Röntgenstrahlung” (x-rays)

1917 J.H. Radon develops mathematical fundamentals to compute tomographic images from transmission measurements

1960/1970 improvements of computer technology

1972 G.N. Hounsfield und J. Ambrose: first clinical examination with CT

1975 first whole-body CT scanner in clinical use

1979 Nobel Price awarded to Hounsfield and Cormack

1989 first clinical examinations with spiraling CT

1998 first clinical examinations with spiraling multi-slice CT

2000 approx. 30 000 clinical spiraling CT installations worldwide

x-ray computed tomography (CT)

1974

1994

x-ray computed tomography (CT)

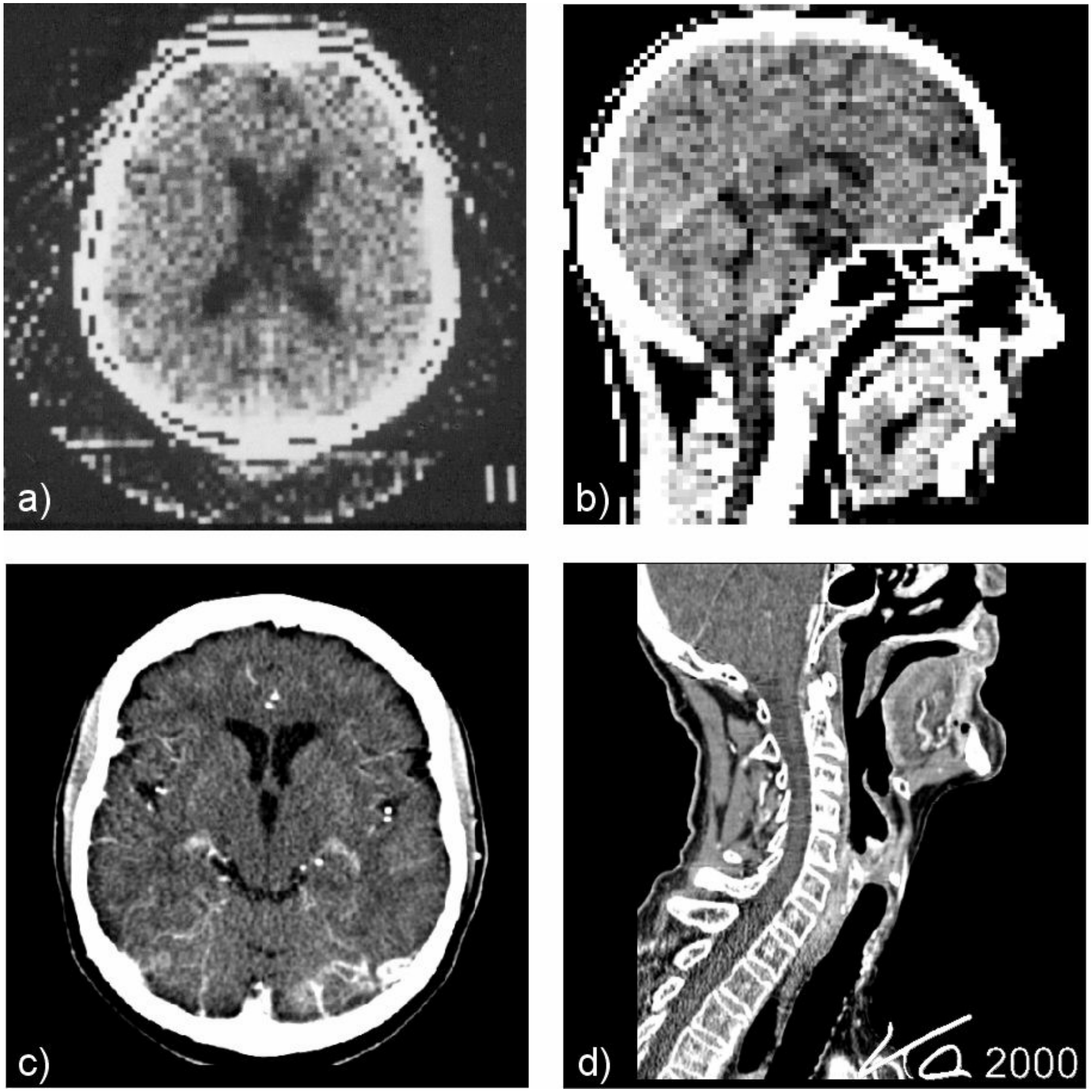

1974
image matrix: 80 x 80

2000
image matrix : 512 x 512
spiraling CT

x-ray computed tomography (CT)

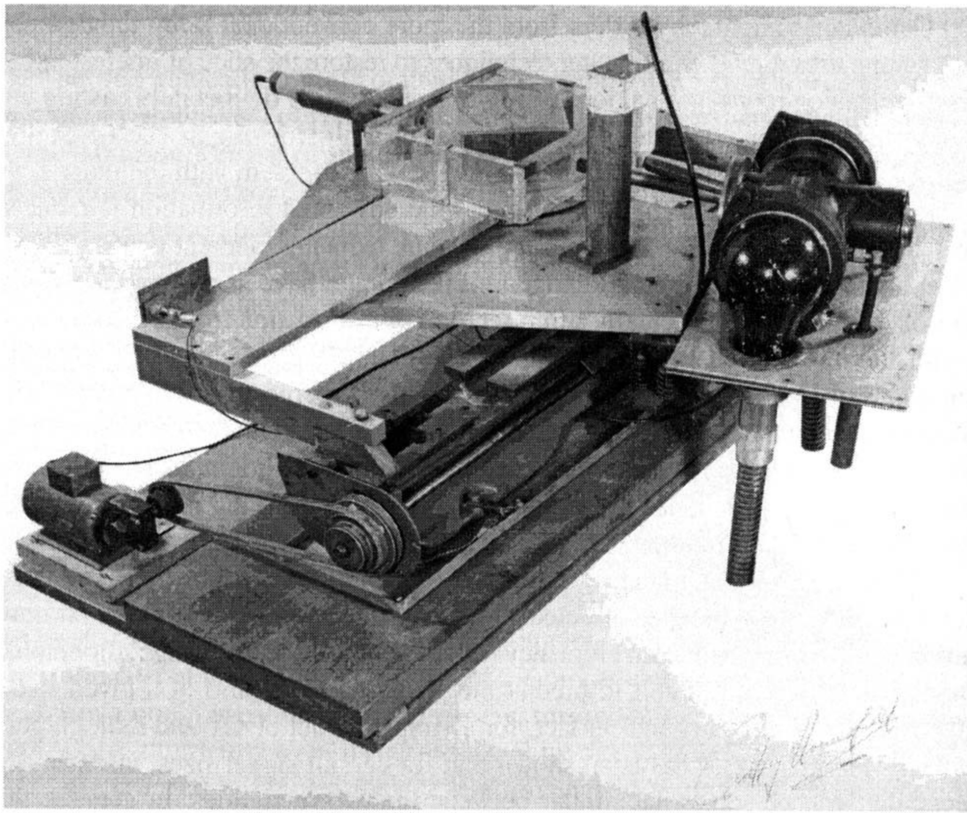

Hounsfield, 1969

modern CT scanner

drawbacks of projection radiography:

x-ray image:

- modulated distribution of γ-quanta transmitted through tissue

- 2D projection der attenuation properties of tissue

- <u>all</u> irradiated volume elements contribute to attenuation

- line integral of attenuation: $J_D = J_0 e^{-\int \mu(x,y,z) dl}$

- contrast mainly from structures with high μ (bones) or profound differences in thickness; soft tissue hard to resolve

- projection radiography is not tomography

?

x-ray computed tomography (CT)

homogeneous object; mono-chromatic radiation

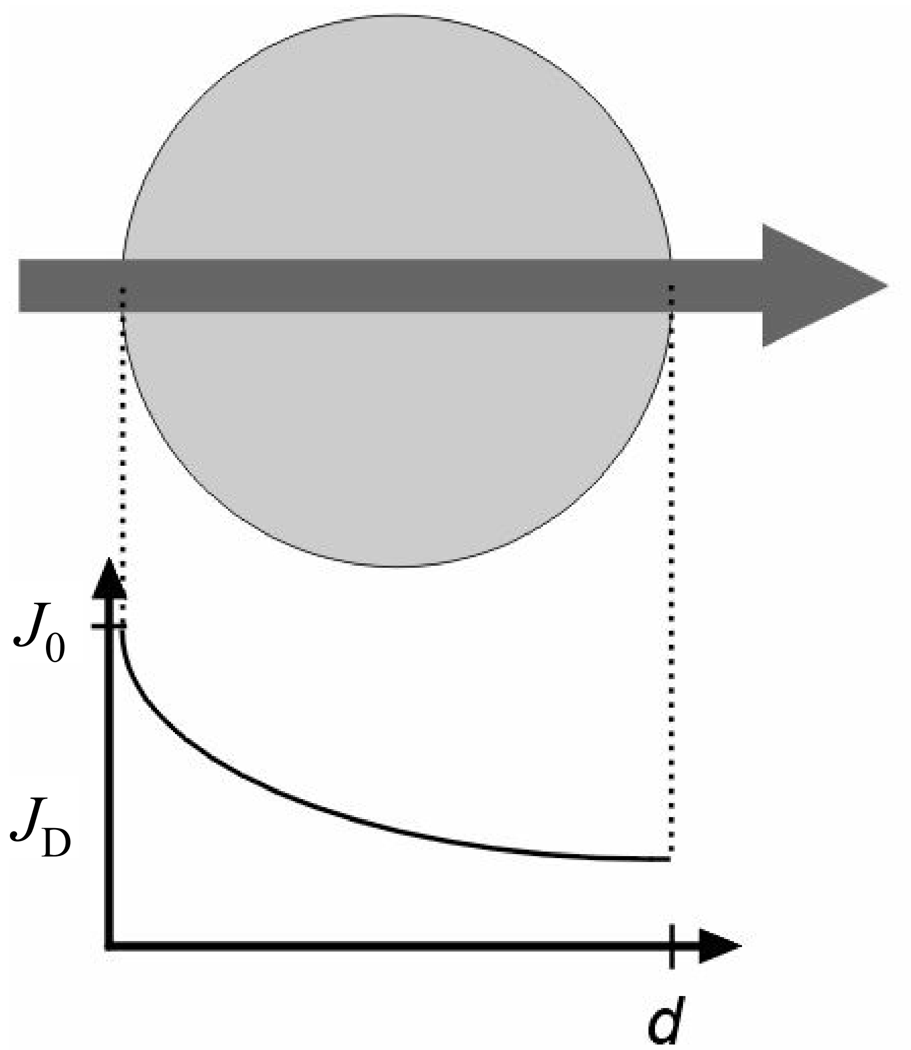

$$J_D = J_0 \cdot e^{-\mu d}$$

$$P = \ln \frac{J_0}{J_D} = \mu \cdot d$$

$$\mu = \frac{1}{d} \cdot \ln \frac{J_0}{J_D}$$

P = projection value

x-ray computed tomography (CT)

non-homogeneous object; mono-chromatic radiation

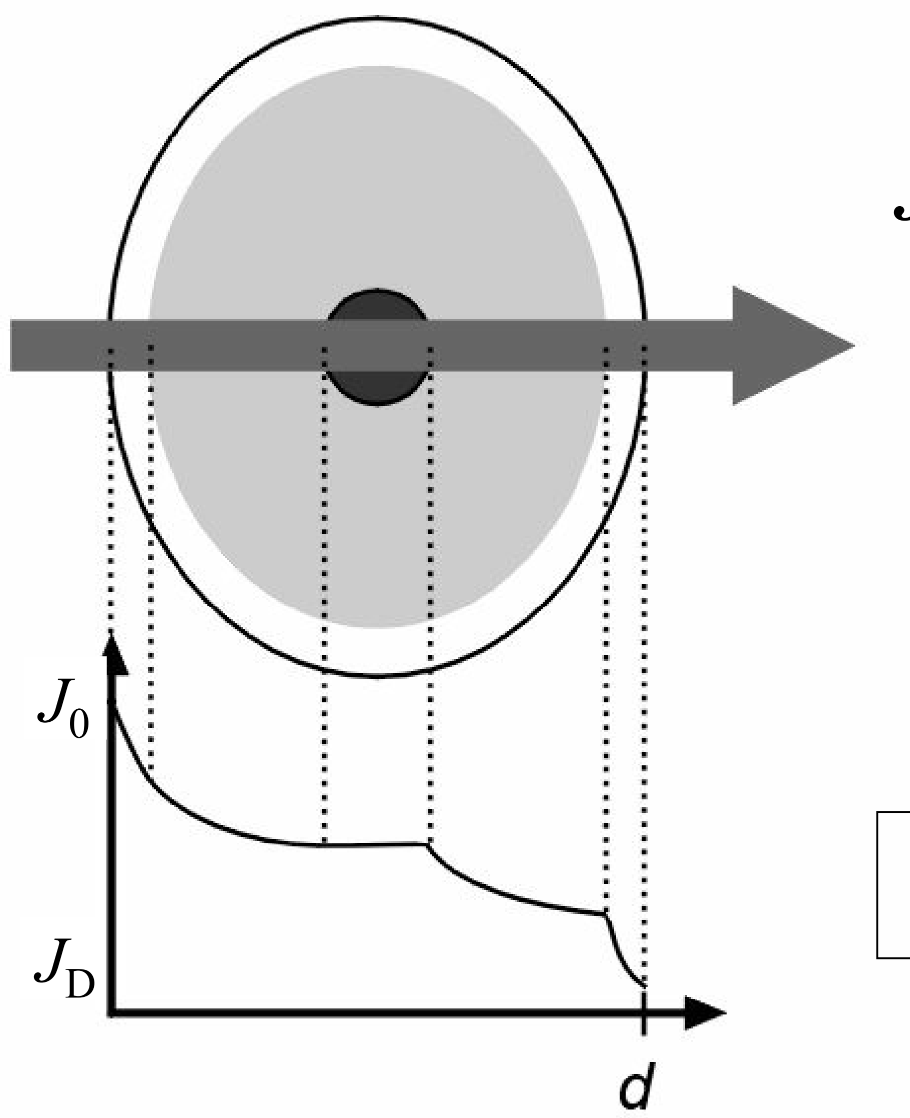

$$J_D = J_0 \cdot e^{-\mu_1 d_1 - \mu_2 d_2 - \mu_3 d_3 - \ldots}$$

$$= J_0 \cdot e^{-\sum_i \mu_i \cdot d_i} = J_0 \cdot e^{-\int_0^d \mu ds}$$

$$P = \ln \frac{J_0}{J_D} = \sum_i \mu_i \cdot d_i$$

$$\mu_i = ??$$

x-ray computed tomography (CT)

non-homogeneous object; poly-chromatic radiation

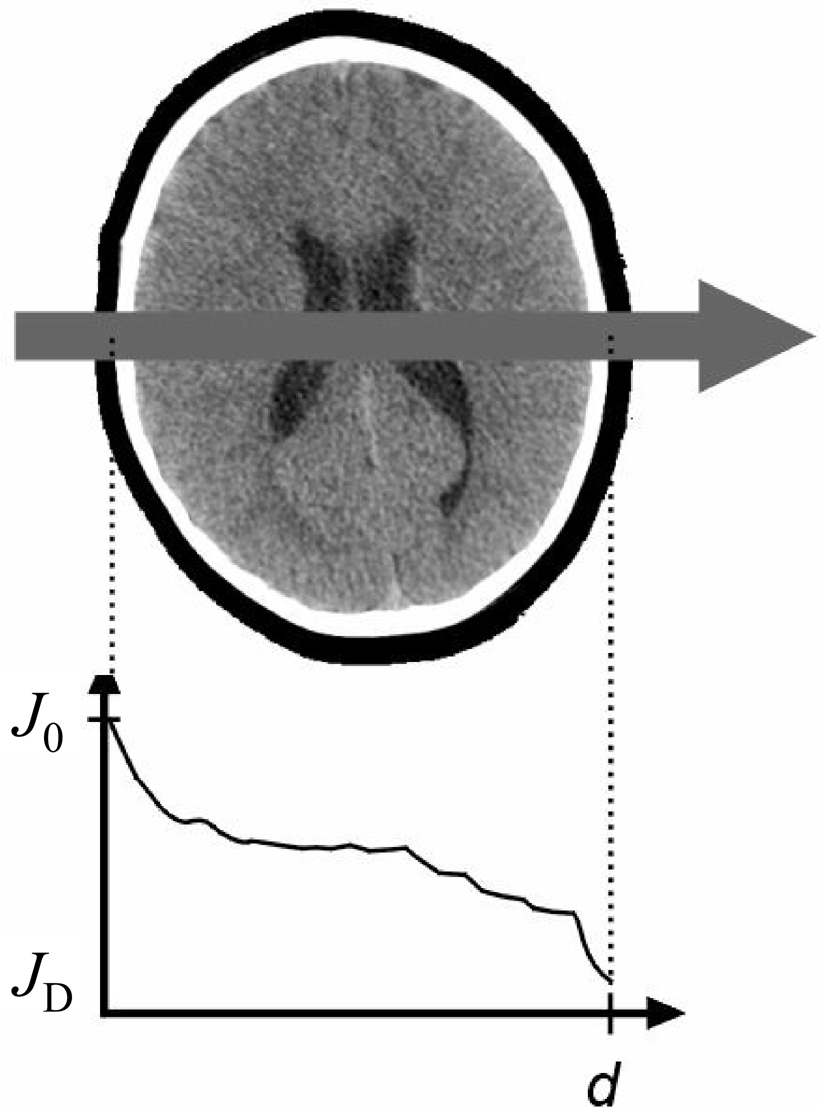

$$J_D = \int_0^{E_{max}} J_0(E) \cdot e^{-\int_0^d \mu ds} dE$$

$$P = \ln \frac{J_0}{J_D}$$

$$\mu(x, y) = ??$$

fundamentals of x-ray computed tomography

fundamentals of computed tomography*:

- measure spatial distribution of physical observable of interest (e.g., attenuation coefficient μ(x,y)) of object of interest

- from measured values estimate non-overlapping images (Radon transform and Fourier-slice theorem)

*holds for any kind of tomographic imaging technique (x-ray CT, PET, MRI, …)

x-ray computed tomography (CT)

idea: record information from single slices

consider human body as being composed of finite many discrete volume elements

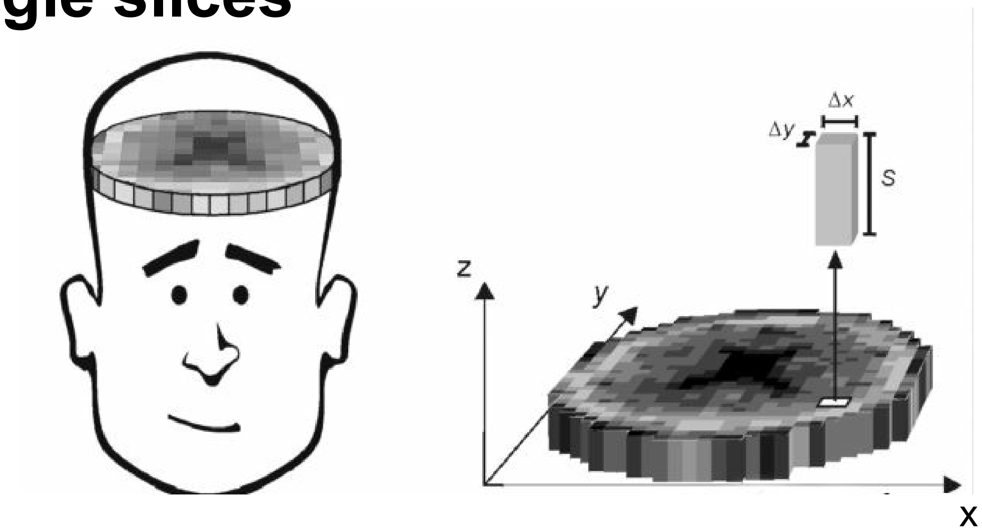

in coarse-grained resolution:

- single transversal slices of thickness *s*
- slices are composed of discrete cuboid volume elements

voxel (volume element)
pixel (picture element)

x-ray computed tomography (CT)

recording tomographic images and inverse problem

inverse problem: given set of N_p recordings (tomographic images) outside of some object, estimate the distribution of some physical property (e.g., $\mu(x,y)$) inside the object

H. von Helmholtz: *the inverse problem has no unique solution*

J. Radon (1917): the 2D distribution of some object property can be fully characterized with an **infinite amount of line integrals**

$\Rightarrow$ a finite number N_p of recordings allows a *sufficiently accurate approximation* of the distribution of some physical property

(**forward problem**: given the distribution of some physical property inside the object, determine result of measurement outside the object)

simplest measurement principle

with Radon's demand:
translation first
(yields a projection),
then rotation
(min. 180°)

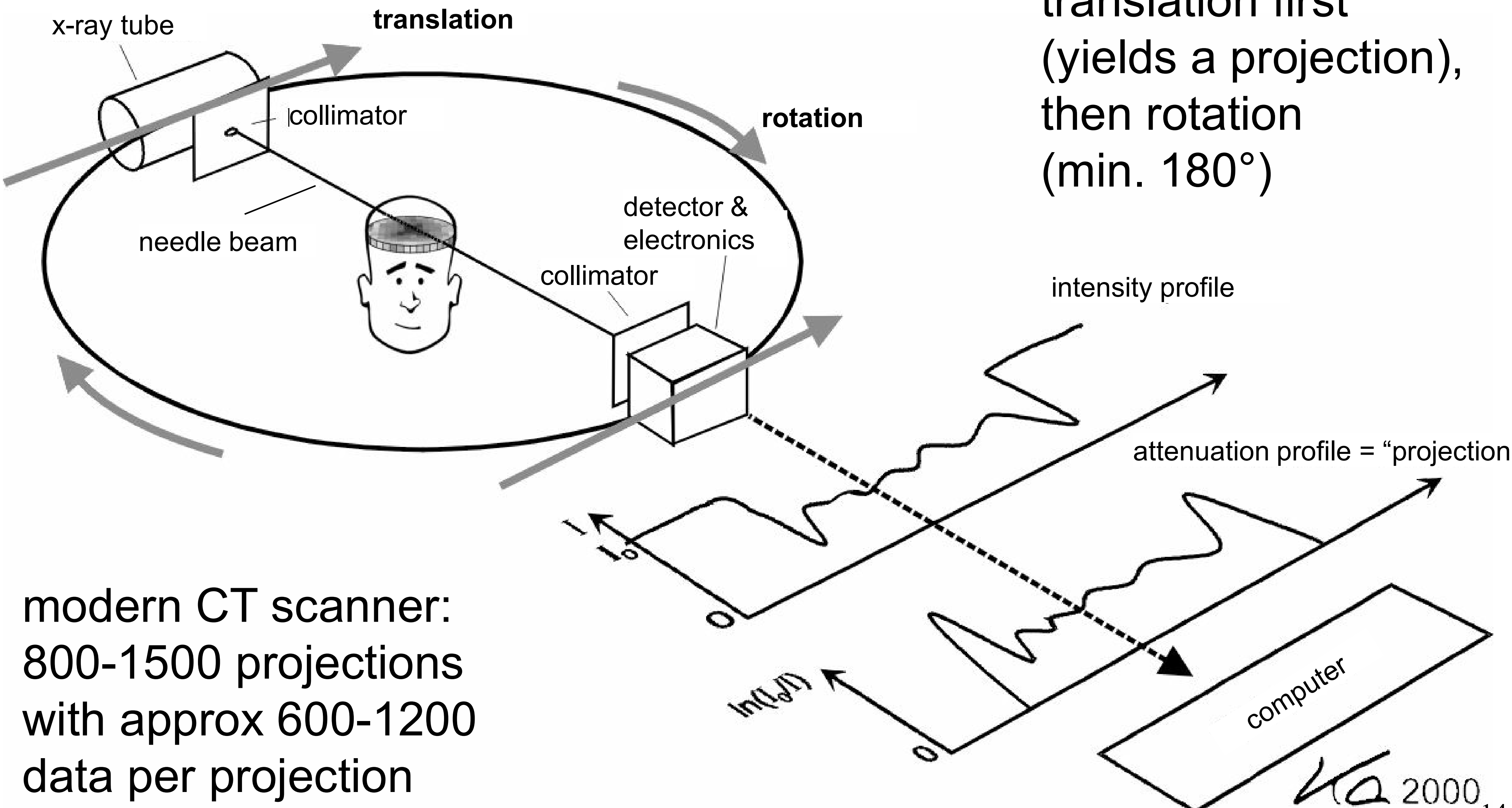

modern CT scanner:
800-1500 projections
with approx 600-1200
data per projection

Radon transform (I)

J. Radon (1917): the 2D distribution of some object property can be fully characterized with an **infinite amount of line integrals**

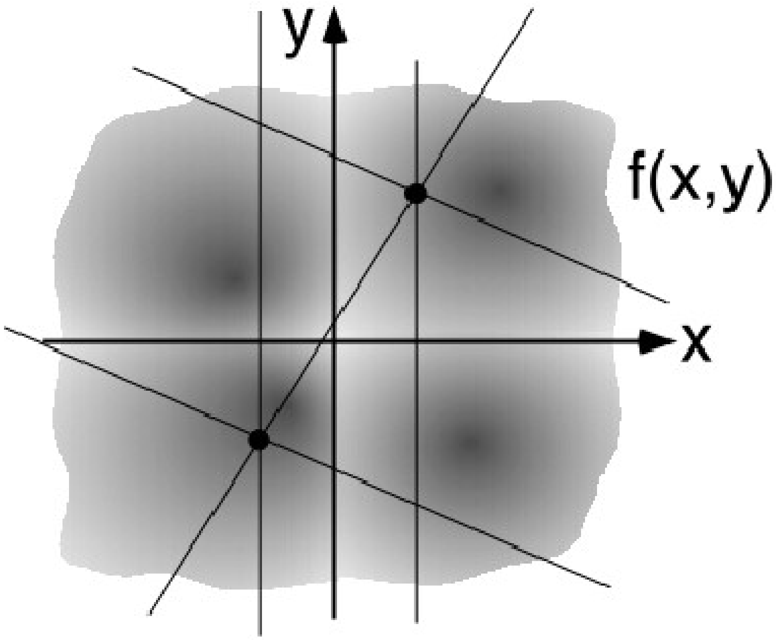

let $f(x,y)$ denote some arbitrary integrable function

characterize $f(x,y)$ with all straight line integrals passing through the area on which $f(x,y)$ is defined:

$$\int_{-\infty}^{+\infty} f\big(x(l), y(l)\big)\, dl$$

x-ray computed tomography (CT)

Radon transform (II)

naïve ansatz: successive integration through all points and along all directions

⇒ some line integrals are identical

⇒ choose appropriate ordering scheme such that all line integrals are unique (e.g., Hesse normal form)

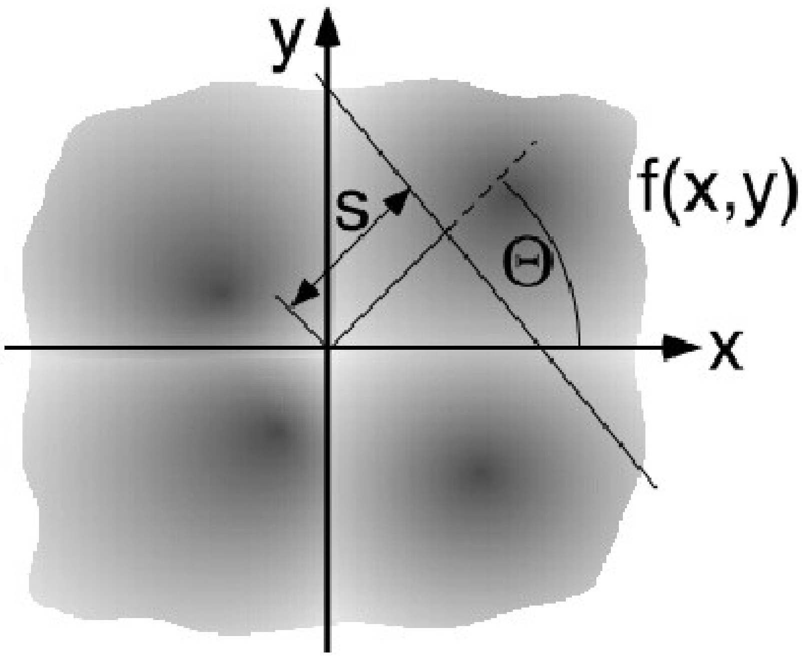

$$\int_{\vec{e}\cdot\vec{r}=s} f(x,y)\,dl = p_{\Theta}(s)$$

$\vec{e}$ = unit vector in direction Θ

Θ = angle between line of integration and normal passing through origin

Radon transform (II)

with $\Theta \in [0°,180°]$ and with all s: $(s_{min} < s < s_{max})$
$\Rightarrow$ all possible line integrals $p_\Theta(s)$ through function $f(x,y)$

assign values of line integrals to $p(\Theta,s)$-diagram

a line in Radon space with Θ =*const* is called projection $p_\Theta(s)$

$p_\Theta(s)$ = sequence of values of line integrals passing through $f(x,y)$ with Θ=const. and distance s to the origin

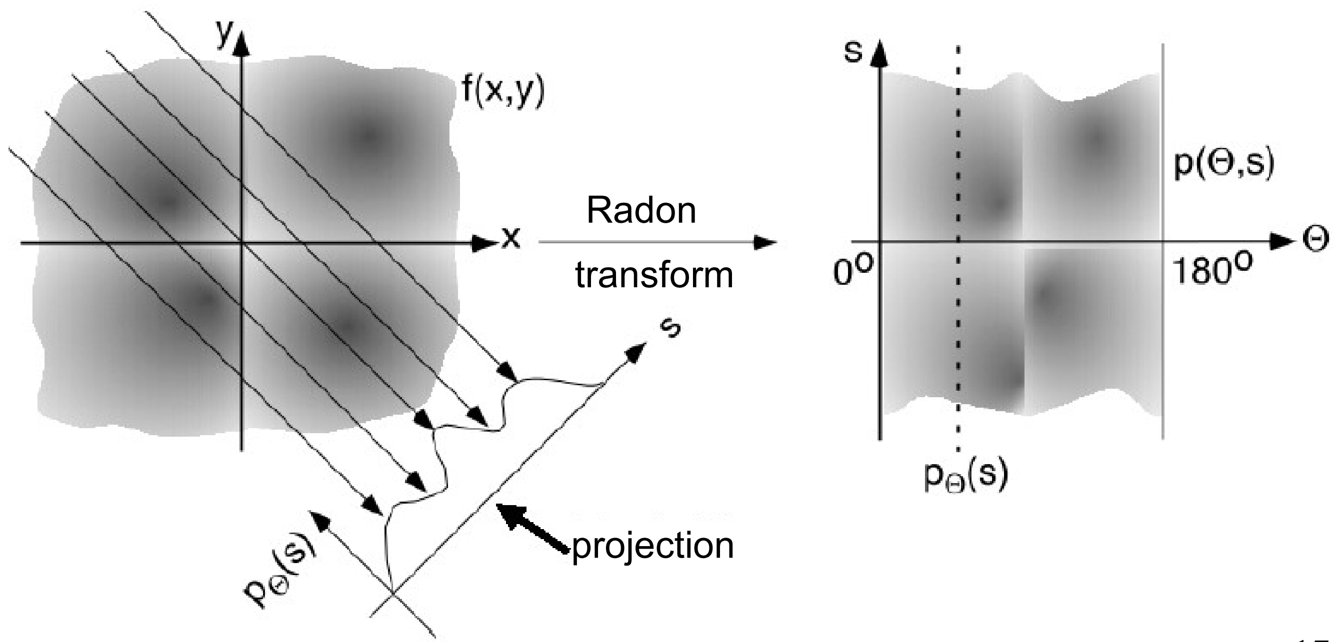

Radon transform (III-1)

estimate Radon transform for Θ=0

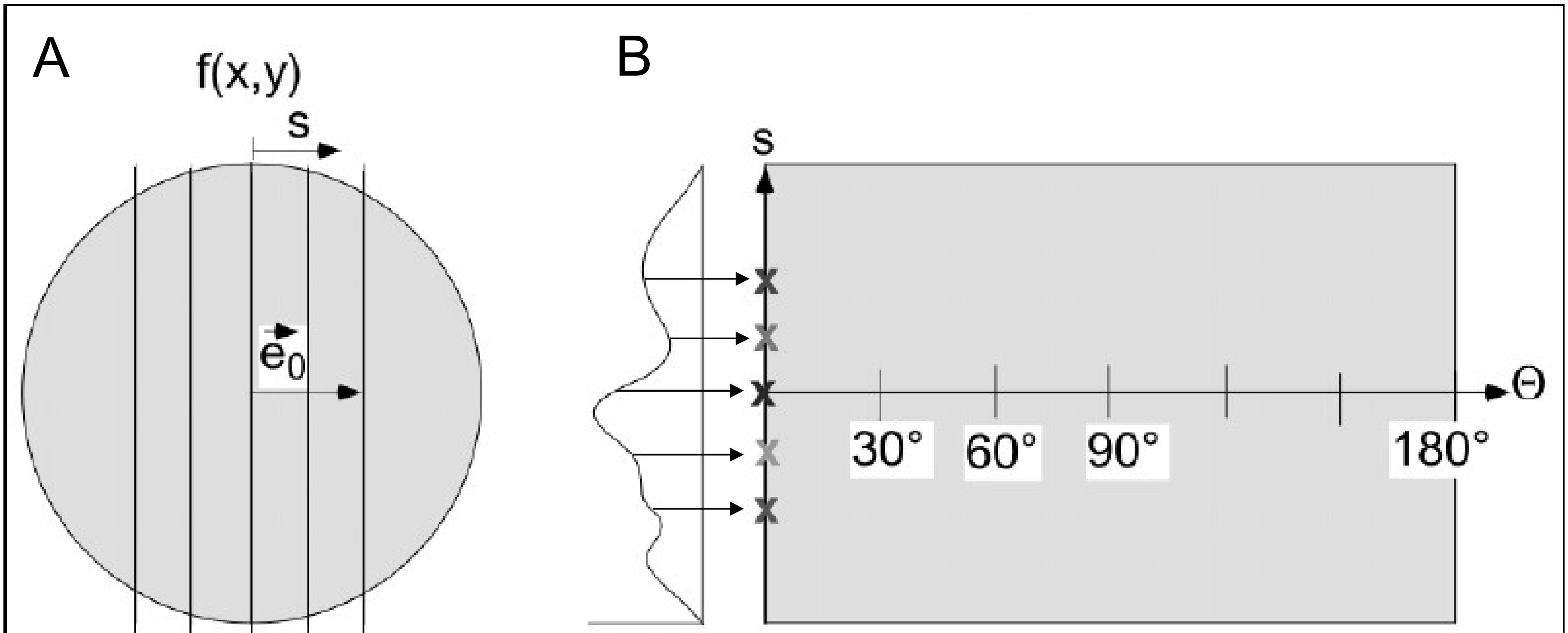

$$\int_{\vec{e}\cdot\vec{r}=s} f(x,y)\,dl = p_\Theta(s)$$

Radon transform (III-2)

estimate Radon transform for $\Theta \neq 0$

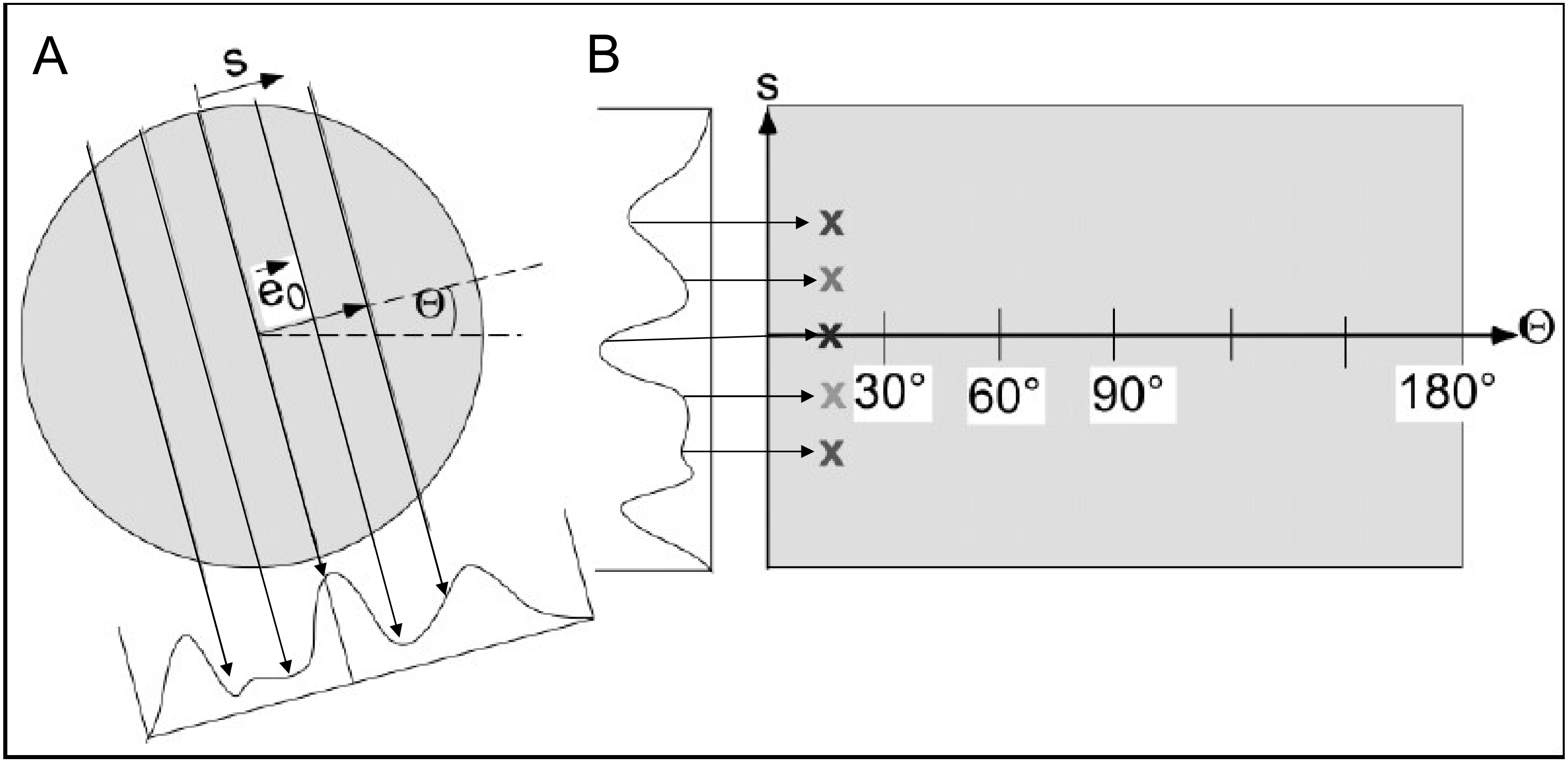

x-ray computed tomography (CT)

Fourier-slice theorem (or projection-slice theorem or central slice theorem)

the results of the following two calculations are equal:

- take a 2D function $f(x,y)$, project it onto a (1D) line (projection operator P_1), and do a Fourier transform (F_1) of that projection

- take that same function, but do a 2D Fourier transform (F_2) first, and then slice it through its origin (slicing operator S_1), which is parallel to the projection line

$$F_1 P_1 = S_1 F_2$$

R. N. Bracewell (1956). Strip integration in radio astronomy. Aust. J. Phys. 9 (2): 198

Fourier-slice theorem

- a recording with a needle beam (line integral) for given angle Θ and distance s from the origin (i.e., projection values $p_\Theta(s)$) corresponds to the Radon transform of an image.
- the Fourier-slice theorem allows one to determine the function $f(x,y)$ (i.e., μ(*x,y*)) from the Radom transform

relation between Radon- und Fourier-transform:

let $R\, f(\vec{e}, s) = \int_{\vec{e}\cdot\vec{r}} f(\vec{r})\, d\vec{r}$ denote the Radon transform of function f

with $G(\alpha) = F(u, v)$ for $(u, v) = \alpha \cdot (\cos\Theta, \sin\Theta)$

we have

$$G(\alpha) = F_1\left\{R_\Theta f(s)\right\}$$

$$F(u, v) = F_2\left\{f(x, y)\right\}$$

→ find μ(*x,y*) with inverse 2D-FT

Fourier-slice theorem (proof for Θ=0)

projections for Θ=0

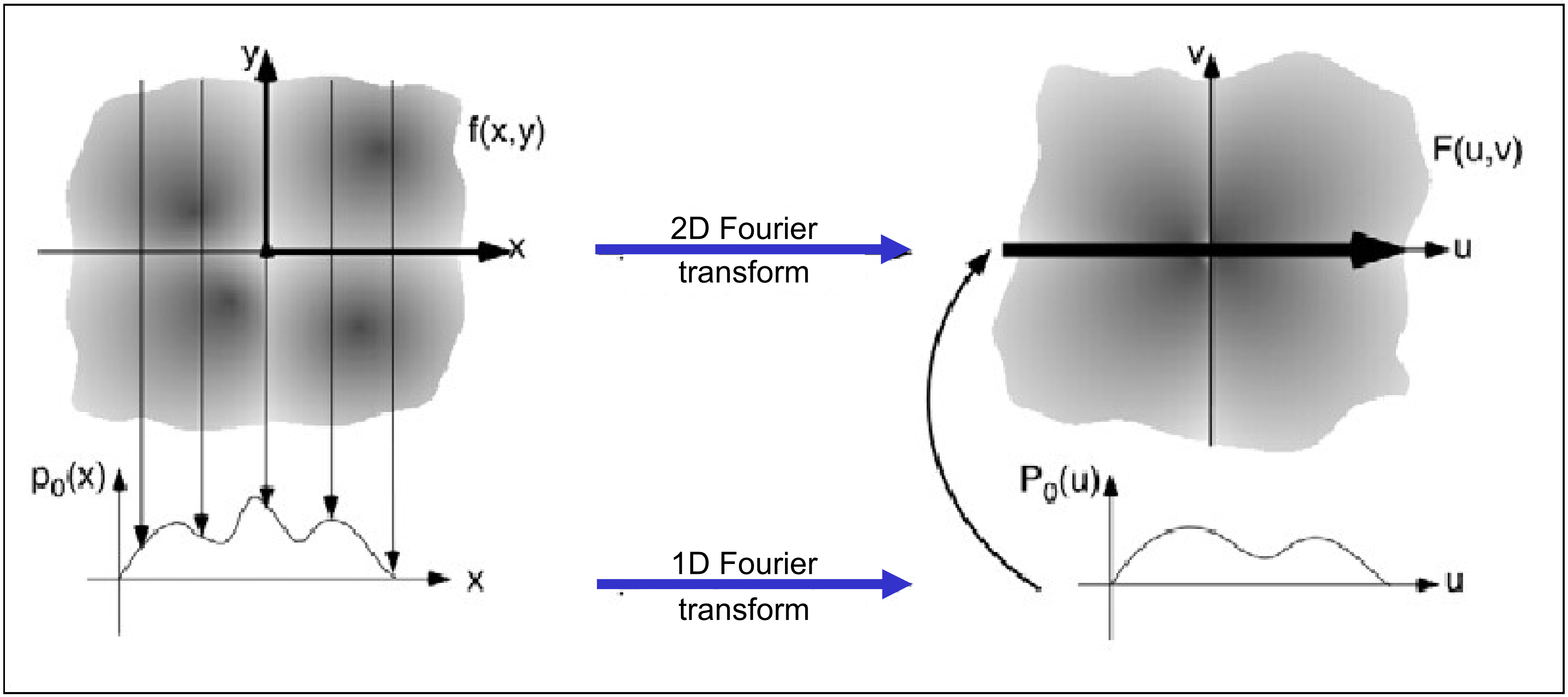

Fourier-slice theorem (proof for Θ=0)

$$p_0(s) = p_0(x) = \int_{-\infty}^{+\infty} f(x,y)\,dy \qquad \text{for} \quad \Theta = 0^{\circ}$$

1D Fourier transform of $p_0(x)$ is defined as:

$$P_0(u) = \int_{-\infty}^{+\infty} p_0(x) e^{-j2\pi ux} dx$$

this can be rearranged as:

$$P_0(u) = \int_{-\infty}^{+\infty} \left[\int f(x,y)\,dy\right] e^{-j\cdot 2\pi ux} dx = \int\int f(x,y) e^{-j\cdot 2\pi(ux+0\cdot y)} dx\,dy = F(u,0)$$

where: $f(x,y) \;\circ\!\!\xrightarrow{\text{2D-FT}}\!\!\circ\; F(u,v)$

1D-FT($p_{\Theta=0}(s)$) yields results of 2D-FT($f(x,y)$) on the u-axis

Fourier-slice theorem (proof for $\Theta \neq 0$)

projections for $\Theta \neq 0$

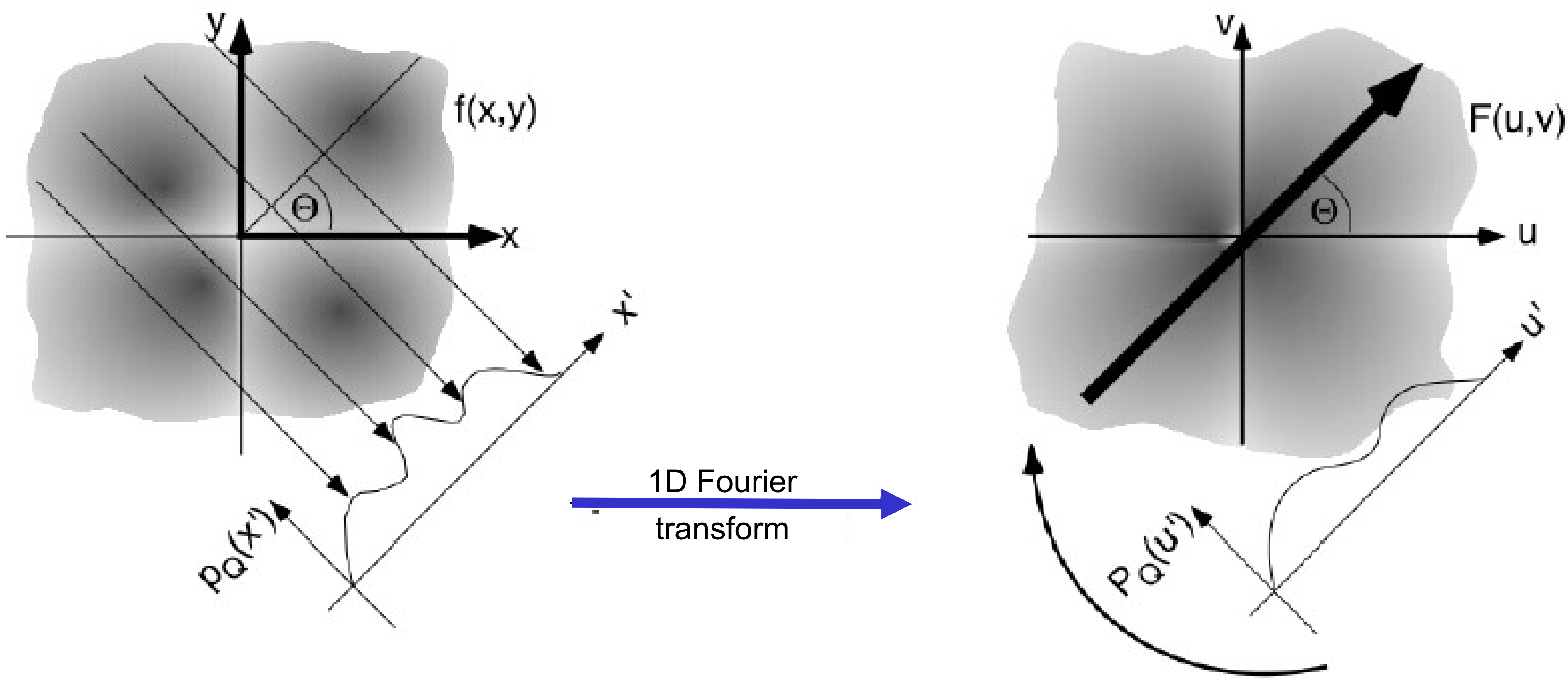

Fourier-slice theorem (proof for $\Theta \neq 0$)

projection $p_\Theta(s)$ can be regarded as a projection onto the x´-axis of a rotated coordinate system.

the same derivation as with $\Theta=0$ holds:
1D-FT($p_\Theta(s)$) yields results of 2D-FT($f(x,y)$) on the u'-axis

in general, we have:
FT of some function $f(x,y)$ rotated by an angle Θ is rotated by the same angle Θ with respect to FT of $F(u,v)$.

□

Fourier-slice theorem

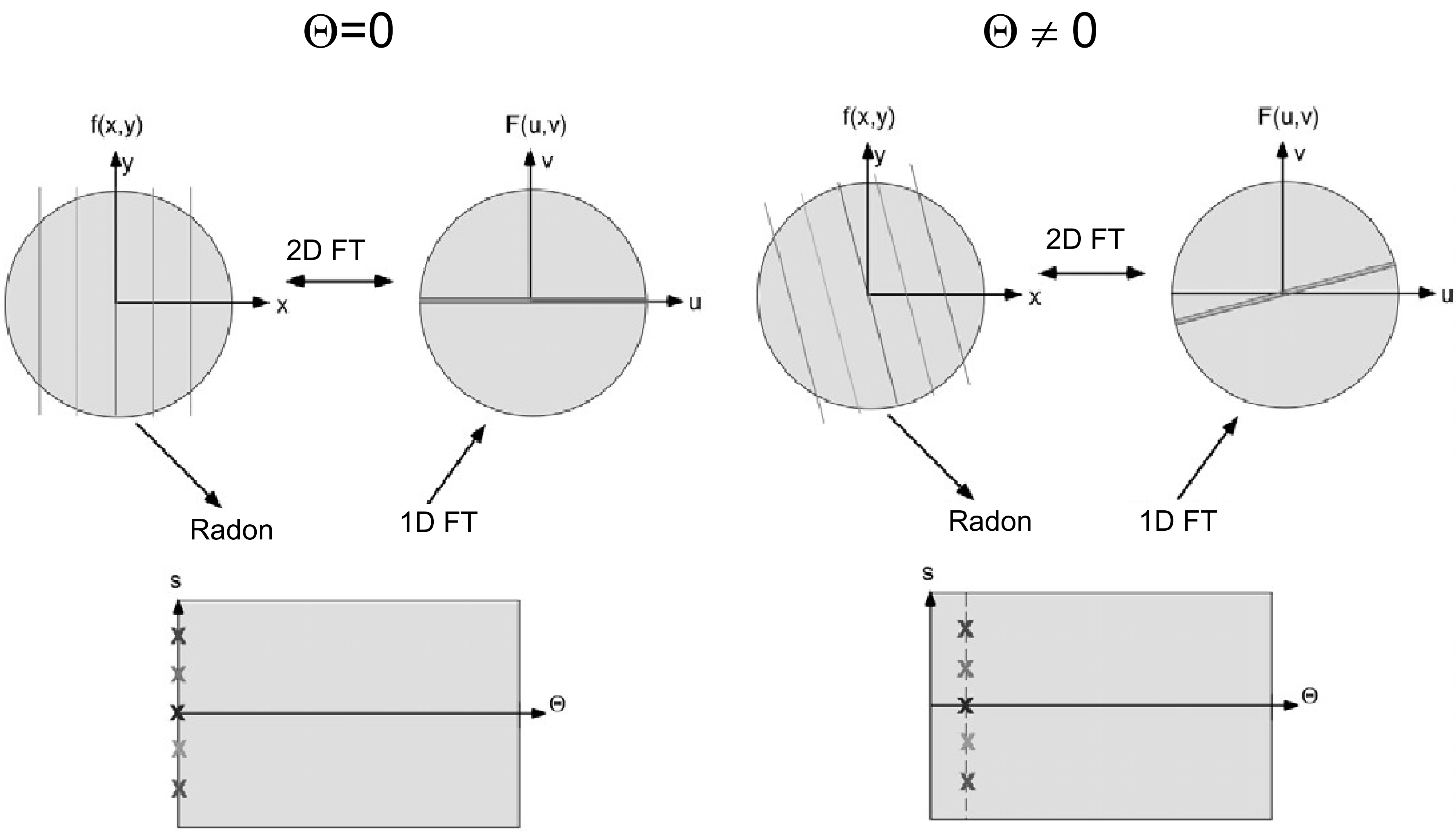

Fourier-slice theorem

given a function f(x,y) and its 2D FT F(u,v)

$$f(x,y) \;\circ\!\!\stackrel{\text{2D-FT}}{\longrightarrow}\!\!\circ\; F(u,v)$$

and let $p_\Theta(s)$ denote a projection of f(x,y) and $P_\Theta(w)$ its 1D FT

$$p_\Theta(s) \;\circ\!\!\stackrel{\text{1D-FT}}{\longrightarrow}\!\!\circ\; P_\Theta(w)$$

Then, $P_\Theta(w)$ equals the values of F(u,v) on a radial beam with angle Θ.

x-ray computed tomography (CT)

Radon transform and computed tomography

passage of a needle-like x-ray beam through the body

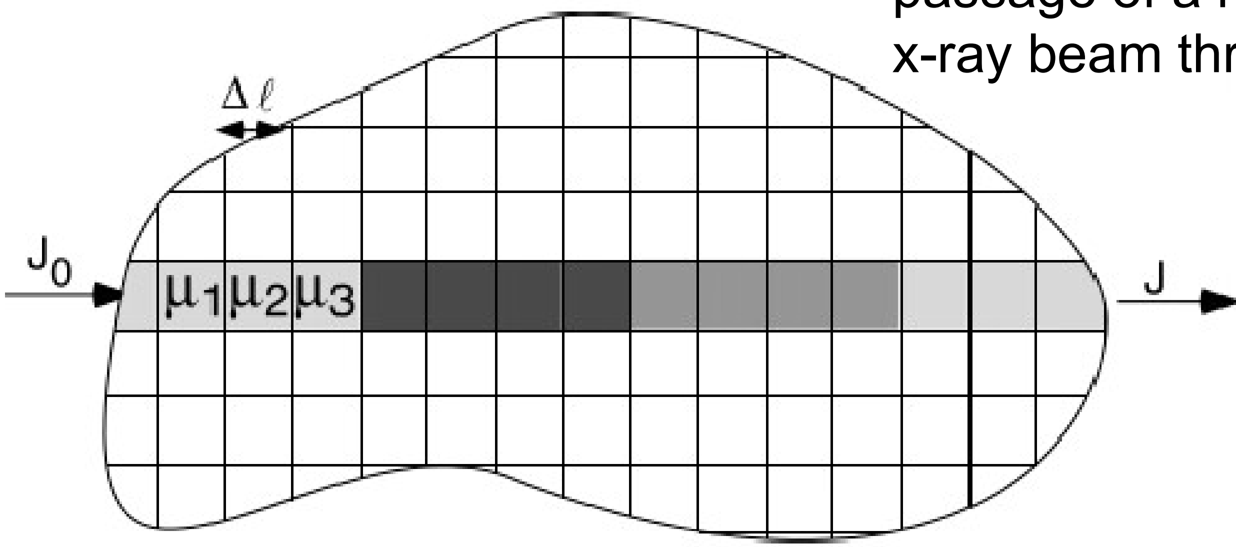

$$J \approx J_0 \cdot e^{-\mu_1 \cdot \Delta \ell} \cdot e^{-\mu_2 \cdot \Delta \ell} \cdot \ldots\ldots e^{-\mu_N \cdot \Delta \ell}$$

$$J \approx J_0 \cdot e^{-\sum_{i=1}^{N} \mu_i \cdot \Delta \ell}$$

$$J = J_0 \cdot e^{-\int \mu(\ell) d\ell}$$

$$\ln\left(\frac{J_0}{J}\right) = \int \mu(\ell) d\ell.$$

measured values (projections) are the line integrals of the attenuation coefficients

x-ray computed tomography (CT)

reconstructing $f(x,y) = \mu(x,y)$ from Radon transform

given sufficient number of projections $p_\Theta(s)$:

- estimate all 1D FT of $p_\Theta(s)$ (= $P_\Theta(w)$)

- for given angle Θ, assign these values to matrix $F(u,v)$

- estimate inverse FT of $F(u,v)$ (= $f(x,y)$)

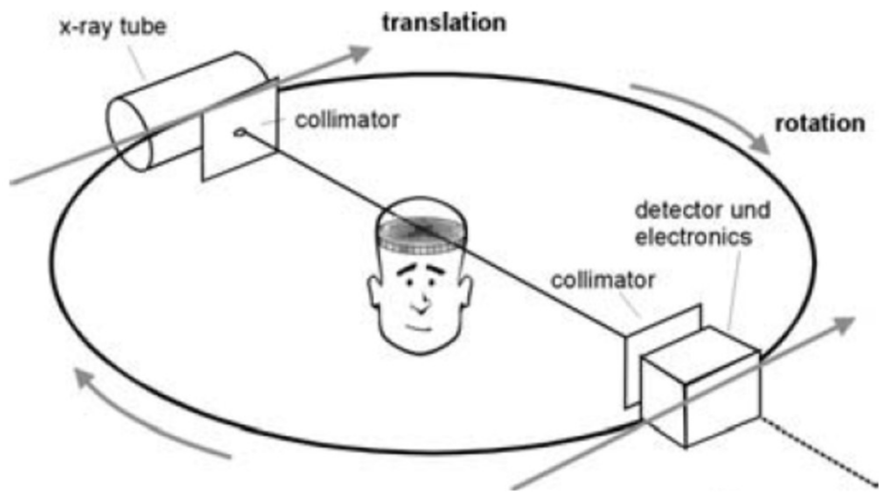

Radon transform and computed tomography

caveat:

- recorded data stem from radial beams !

- fast Fourier transform (FFT) requires interpolation onto square lattice (polar coordinates $\rightarrow$ Cartesian coordinates)

- interpolation can lead to serious artifacts !

(modern scanner allow sampling on square lattice)

iterative image reconstruction (I)

- unknown distribution μ(x,y) only available as projection values (Radon transform) at the end of recording

- use appropriate back transform to find μ(x,y)

simplest ansatz:

wanted: N x N pixels in matrix: N^2 values

given: $M = N_p \times N_d$

= number of projections x number of data/projection

for $M \geq N$: over-determined problem ⇒ can be solved !

iterative image reconstruction (II)

- let f(x,y) = µ(x,y)

- for digital processing: succession of lines of an image matrix yields numerical sequence with index f_i

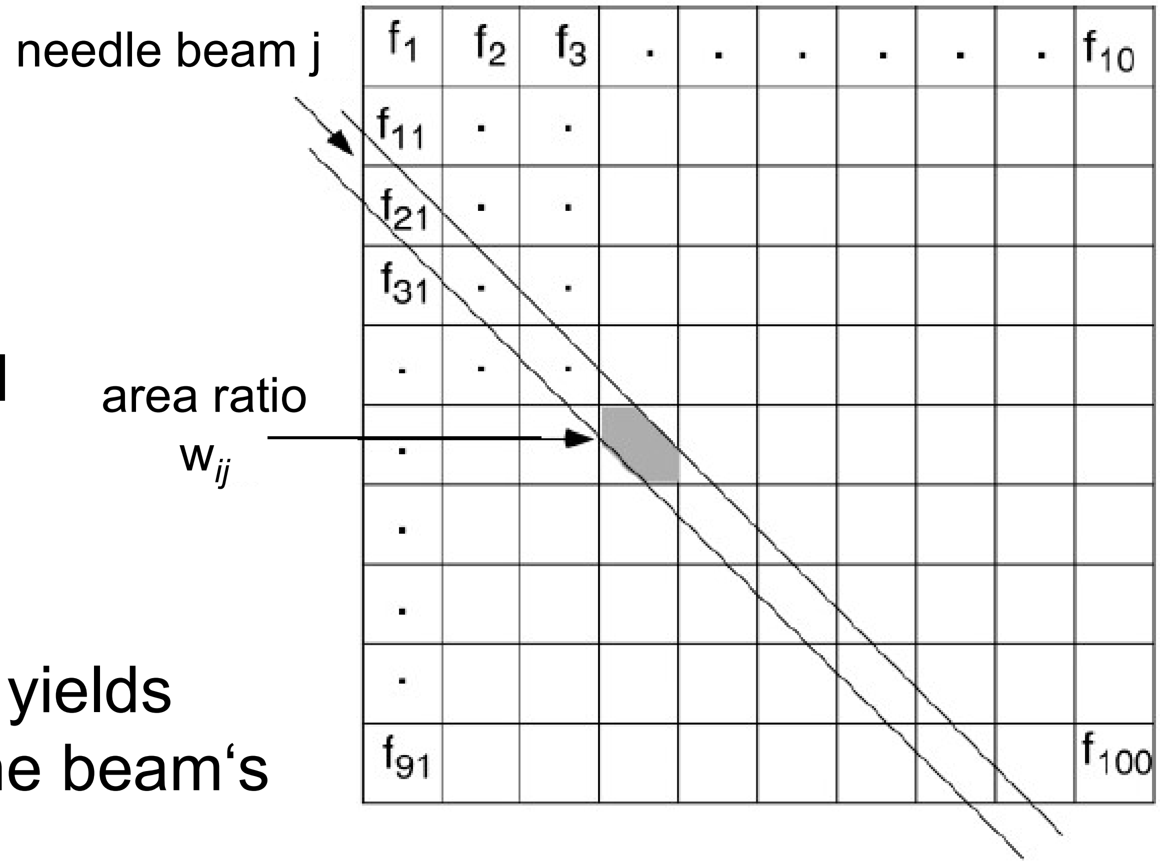

- recording with needle beam *j* yields integral over values f_i along the beam's trajectory:

  values f_i are multiplied with weight w_{ij} and summed up
  w_{ij} denotes area ratio of beam *j* to pixel *i*
  (for a needle beam, most w_{ij}=0)

iterative image reconstruction (III)

recorded data p_i (line integrals) can be written as:

$$p_1 = w_{11} f_1 + w_{12} f_2 + ... + w_{1N} f_N$$

$$p_2 = w_{21} f_1 + w_{22} f_2 + ... + w_{2N} f_N$$

$$\vdots$$

$$p_M = w_{M1} f_1 + w_{M2} f_2 + ... + w_{MN} f_N$$

$\Rightarrow$ linear mapping !!

example: matrix size: 512 x 512 $\Rightarrow$ N^2 = 262.144
given: 1.000 projection values/detector with 800 detectors
$\Rightarrow$ M = 1.000 x 800 = 800.000 (over-determined problem!)

800.000 equations with 262.144 unknown !!

iterative image reconstruction (IV)

solving the system of linear equations:

(1) direct methods

e.g., Gauss elimination impracticable for large matrices

(2) iterative methods:

$$\vec{f}^{(k)} = \vec{f}^{(k-1)} - \frac{\left(\vec{f}^{T(k-1)} \cdot \vec{w}_k\right) - p_k}{\left(\vec{w}_k \cdot \vec{w}_k\right)} \cdot \vec{w}_k$$

$\vec{f}^{(k)} = \left(f_1^{(k)}, \ldots\ldots f_N^{(k)}\right)^T$ vector containing solutions after k-th iteration

$\vec{w}_j = \left(w_{j1}, \ldots\ldots w_{jN}\right)^T$ weight factors for needle beam j

$p_j =$ data of beam j

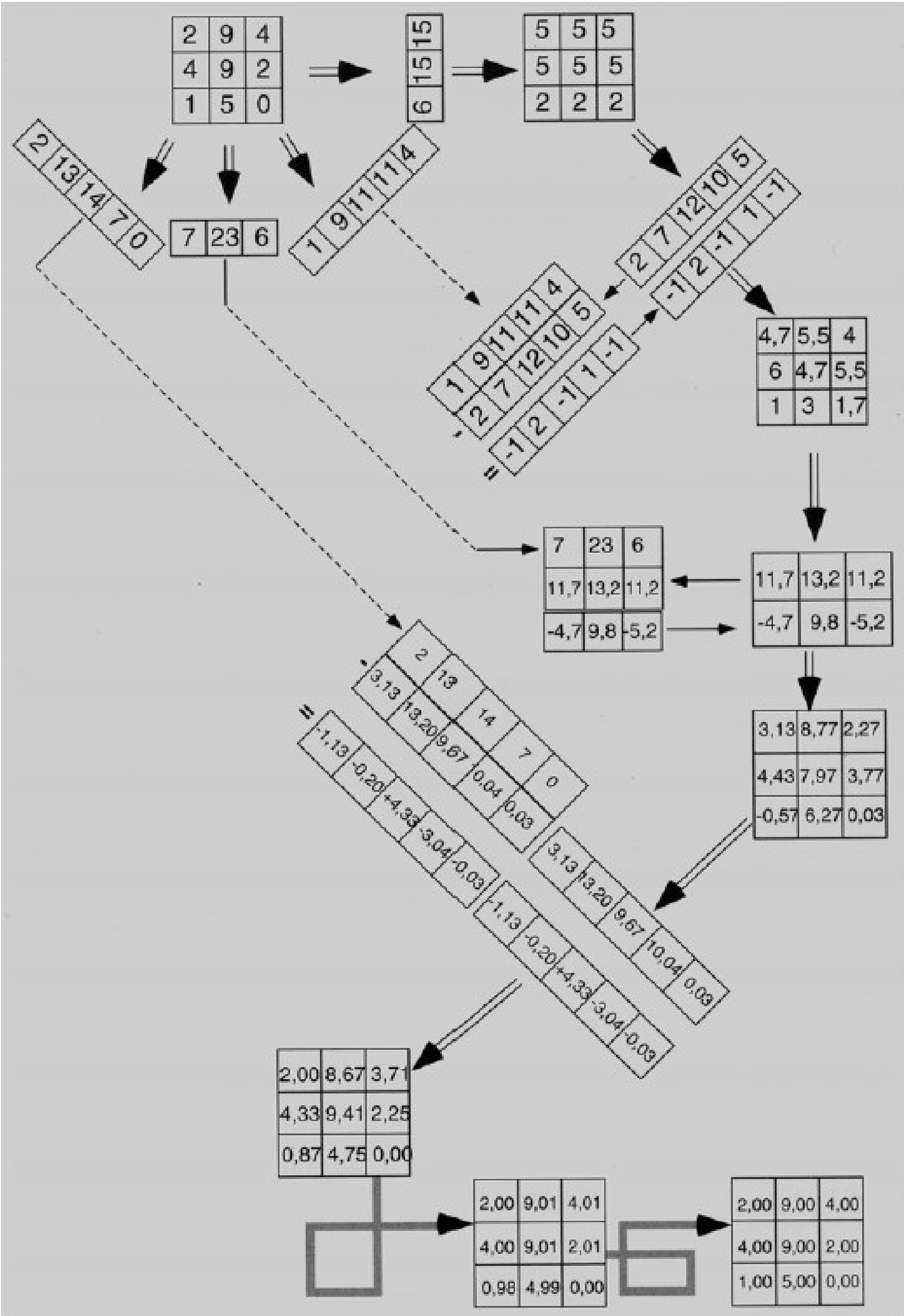

iterative reconstruction scheme

- processing of data from 1. projection:

  distribute data equally to all pixel that contribute to that projection

- processing of data from 2. projection:

  use difference between “forward” calculated data and true data as correction value; distribute correction value equally to all pixels that contributed to that projection

- process data from remaining projections in the same manner

iterative image reconstruction (V)

- method always converges
- method no longer in use in x-ray CT
- method repeatedly applied for PET/SPECT imaging

x-ray computed tomography (CT)

image reconstruction with filtered back projection

recap:
a recording with needle beam under given angle Θ und distance s from origin (i.e., projections $p_\Theta(s)$) corresponds to the ***Radon transform*** of the spatial distribution of μ(x,y).

with ***Fourier-slice theorem***, we have:

- the 1D-FT of projection $p_\Theta(s)$ is the 2D-FT of μ(x,y) along a line in direction of Θ

- reconstruct μ(x,y) by inverse 2D-FT

but: data in polar coordinates;
FFT requires Cartesian coordinates

x-ray computed tomography (CT)

image reconstruction with filtered back projection (I)

back projection:

data (projection values $p_\Theta(s)$) are line integrals of μ(x,y).

however:
integral value = sum over all contributions **without** location information

ansatz:
- distribute integral value equally along the initial line of integration

- superposition of all back projections at (x,y) approximates μ(x,y)

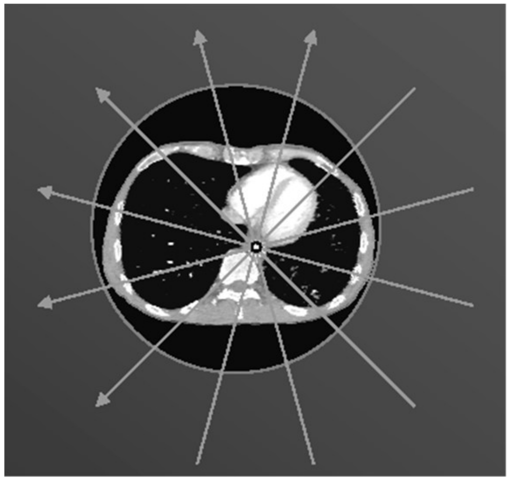

image reconstruction with filtered back projection (II)

back projection:

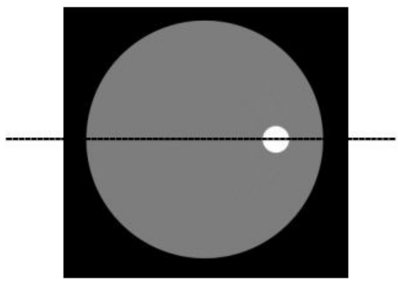

attenuation profile:

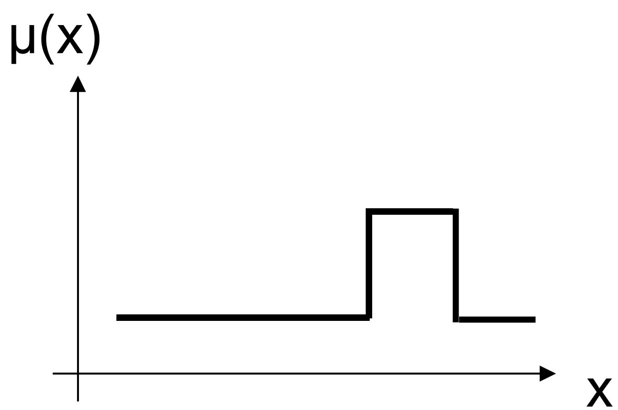

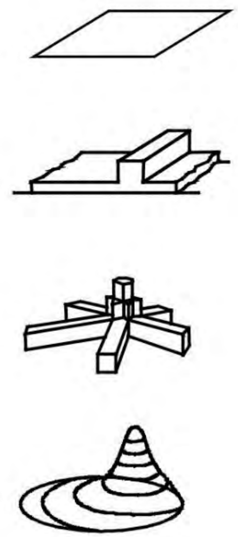

0. back projection

1. back projection

3. back projection

N. back projection

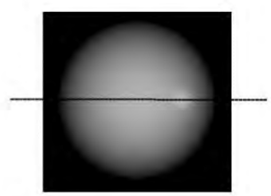

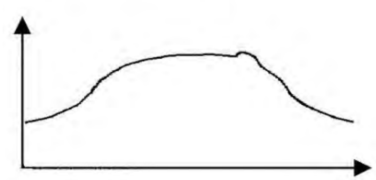

attenuation profile
after N ($\neq \infty$) back projections

image reconstruction with filtered back projection (III)

back projection:

b.p. with finite number of projections
has **point spread function** (PSF) **~ 1/r**

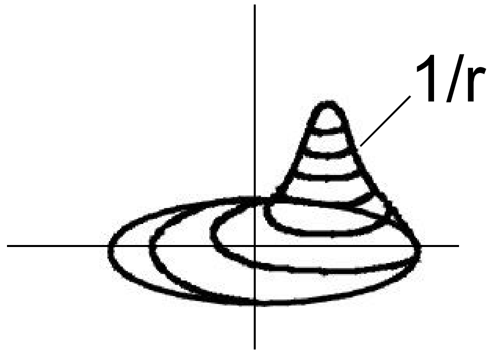

such a PSF can be assigned to each pixel,
weighted with the local μ(x,y)

back projection = 1/r ∗ μ(x,y) (convolution)

back projection leads to **blurred image**:
differences in contrast and/or fine structures not recognizable

image reconstruction with filtered back projection (IV)

filtered back projection:

idea:

modify point spread function such that blurring is minimized (ideally: prevented).

ansatz:

convolve attenuation profile with suitable filter (convolution kernel)

image reconstruction with filtered back projection (IV-a)

filtered back projection:

attenuation profile $*$ convolution kernel = filtered profile

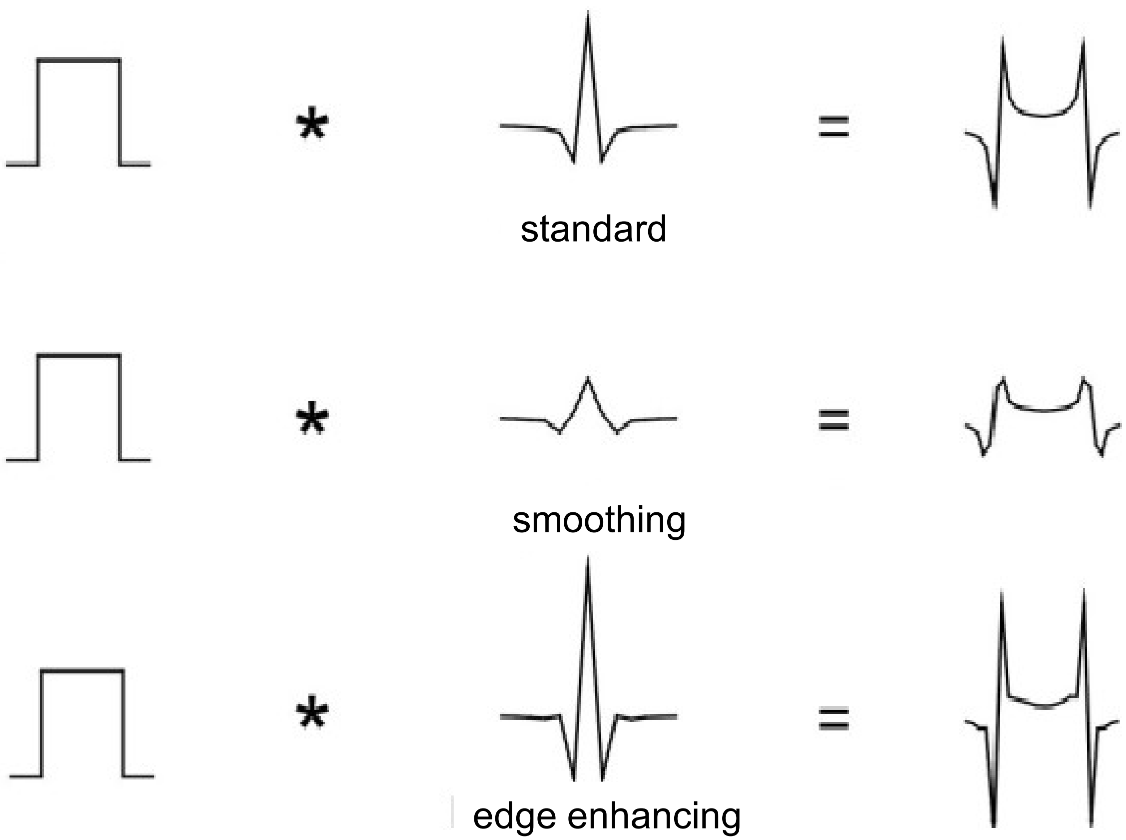

x-ray computed tomography (CT)

image reconstruction with filtered back projection (V)

filtered back projection

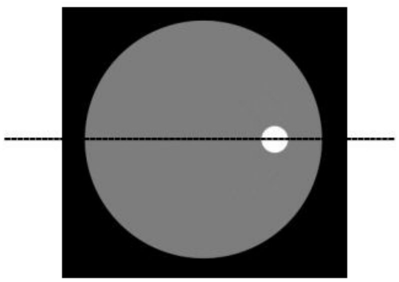

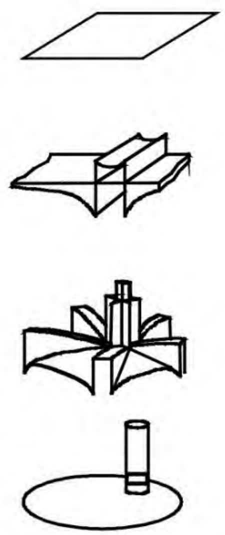

0. back projection

1. back projection

3. back projection

N. back projection

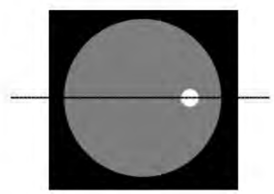

attenuation profile:

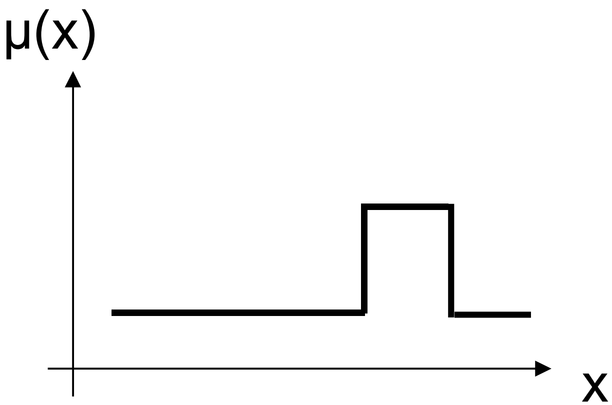

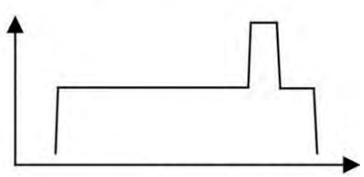

attenuation profile after N ($\neq \infty$) filtered back projections

image reconstruction with filtered back projection (V-a)

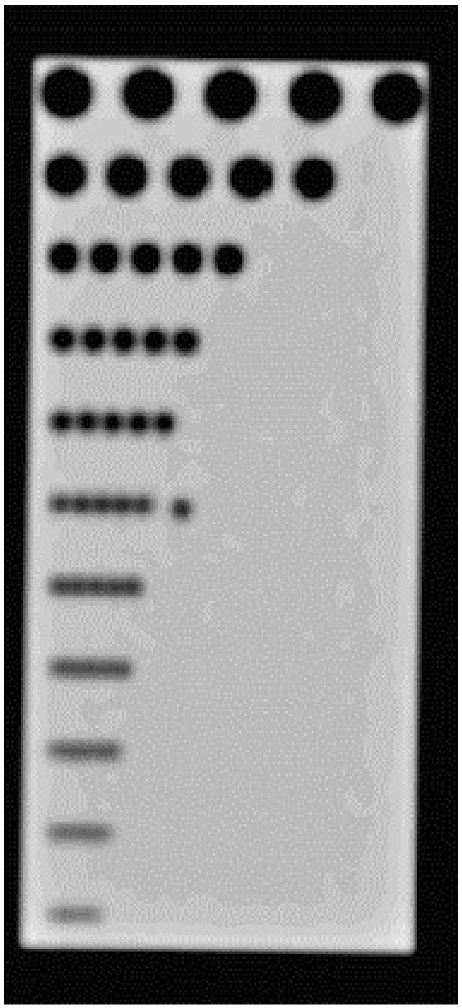

smoothing

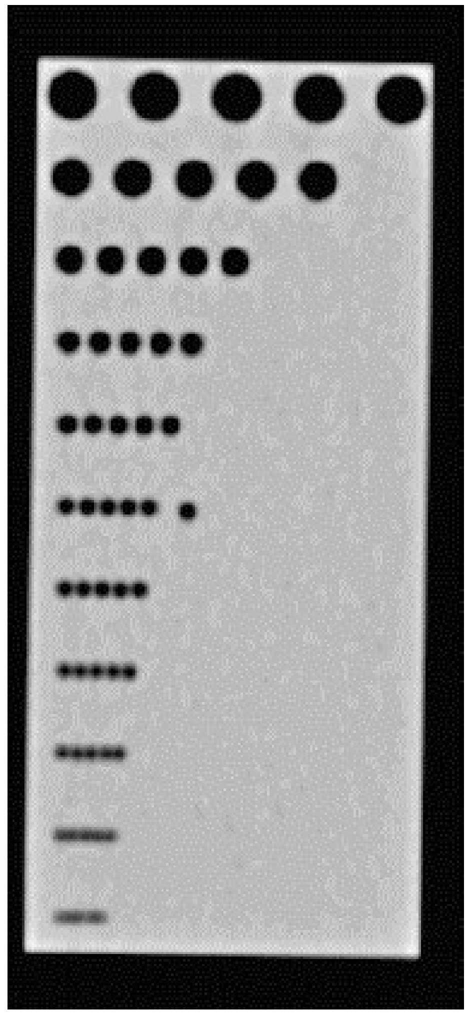

standard

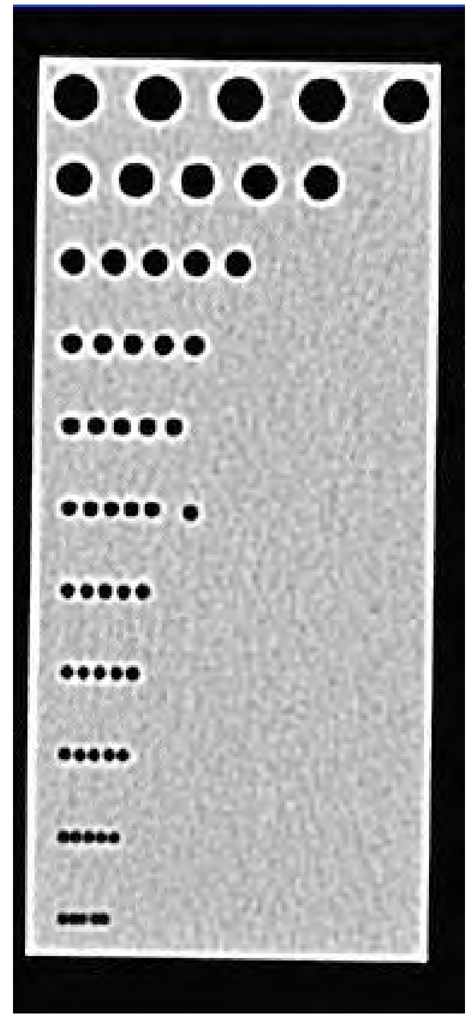

edge enhancing

image reconstruction with filtered back projection (V-b)

impact of convolution kernel

smoothing
"soft"

standard

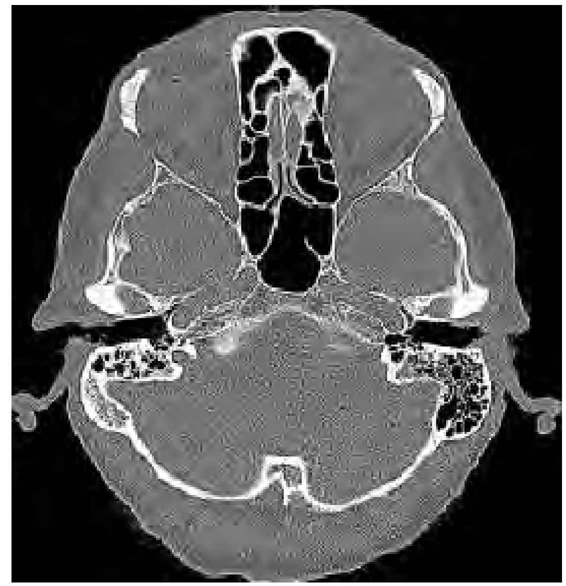

edge enhancing
"bone"

image reconstruction with filtered back projection (VI)

can we derive an analytic form for the filter?

wanted: f(x,y) = μ(x,y) from inverse 2D-FT of F(u,v), i.e.:

$$f(x,y) = \int_{-\infty}^{+\infty}\int_{-\infty}^{+\infty} F(u,v) \cdot e^{j \cdot 2\pi \cdot (ux+vy)} du dv$$

with cylindrical coordinates in Fourier space

$u = w \cdot \cos\Theta$

$v = w \cdot \sin\Theta$

$du dv = w \cdot dw \cdot d\Theta$,

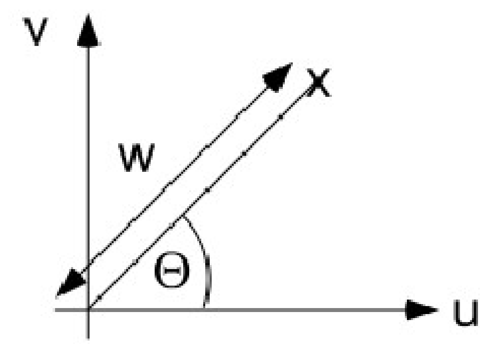

we have:

$$f(x,y) = \int_{0}^{2\pi}\int_{0}^{\infty} F(w,\Theta) \cdot e^{j \cdot 2\pi \cdot w(x\cos\Theta + y\sin\Theta)} w dw d\Theta$$

image reconstruction with filtered back projection (VI-a)

integration can be reduced to $[0,\pi]$ (Hesse normal form):

$$f(x,y) = \int_0^{\pi} \int_{-\infty}^{+\infty} F(w,\Theta) \cdot e^{j \cdot 2\pi \cdot w (x\cos\Theta + y\sin\Theta)} |w| \, dw \, d\Theta$$

(use absolute value of w, to avoid negative radii)

$F(w,\Theta) = P_\Theta(w)$ (with Fourier-slice theorem)

$p_\Theta(s) \; \circ\!\!\xrightarrow{\text{1D-FT}}\!\!\circ \; P_\Theta(w)$ (1D FT of a projection)

$$f(x,y) = \int_0^{\pi} \left[\int_{-\infty}^{+\infty} P_\Theta(w) \cdot |w| \cdot e^{j \cdot 2\pi \cdot ws} \, dw \right] d\Theta$$

$s = x\cos\Theta + y\sin\Theta$

x-ray computed tomography (CT)

image reconstruction with filtered back projection (VI-b)

substitution: $\tilde{p}_\Theta(s) = \int_{-\infty}^{+\infty} P_\Theta(w) \cdot |w| \cdot e^{j \cdot 2\pi \cdot ws} dw$

if |w| were not part of the integral, an inverse FT would immediately recover the original projection $p_\Theta(s)$, i.e.:

$$p_\Theta(s) \circ\!\!-\!\!\!-\!\!\!-\!\!\circ P_\Theta(w)$$

due to the multiplication with |w| in Fourier space, we have a filtering of the projection $p_\Theta(s)$:

$$\tilde{p}_\Theta(s) = p_\Theta(s) * h(s) \circ\!\!-\!\!\!-\!\!\!-\!\!\circ P_\Theta(w) \cdot |w|$$

$\tilde{p}_\Theta(s)$ is the **filtered projection** (using the convolution theorem).
h(s) is the impulse response function of the filter (= convolution kernel)

$$h(s) \circ\!\!-\!\!\!-\!\!\!-\!\!\circ |w|$$

image reconstruction with filtered back projection (VI-c)

is there a function h(s) that represents FT of |w| ?

problem: h(s) only defined as limiting process

with ansatz: $|w| \approx |w| \cdot \exp(-\varepsilon |w|)$

we find: $$\frac{\varepsilon^2 - (2\pi s)^2}{\left(\varepsilon^2 + (2\pi s)^2\right)^2} \circ\!\!-\!\!\circ \; |w| \cdot e^{-\varepsilon|w|}$$

inverse FT of $|w| \cdot \exp(-\varepsilon |w|)$

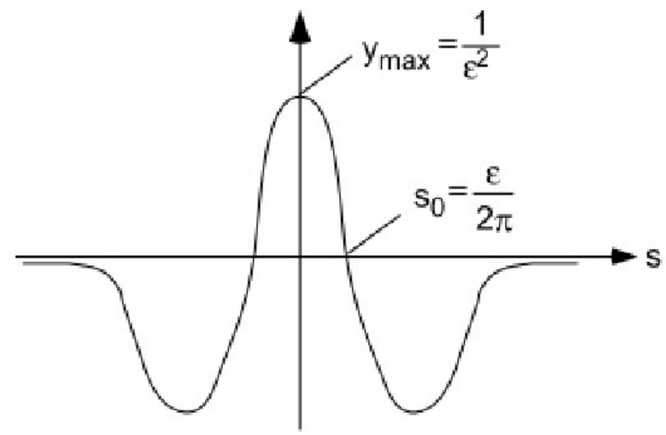

consider limes $\varepsilon \to 0$:

- l.h.s. turns into $-1/2\pi s^2$ and r.h.s. turns into |w|
- peak at s=0 the more narrow and larger the smaller ε

image reconstruction with filtered back projection (VI-d)

what is the meaning of the integral over Θ ?

$$f(x,y) = \int_0^\pi \tilde{p}_\Theta(s)\,d\Theta = \int_0^\pi \tilde{p}_\Theta(x\cos\Theta + y\sin\Theta)\,d\Theta$$

back projection:

in order to derive f(x,y)=μ(x,y) at position (x,y), take all filtered projections $\tilde{p}_\Theta(s)$ at position xcosΘ+ysinΘ und sum them up.

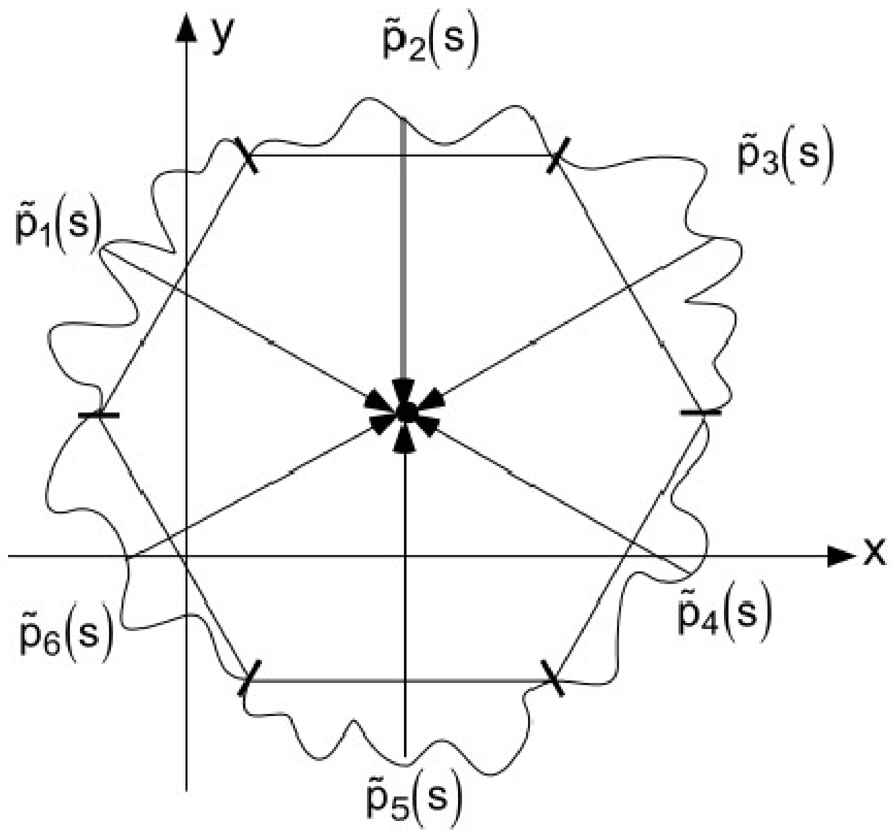

image reconstruction with filtered back projection (VII)

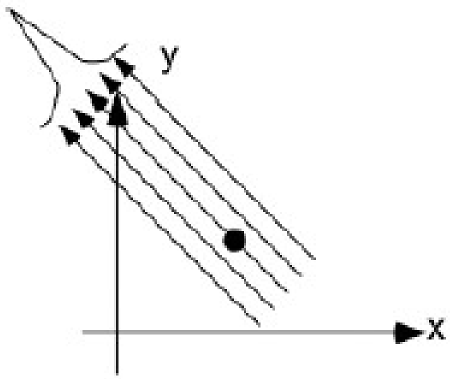

projection
(measurement)

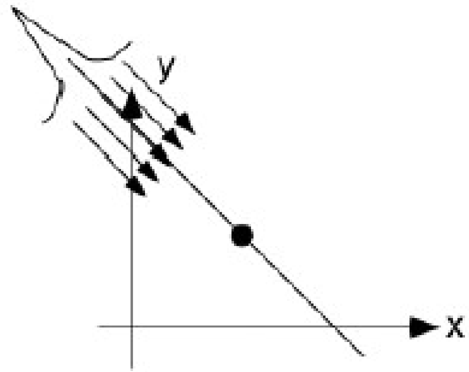

unfiltered back projection
(single measurement)

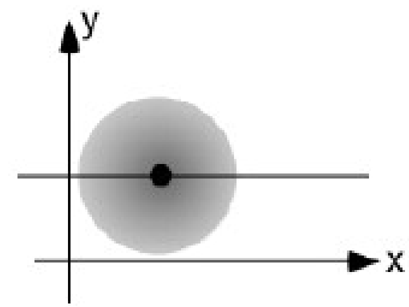

unfiltered back projection
(all measurements)

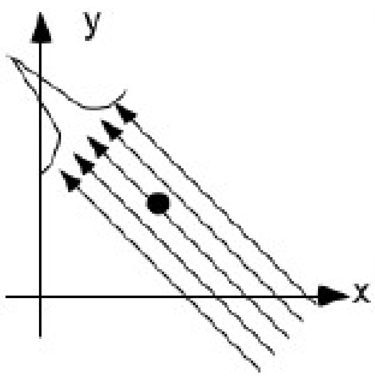

projection
(measurement)

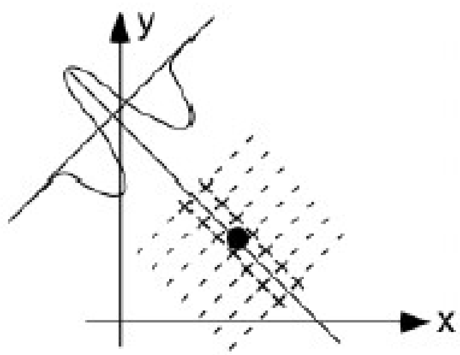

filtered back projection
(single measurement)

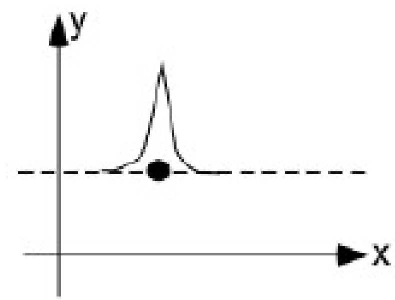

filtered back projection
(all measurements)

image reconstruction with filtered back projection (VIII)

linear interpolation:

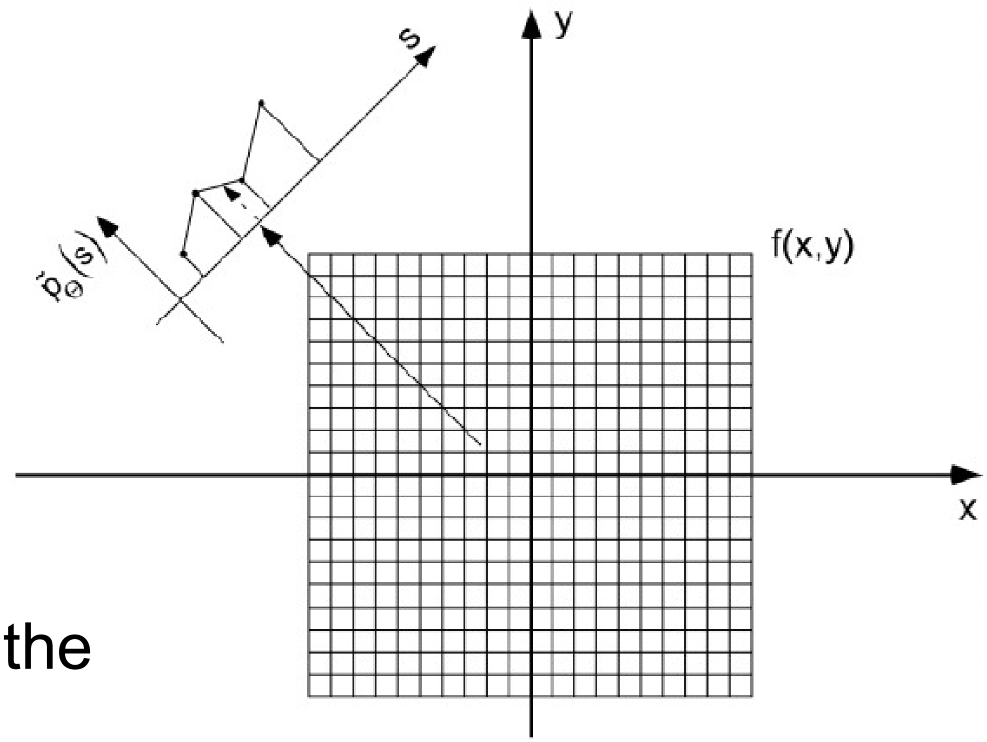

problem:
a back projection may not always hit the center of quadratically arranged pixel

solution (go backward)
1) from the center of a pixel target at the filtered projection under angle Θ
2) perform *linear interpolation* between adjacent values to approximate measurement position of the detector.

image reconstruction with filtered back projection (IX)

Nyquist theorem and noise:

- digital sampling leads to maximum frequency $w_{max} = 1/2\Delta S$ in the projections, where ΔS denotes the distance between detectors

- since spatial frequencies larger than w_{max} are not known a priori, the filtered back projection has a degraded performance in applications (high spatial frequencies over-emphasized)

- at spatial frequencies $w < w_{max}$ the spectrum $P_\Theta(w)$ is dominated by noise

- multiplication with $|w|$ enhances noise additionally

ansatz: replace $|w|$ with a "more suitable" filter function

image reconstruction with filtered back projection (IX-a)

alternative filter functions according to Shepp & Logan and Ramachandran & Lakshminarayan

convolution kernel

	Shepp und Logan	Ramachandran u. Lakshminarayan
hk	$-\frac{2}{\pi^2 a^2}\frac{1}{4k^2-1}$	$\frac{1}{4a^2}$ $k=0$ 0 $k=$ even $,\neq 0$ $-\frac{1}{\pi^2 a^2 k^2}$ $k=$ odd
h(s)	$-\frac{2}{\pi^2 a^2}\frac{1-2\frac{s}{a}\sin\pi\frac{s}{a}}{4\left(\frac{s}{a}\right)^2-1}$	$\frac{1}{2a^2}\left\{\frac{\sin\pi\frac{s}{a}}{\pi\frac{s}{a}}+\frac{\cos\pi\frac{s}{a}-1}{\left(\pi\frac{s}{a}\right)^2}\right\}$
$H(\|w\|)$	$\|w\|\cdot\left\|\frac{\sin\pi wa}{\pi wa}\right\|\mathrm{rect}(2aw)$	$\|w\|\cdot\mathrm{rect}(2aw)$

image reconstruction with filtered back projection (IX-b)

alternative filter functions according to Shepp & Logan and Ramachandran & Lakshminarayan

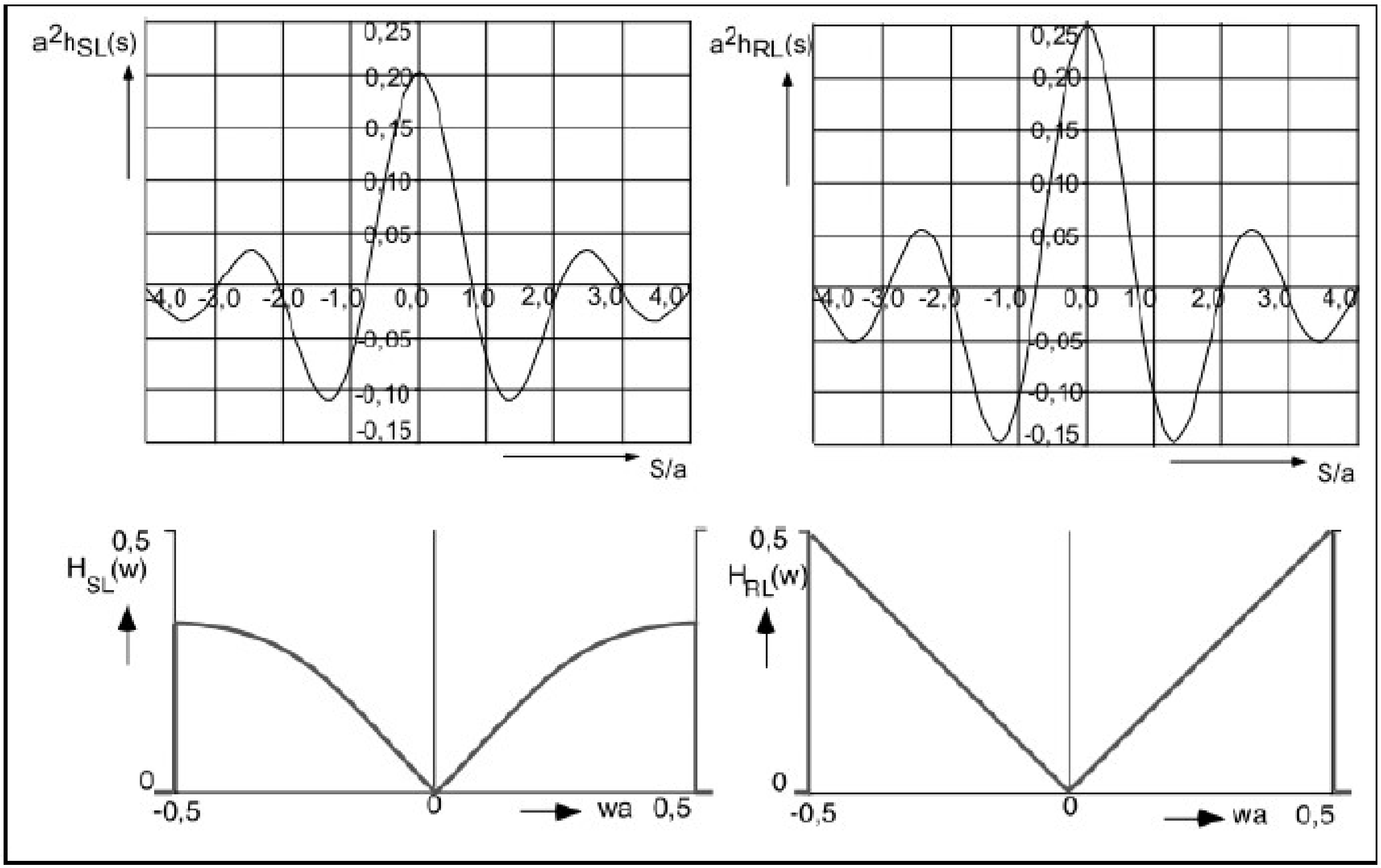

image reconstruction with filtered back projection (X)

analog and digital filtering:

analog

$$\tilde{p}_{\Theta}(s) = \int_{-\infty}^{+\infty} p_{\Theta}(s) \cdot h(s - s')ds'$$

digital

$$\tilde{p}_{\Theta}(n \cdot \Delta s) = \Delta s \cdot \sum p_{\Theta}(k \cdot \Delta s) \cdot h(n \cdot \Delta s - k \cdot \Delta s)$$

$$= \Delta s \cdot \sum_{k=-K}^{k=+K} p_{\Theta}(n \cdot \Delta s - k \cdot \Delta s) \cdot h(k \cdot \Delta s).$$

x-ray computed tomography (CT)

image reconstruction with filtered back projection (X)

analog and digital filtering:

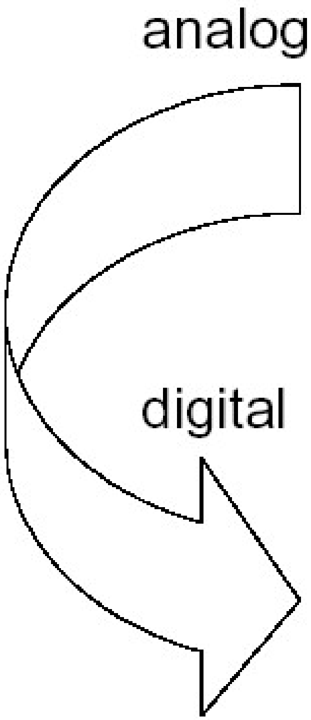

$$f(x,y) = \int_0^{\pi} \tilde{p}_{\Theta}(s)\ d\Theta \qquad d\Theta \approx \frac{\pi}{M}$$

M =
number of projections

$$f(x,y) = \frac{\pi}{M}\sum_{i=1}^{M} \tilde{p}_{\Theta}(x\cos\Theta_i + y\sin\Theta_i)$$

suitable interpolation

what does a CT image represent?

average of all linear attenuation coefficients in a given volume element (voxel)
in Hounsfield units

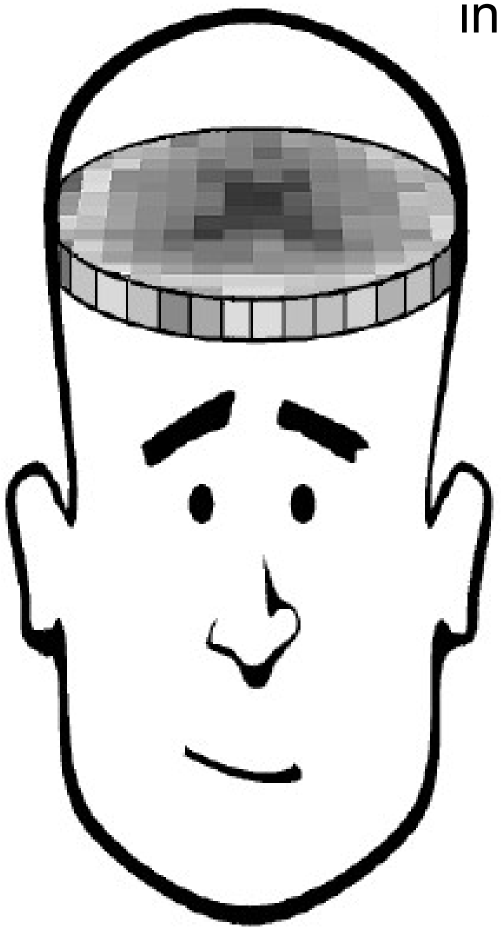

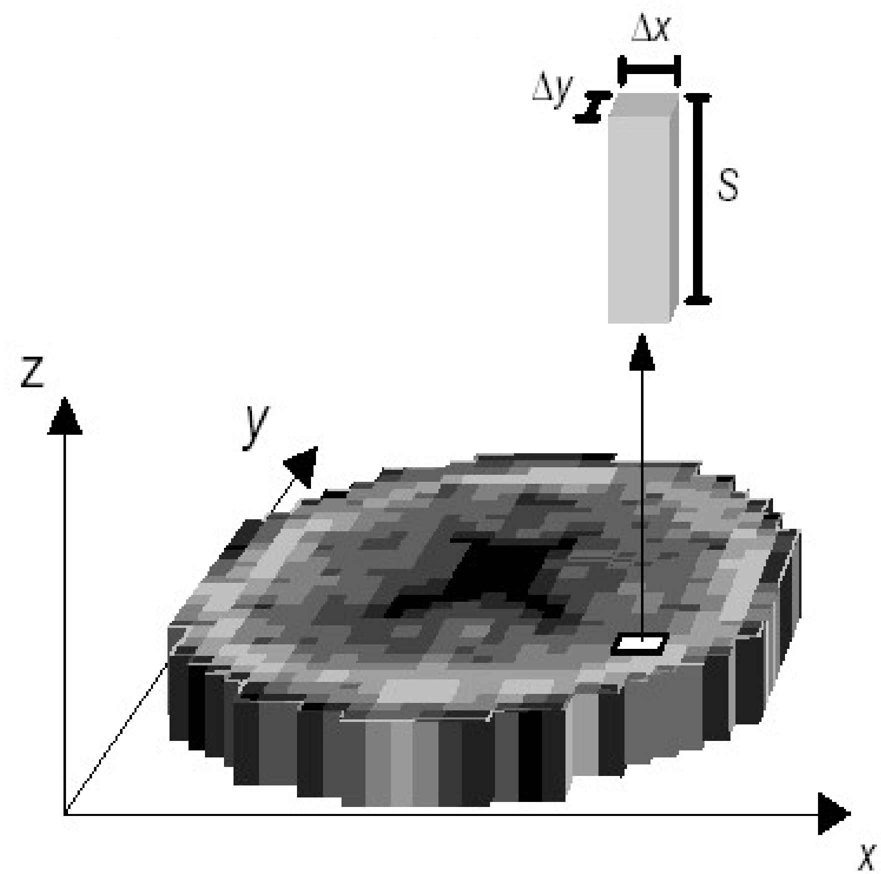

Hounsfield scale

absorption- or attenuation coefficient

in nuclear physics:

$$[\mu] = \mathrm{cm}^{-1}$$ (μ depends on energy of x-rays!)

in medical imaging: ***relative Hounsfield unit (HU; CT number)***

$$\mu_{rel} = \frac{\mu - \mu_{\text{water}}}{\mu_{\text{water}}} \cdot 1000$$

- human body mostly consists of water (~60 %)
- representation in *per mille* since most soft tissues differ only very little from μ_{water}

x-ray computed tomography (CT)

Hounsfield scale

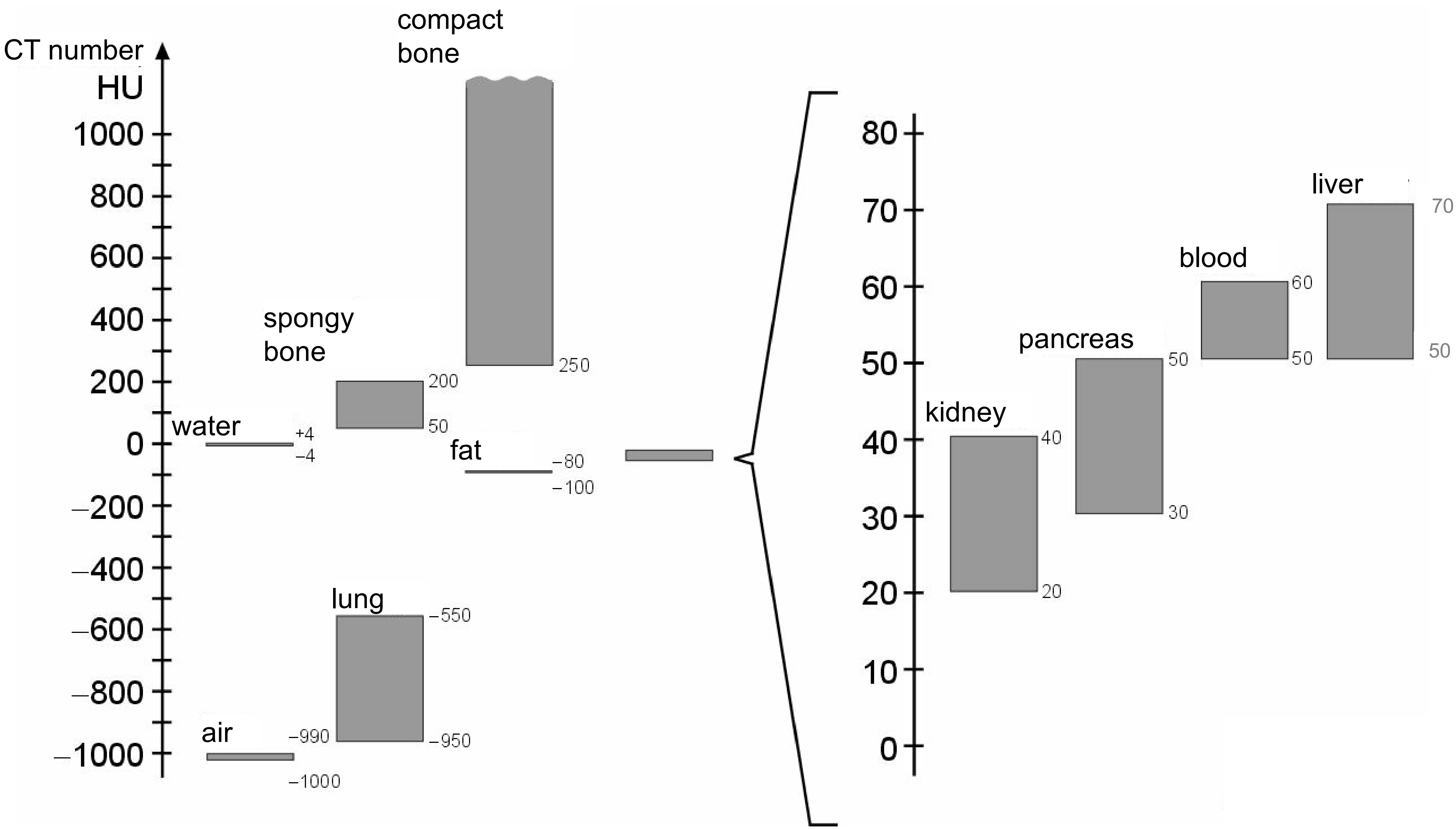

x-ray computed tomography (CT)

Hounsfield scale

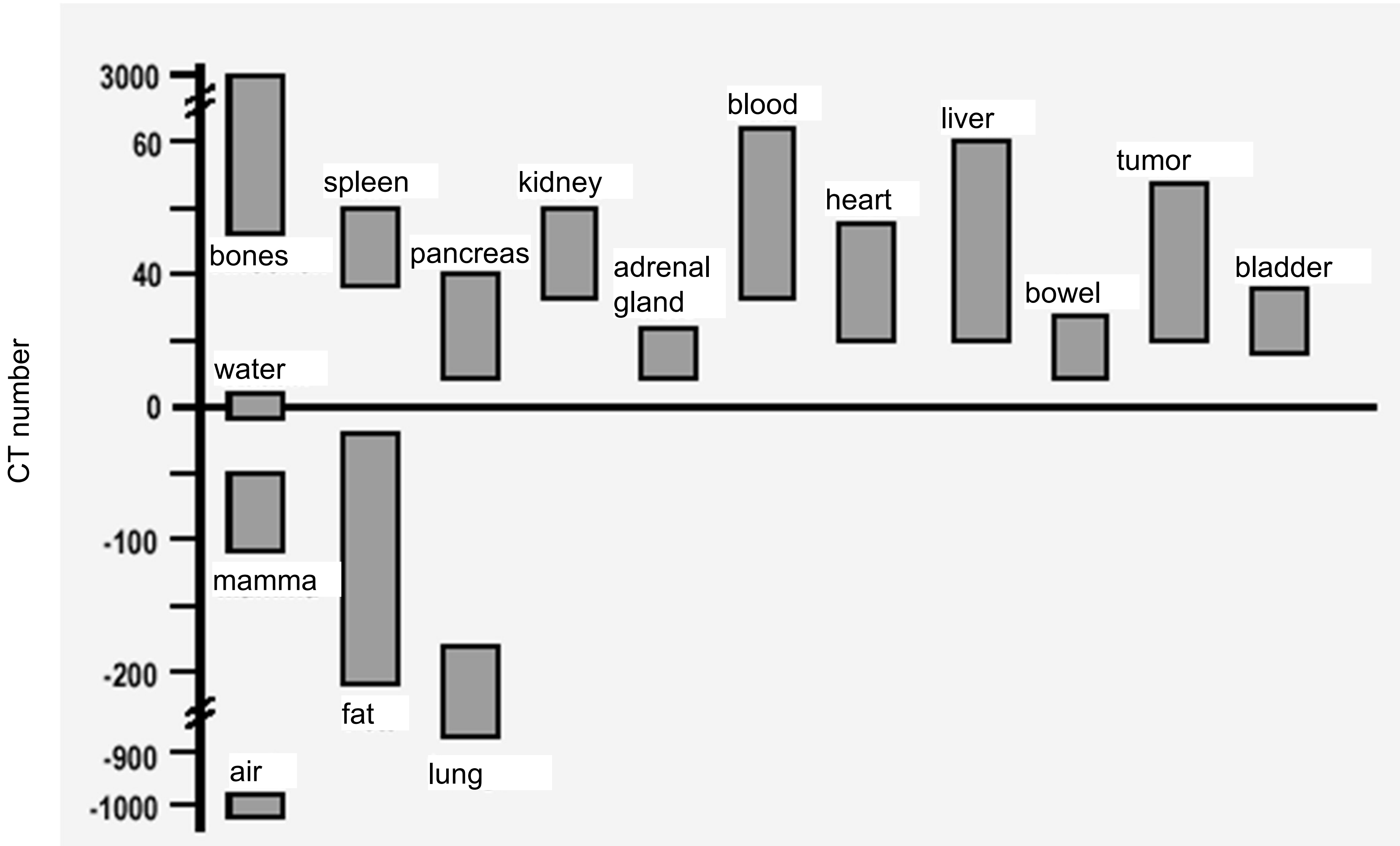

Hounsfield scale and window techniques

improve differentiability of soft tissues with window technique

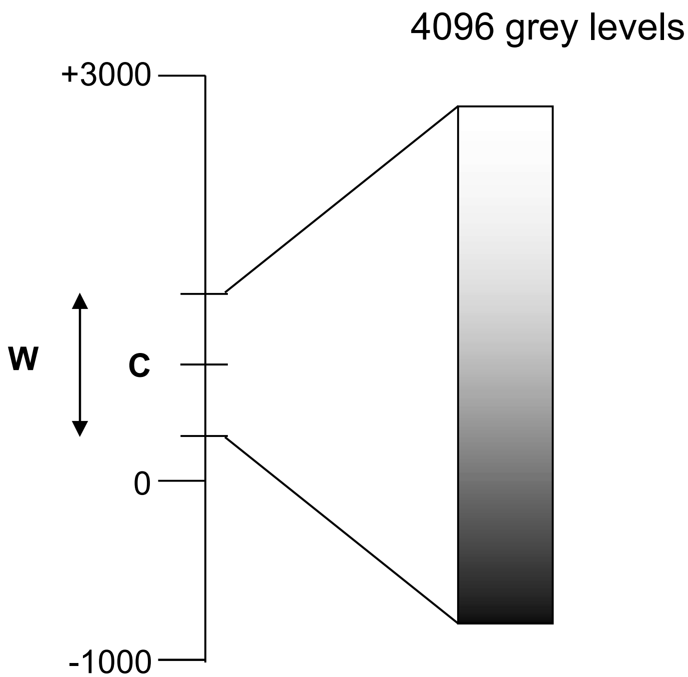

C center
W width

improved interpretability of CT images

e.g.

bone window:	C/W = 1000/2500
mediastinum window:	C/W = -50/ 400
lung window:	C/W = -625/1250

Hounsfield scale and window techniques

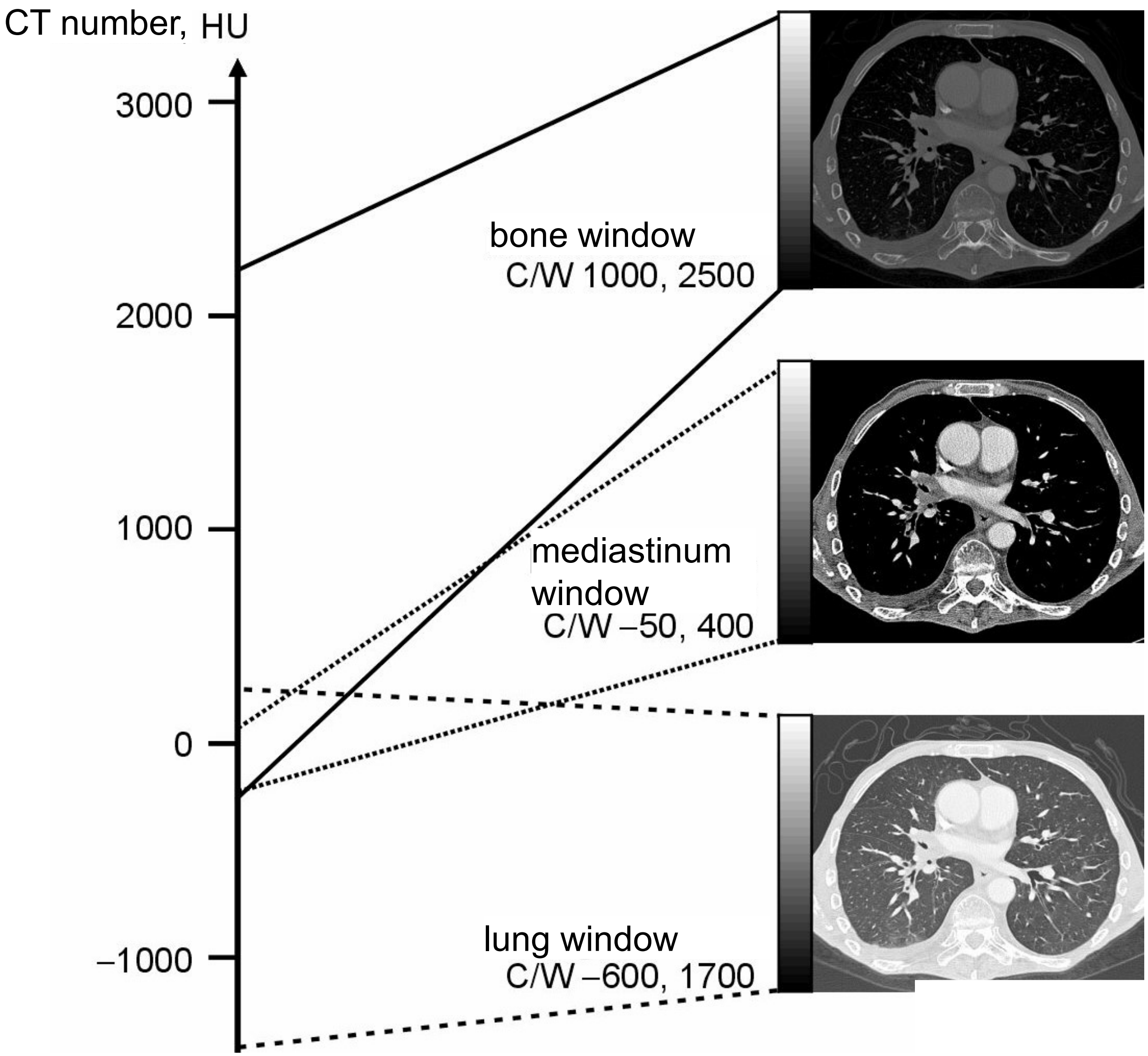

Hounsfield scale and dual-energy CT

- CT number hard to interpret unequivocally
  (note: average of attenuation coefficients of all chemical elements
  in a given voxel!)

- ambiguous diagnostic finding (example):
  observation: area with increased attenuation in soft tissue
  question: recent (bleeding) or existent process (calcium deposit)

- use order-number-dependent energy-dependence of $\mu = f(E,Z)$

- dual energy CT:
  - two recordings with different energies of x-rays
  - subtraction of images yields material-selective image

Hounsfield scale and dual-energy CT

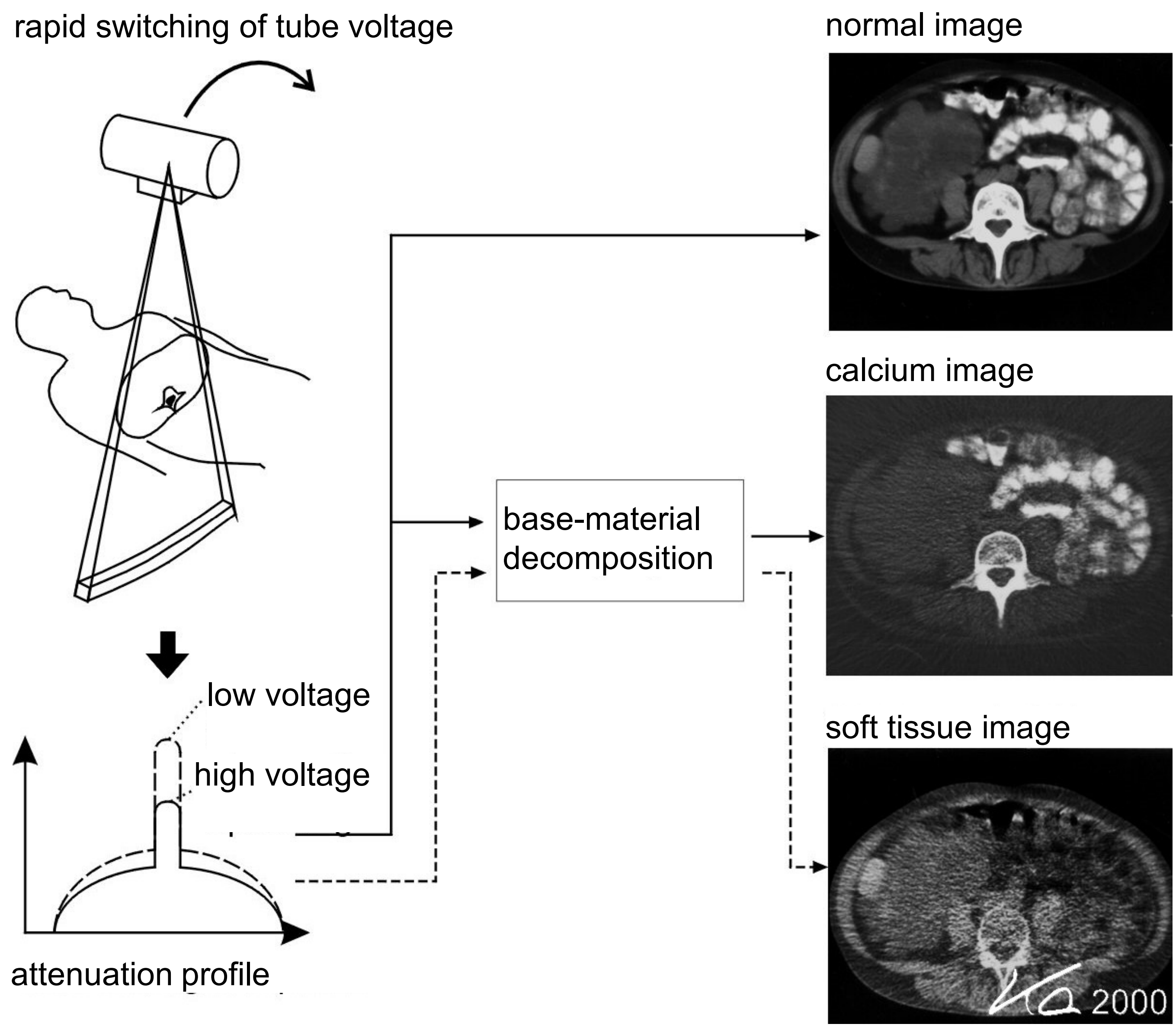

x-ray computed tomography (CT)

estimating homogeneity

tolerance:
± 4HU
from set value
(water: 0 HU)

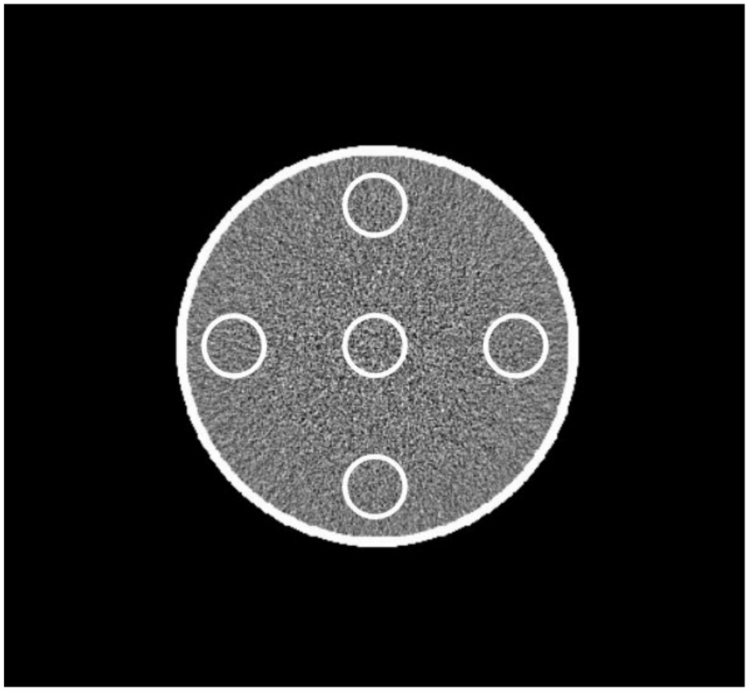

20 cm water phantom

	mean	σ
middle	–1,6 HU	21,3 HU
top	–0,9 HU	14,8 HU
right	–1,3 HU	14,7 HU
bottom	–0,9 HU	14,6 HU
left	–1,3 HU	14,9 HU

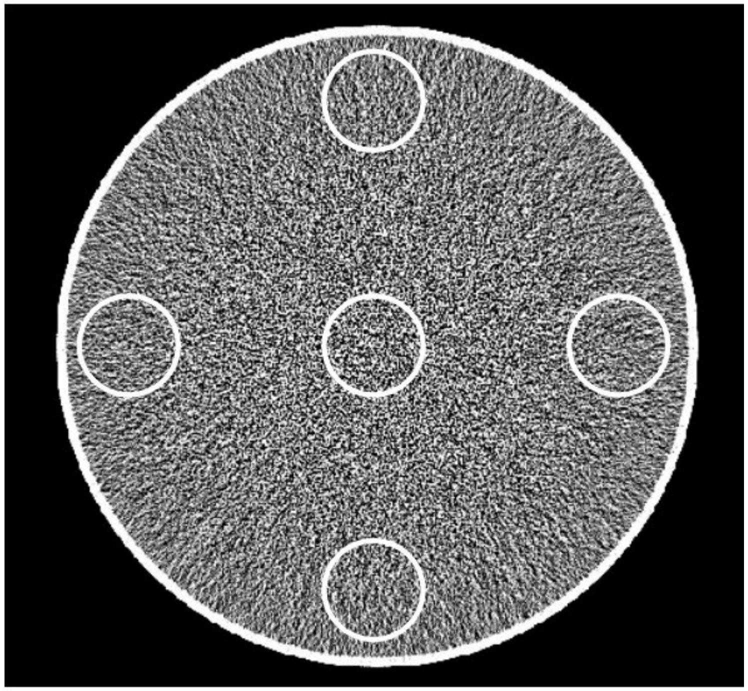

32 cm water phantom

	mean	σ
middle	3,0 HU	68,5 HU
top	–1,6 HU	34,8 HU
right	–0,9 HU	34,2 HU
bottom	–0,9 HU	35,1 HU
left	–0,1 HU	35,3 HU

comparing projection radiography and computed tomography

both techniques:
- imaging with x-rays
- require comparable dose (novel CT-systems even lower dose)

projection radiography:
- contrast = sum of signals (μ) along transmission trajectory
- contrast depends on atomic number *Z* and dose

computed tomography
- contrast = μ-values from adjacent voxel (not due to summation or line integrals); local composition of tissue
- no influence from adjacent or overlapping structures

x-ray computed tomography (CT)

CT image

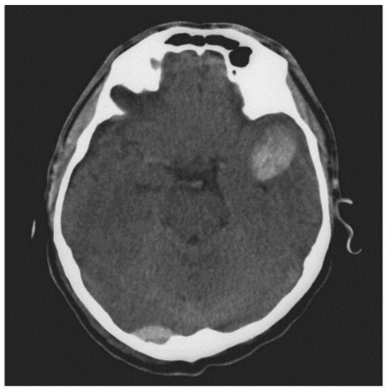

Röntgen image

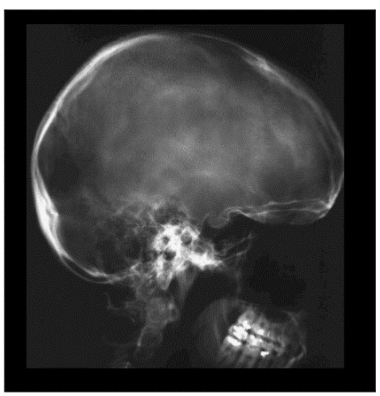

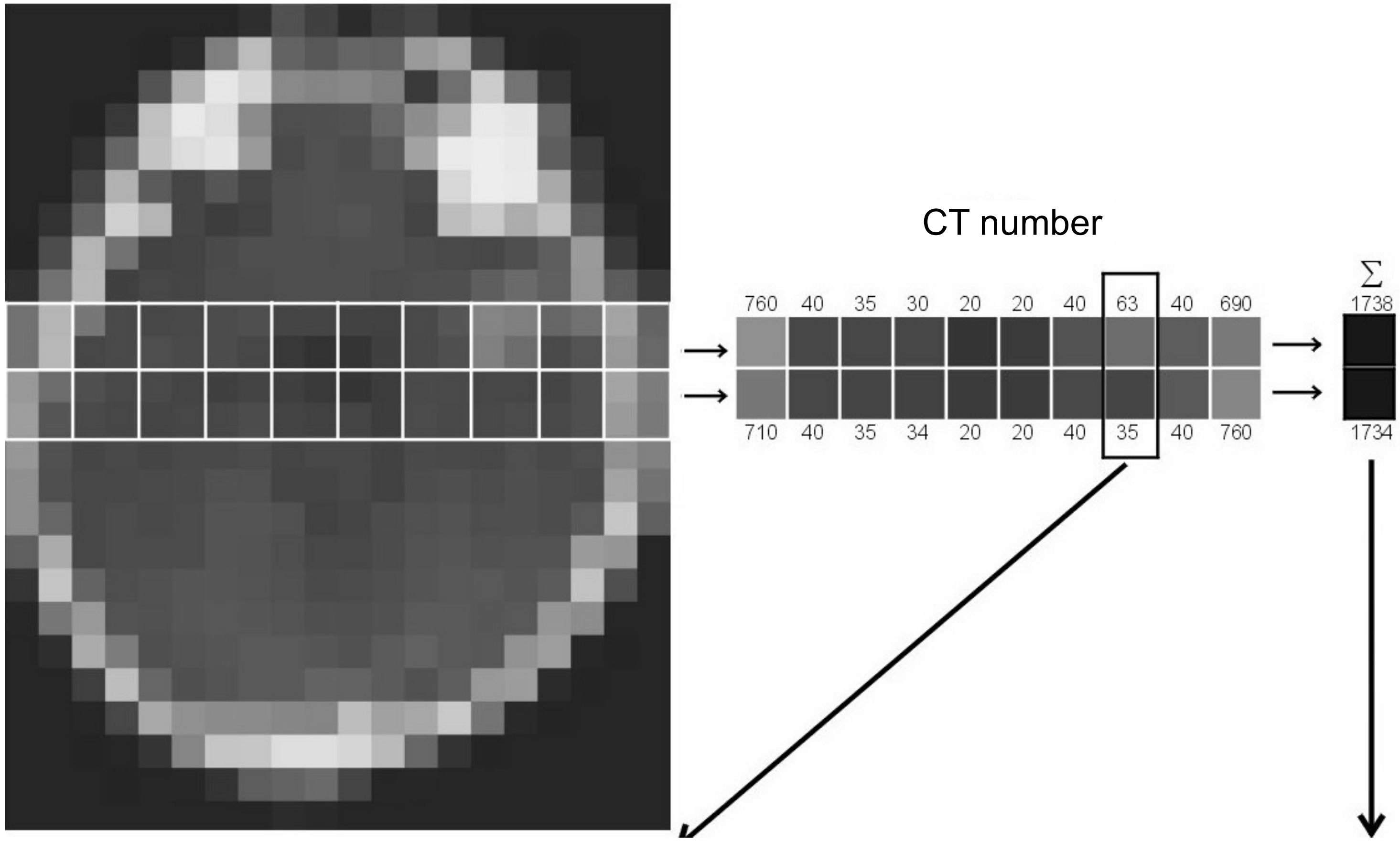

CT image:
high local contrast *K*
$K = \Delta CT = J_1 - J_2$
~ 50 %

Röntgen image:
low soft-tissue contrast
$K = (J_1 - J_2)/((J_1 + J_2)/2)$
~ 0,23 %

measurement devices
for
x-ray computed tomography

data acquisition

1. generation CT scanner

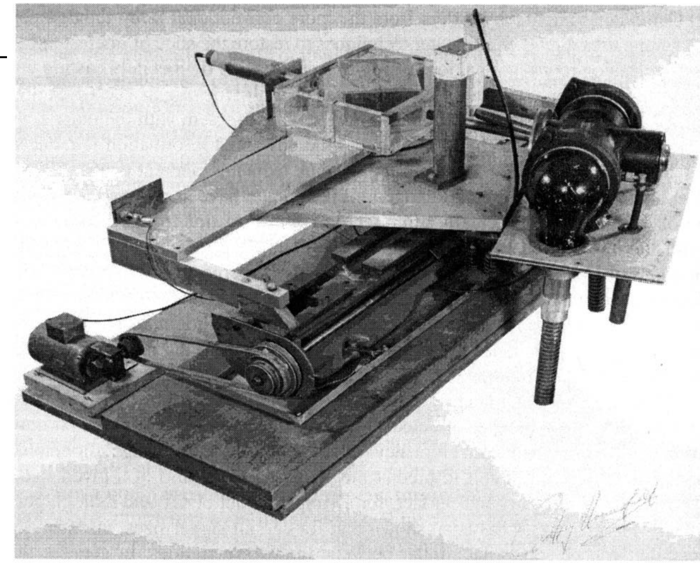

Hounsfield 1969 (phantom measurements)
(*A method of and apparatus for examination of a body by radiation such as x-ray or gamma radiation*, US patent 1970)

technique: *pencil beam* (single x-ray needle-like beam)
principle: translation-rotation
detectors: 1
x-ray source: americum 95
recording duration: 9 days
(image reconstruction: 2.5 hrs; computing center EMI)

x-ray computed tomography (CT)

data acquisition

scheme of recording with
1. generation CT scanner

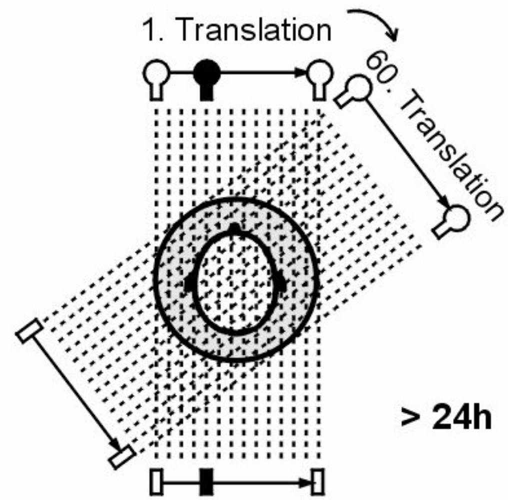

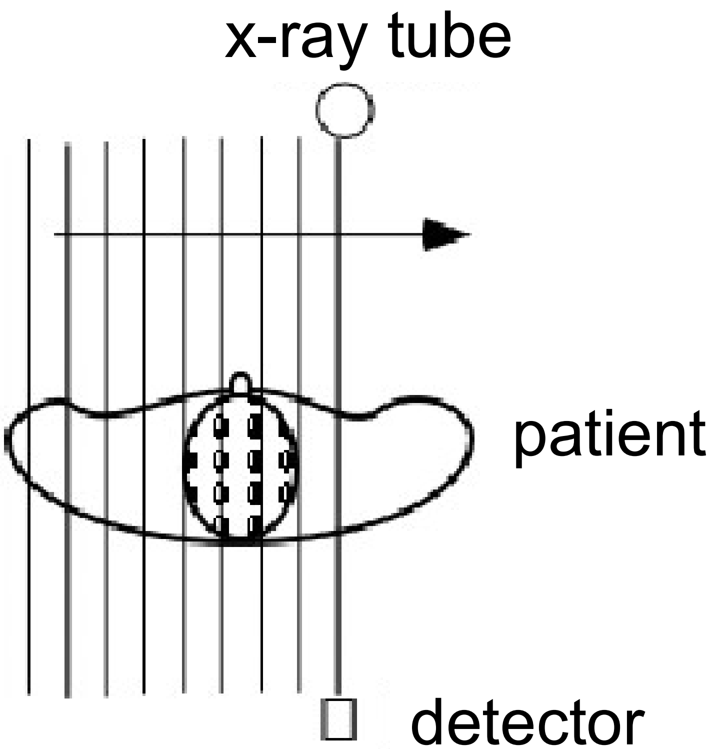

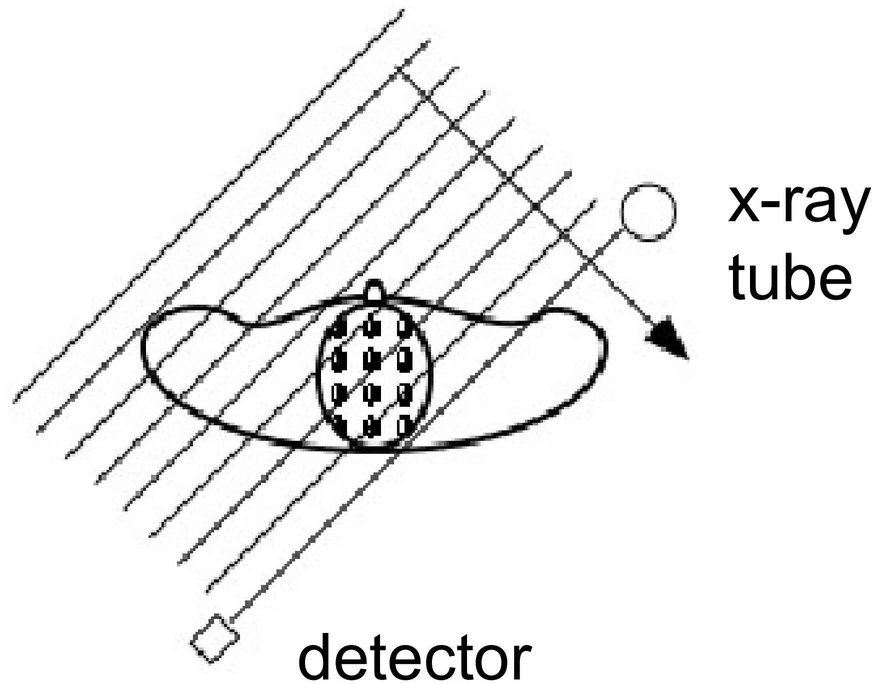

data acquisition

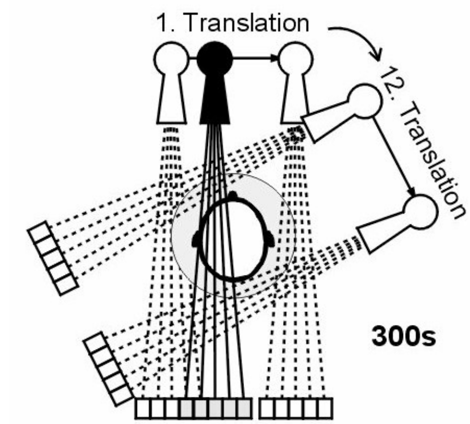

2. generation CT scanner (first commercial system)

Hounsfield 1972-1975

technique: *partial fan beam*
beam width: 10°
principle: translation-rotation
detectors: array (>30)
x-ray source: high performance tube
recording duration: 300 s

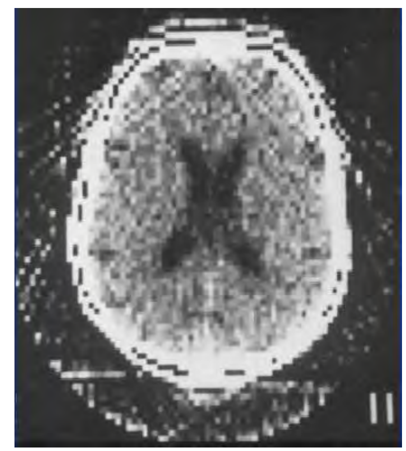

matrix size: 80 x 80 = 6400 pixel

estimated from 180 projections (1°-steps) with 160 data each= 28.800 data/scan

data acquisition

**scheme of recording with
2. generation CT scanner**

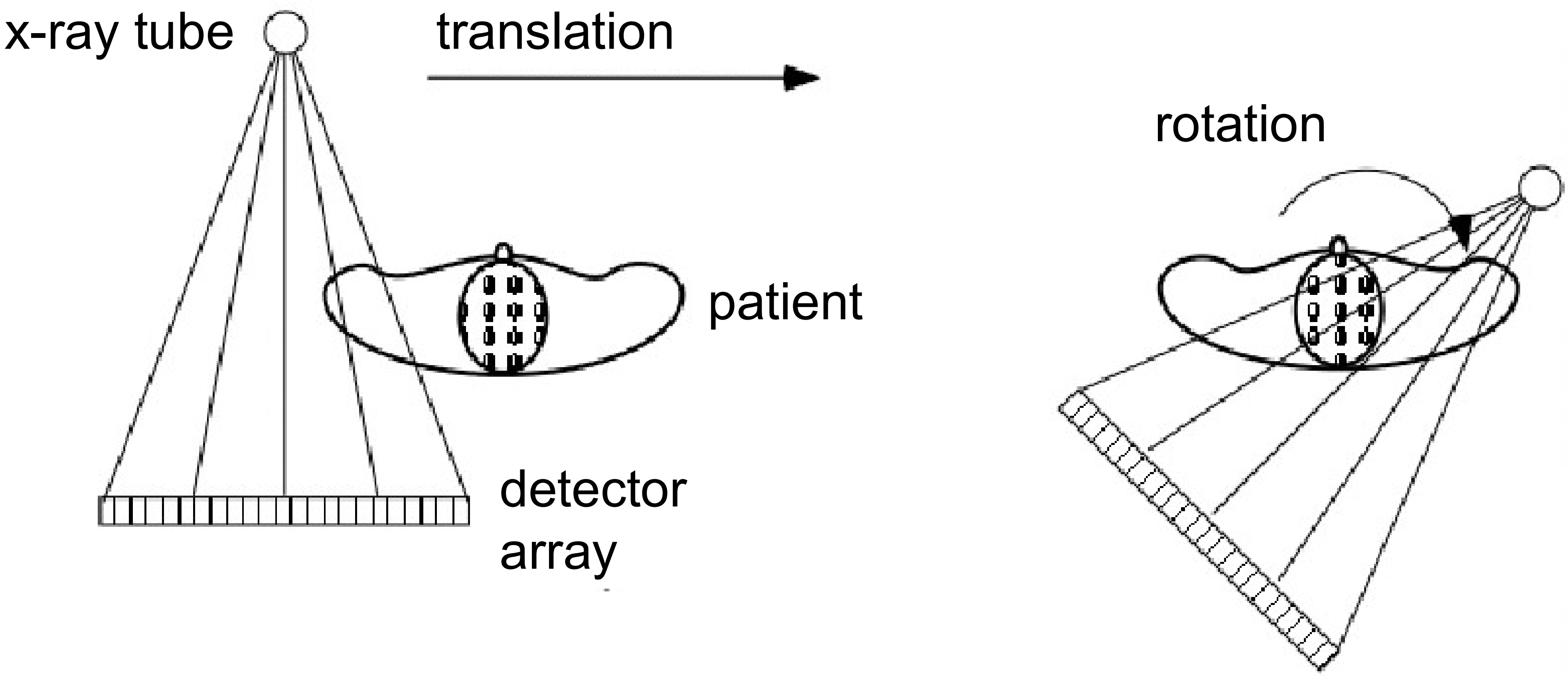

x-ray computed tomography (CT)

data acquisition in Radon space (2. generation CT scanner)

$s = 0,\ \Theta = 0$

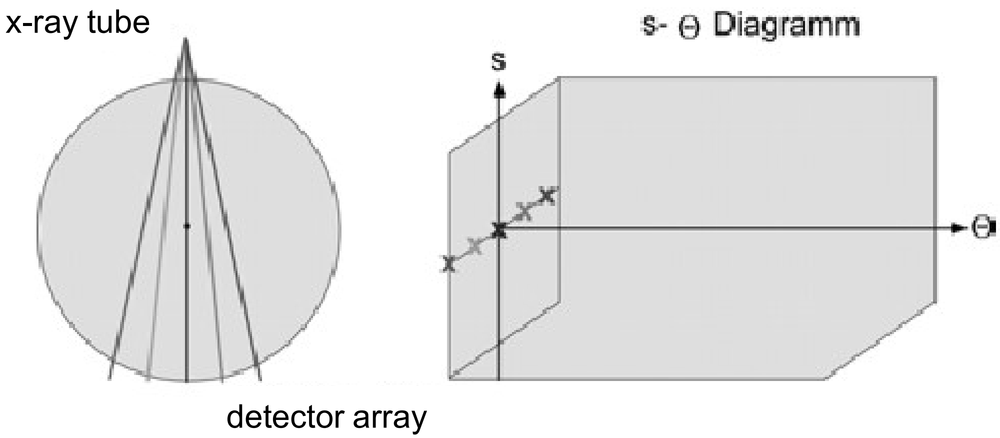

$s \neq 0,\ \Theta = 0$

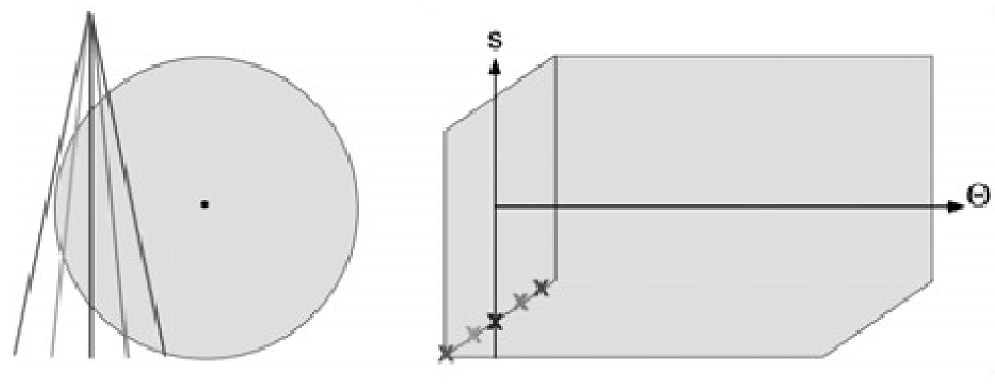

$s \neq 0,\ \Theta \neq 0$

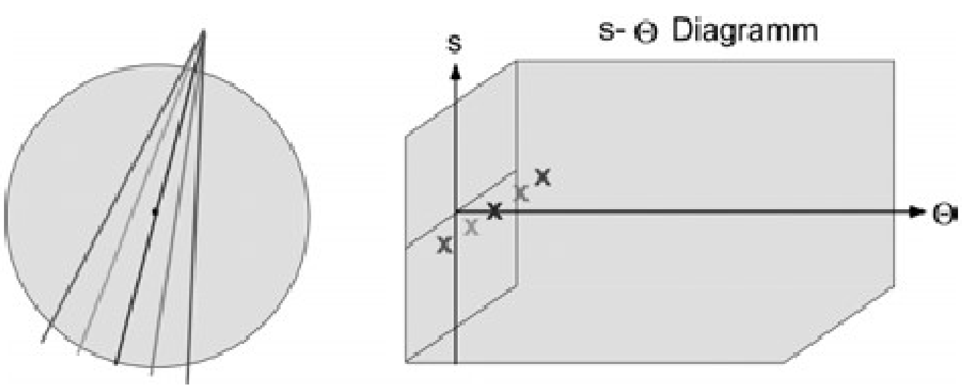

data acquisition

3. generation CT scanner

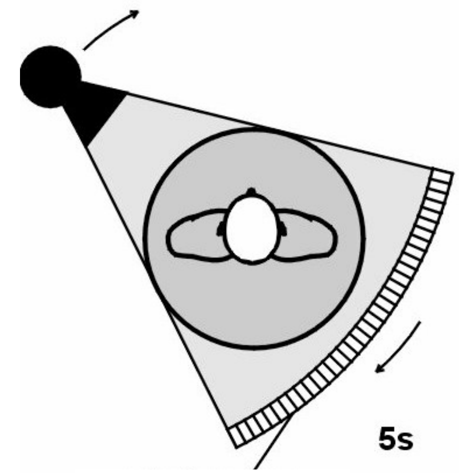

1976
- improved utilization of available dose
- enables whole-body scanning

technique:	*full fan beam*
	beam width: 40° - 60°
principle:	continuous rotation
	(tube and detector array rotate around patient)
detectors:	array (500-800)
x-ray source:	high-performance tube (1-2 ms pulses every 13 ms)
recording duration:	5 s

x-ray computed tomography (CT)

data acquisition

scheme of recording with 3. generation CT scanner

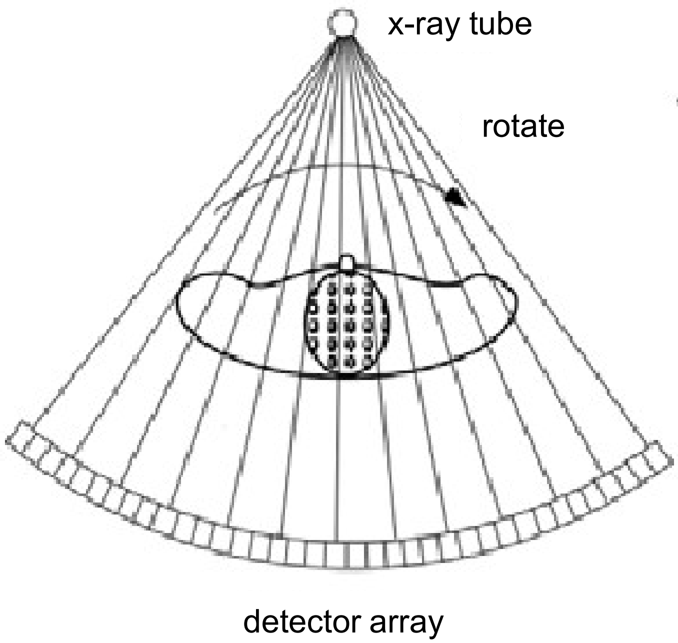

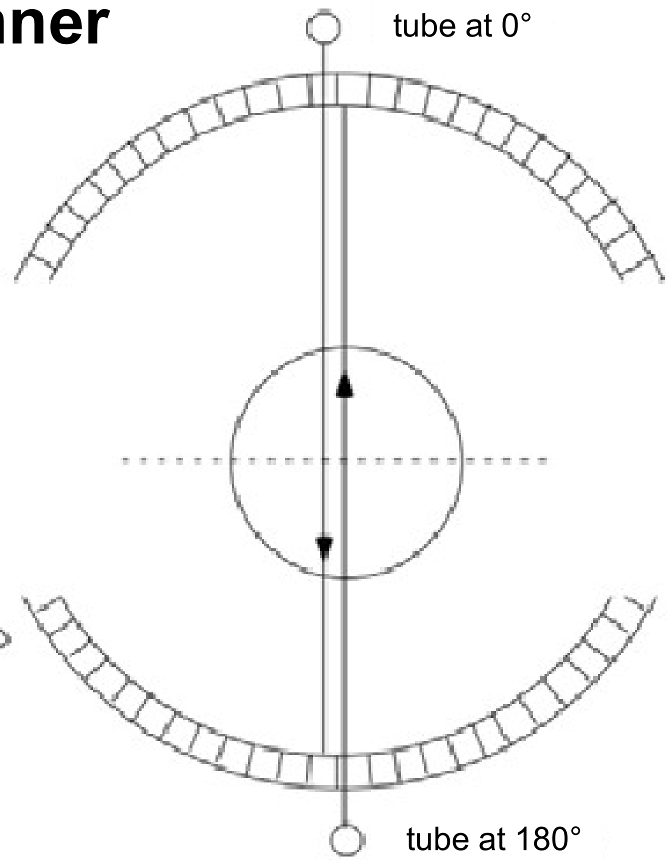

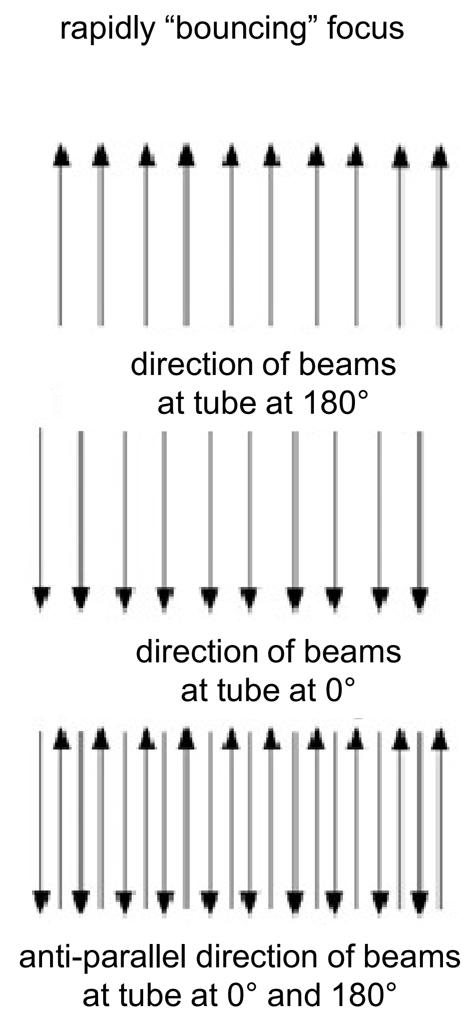

x-ray computed tomography (CT)

data acquisition in Radon space (3. generation CT scanner)

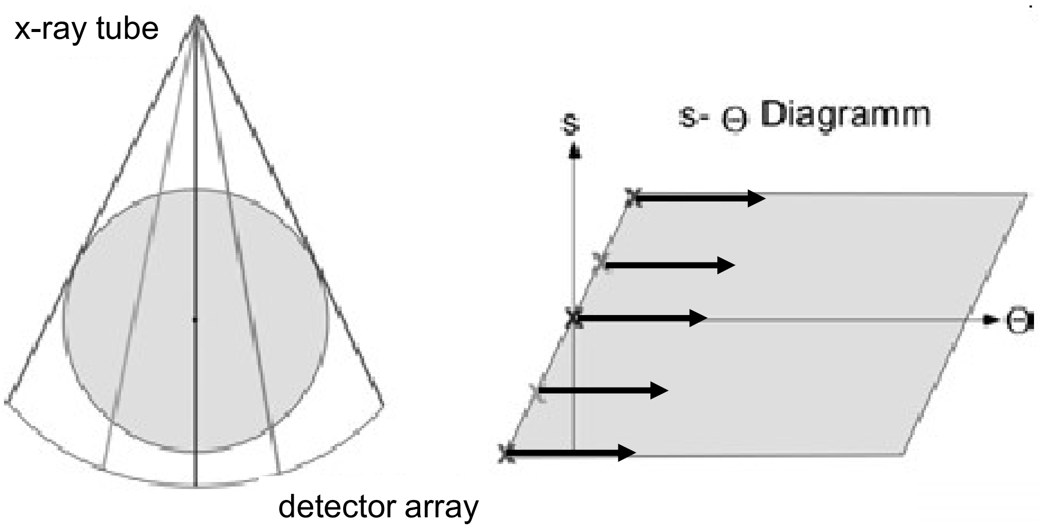

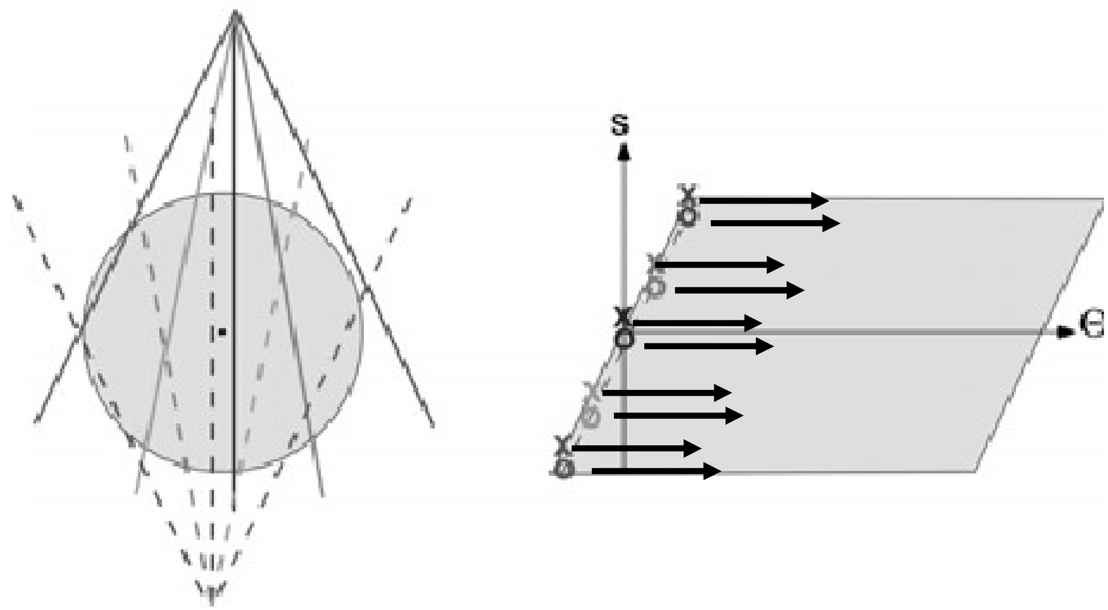

rapidly “bouncing” focus:
- finer sampling of Radon space
- higher resolution

data acquisition

4. generation CT scanner

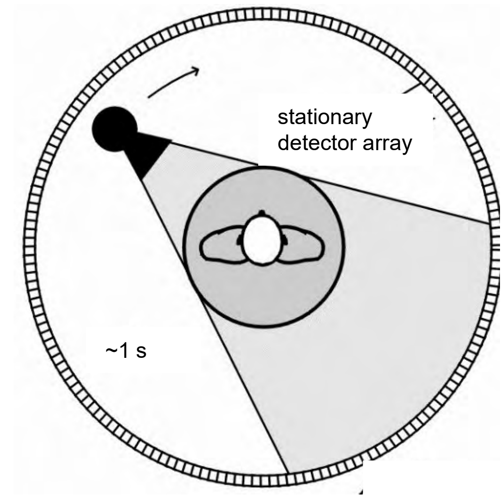

1978
- comparable to 3. generation scanner
- no commercialization (logistics, costs)

technique:	*full fan beam*
	beam width: 40° - 60°
principle:	tube rotates continuously around patient
detectors:	stationary array (~5000)
x-ray source:	continuously emitting high-performance tube
recording duration:	~ 1 s

data acquisition

scheme of recording with 4. generation CT scanner

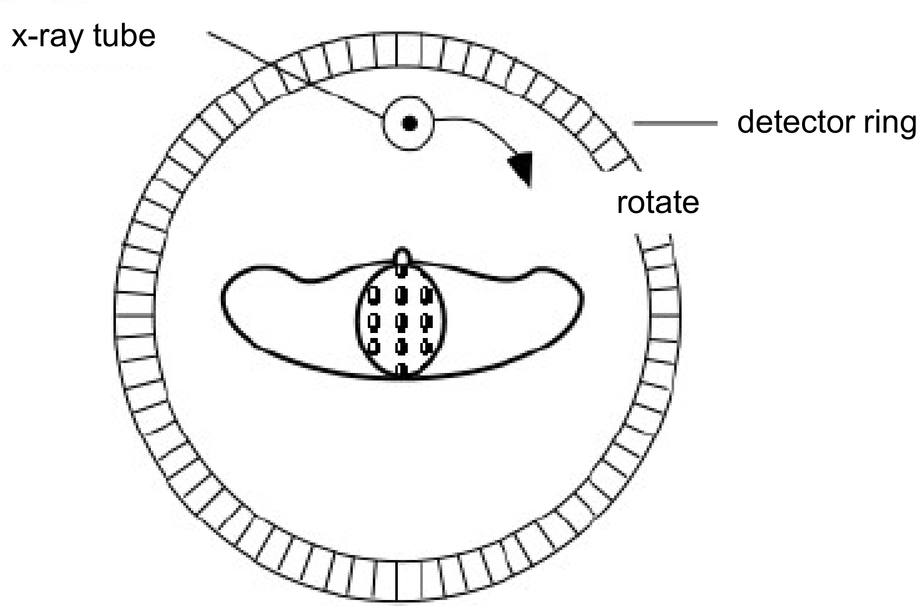

"inside" detector ring

"outside" detector ring

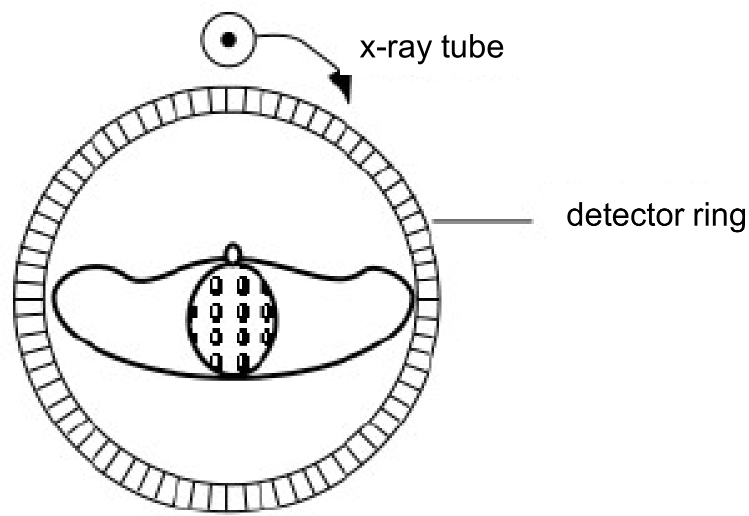

detector ring needs to be tilted wrt rotation-axis of x-ray tube

data acquisition in Radon space (4. generation CT scanner)

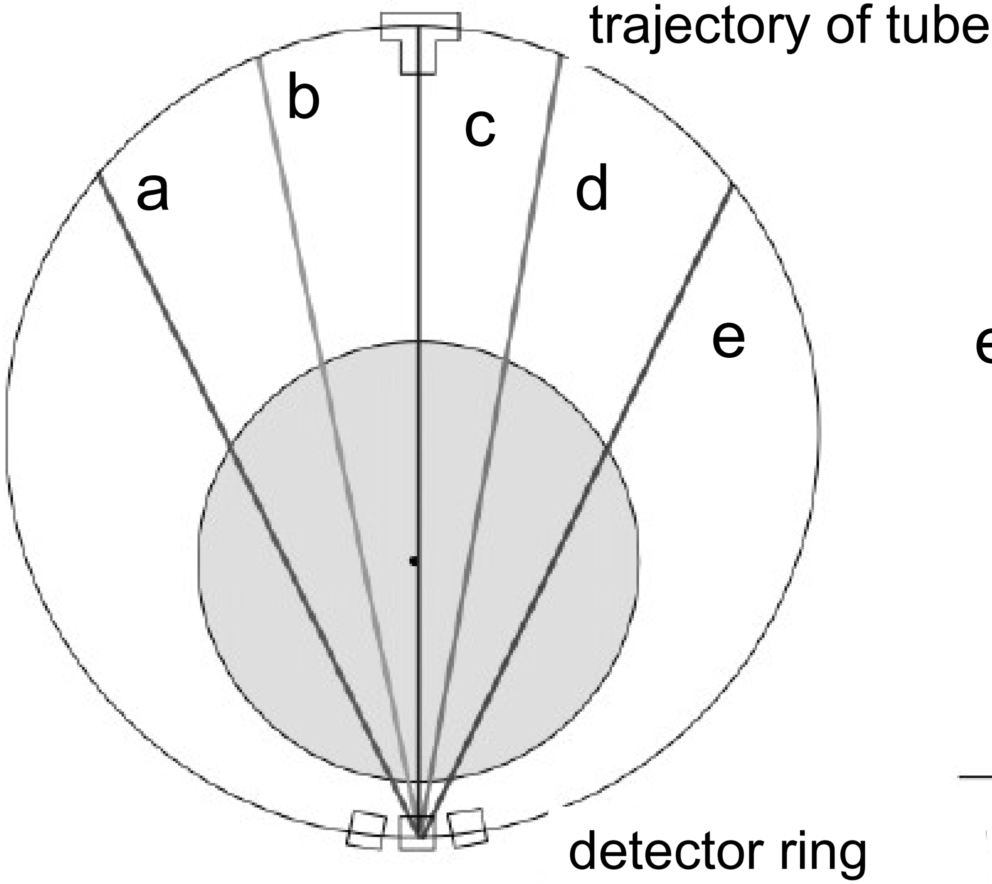

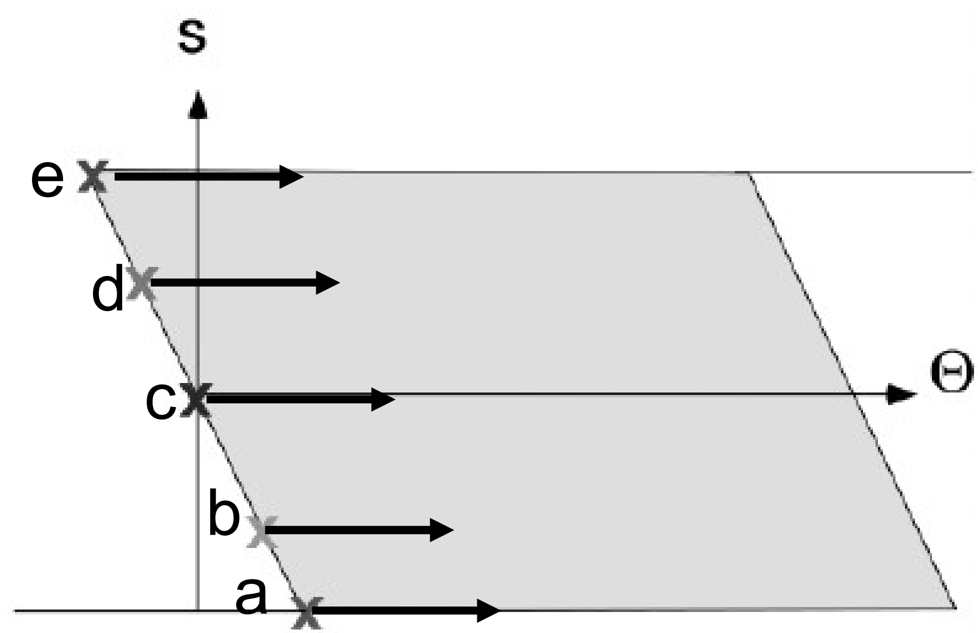

data acquisition with 1. to 4. generation CT scanner

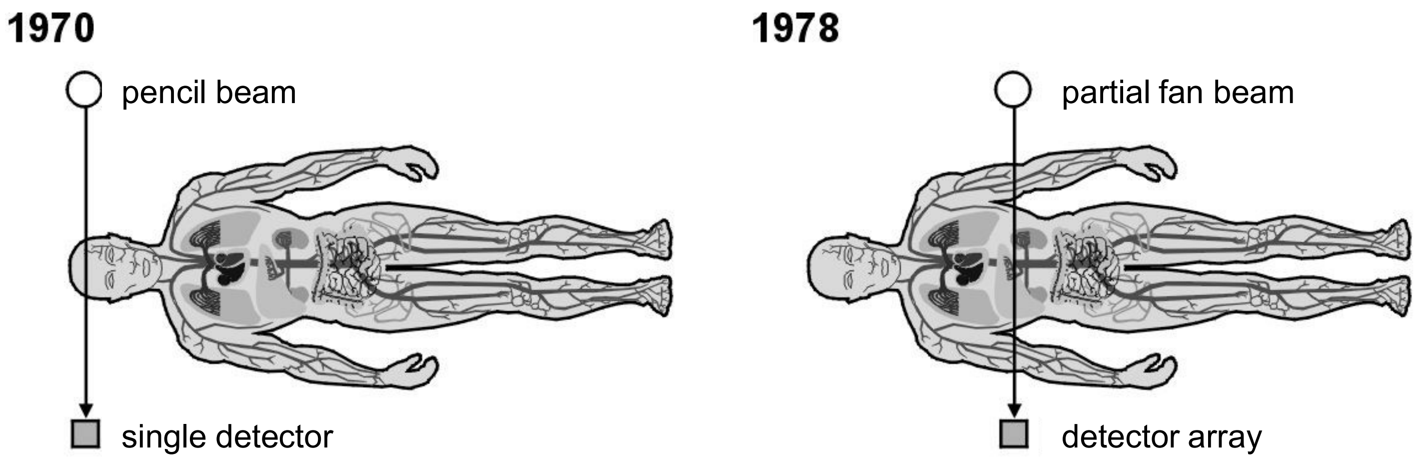

- 1. and 2. generation: head recording only
- image reconstruction of a single slice only (2-5 mm thickness)
- not suitable for large regions or whole-body imaging:
    - record, shift patient (e.g. by 2 mm), record, ...
    - duration, high radiation exposure, artifacts

data acquisition with spiraling CT (W. Kalender, 1989)

idea: slow but continuous translation of patient inside scanner while tube rotates around the center

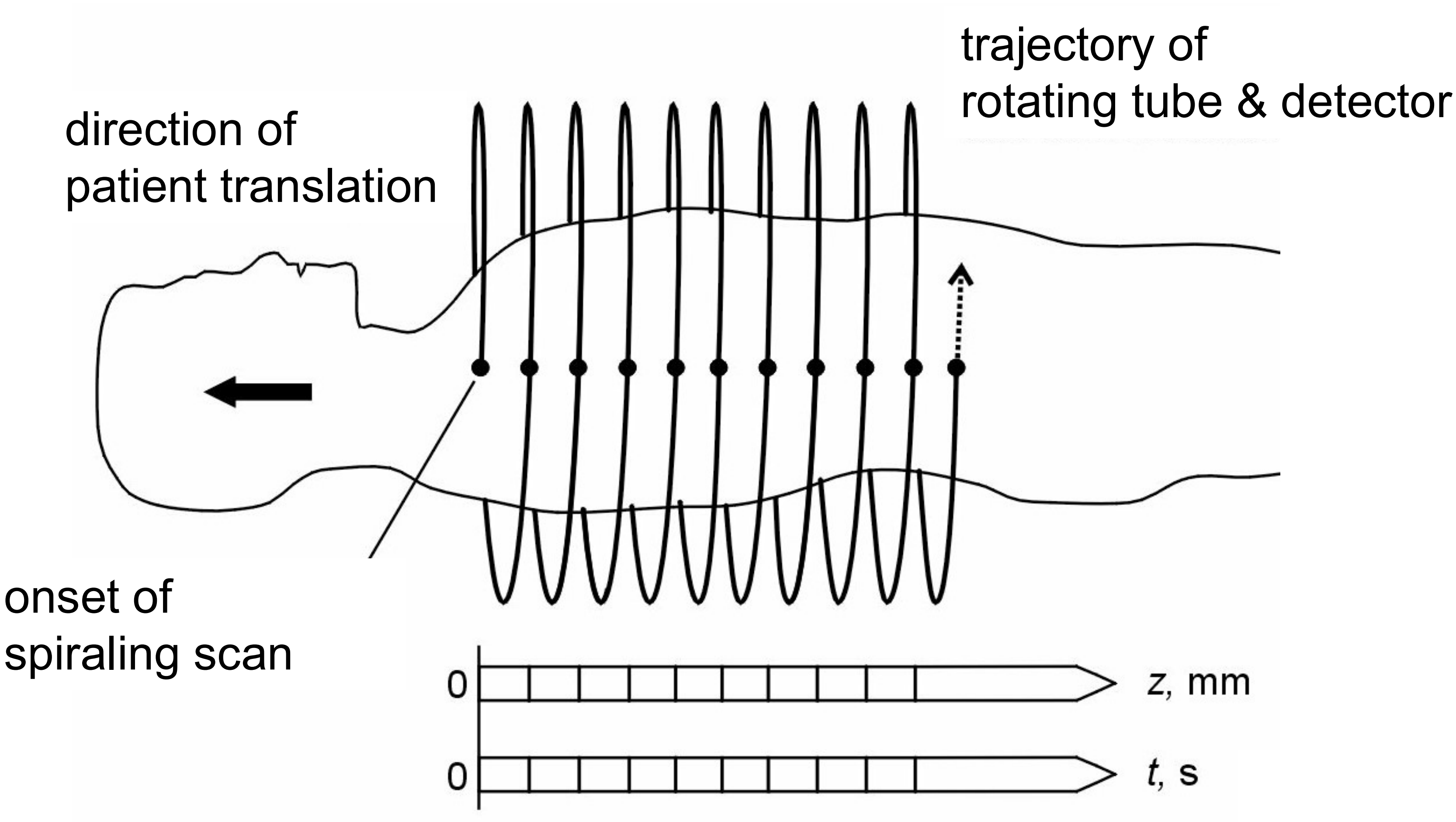

data acquisition with spiraling CT

problem:
- which data to use for image reconstruction ?
- projections under different angles Θ do not fit each other !

ansatz:
- for each Θ, there are several data sets shifted rel. to each other by d (d = patient advance)

- estimate "missing" projections at each intermediate step $z_1<z<z_1+d$ by interpolation (not exact but sufficiently accurate)

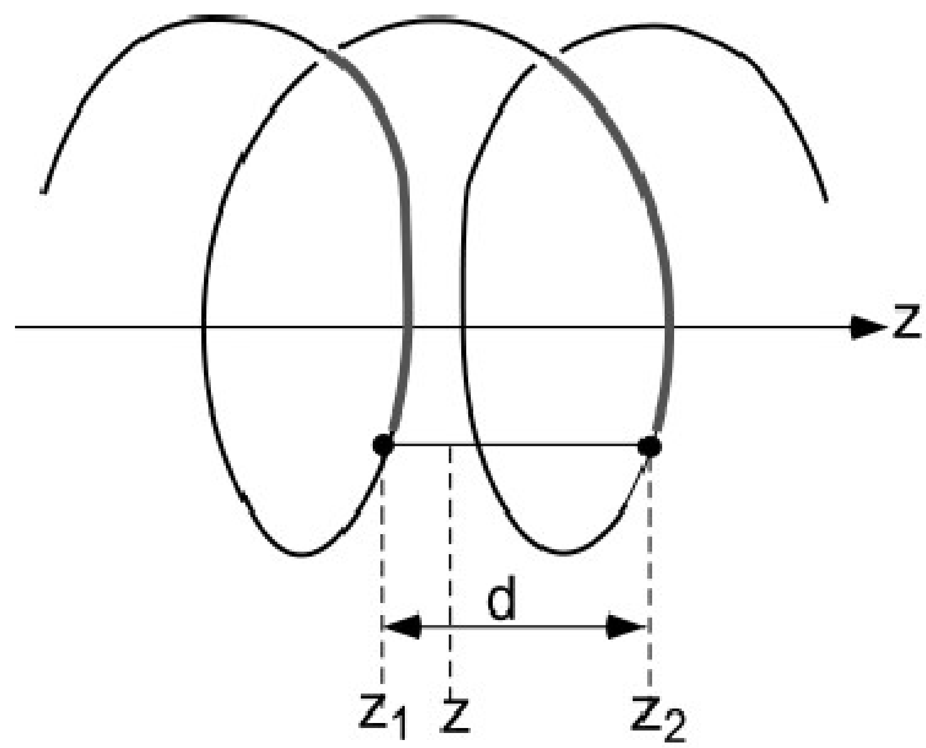

x-ray computed tomography (CT)

data acquisition with spiraling CT

continuously rotating tube:

- for d=0: projections with 180°<Θ<360° are redundant
- for $d \neq 0$: projections with 180°<Θ<360° provide data from intermediate slices
- these can be used for interpolation

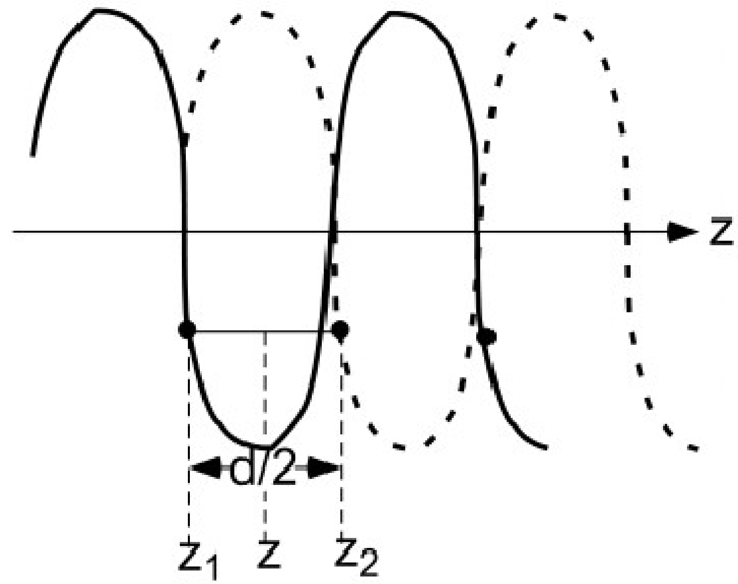

⇒ effectively, interpolation with intermediate slices $0 < z < d/2$ only (corresponding to rotation around 180°)

⇒ **fast 3D-acquisition of body region**

x-ray computed tomography (CT)

data acquisition with spiraling CT

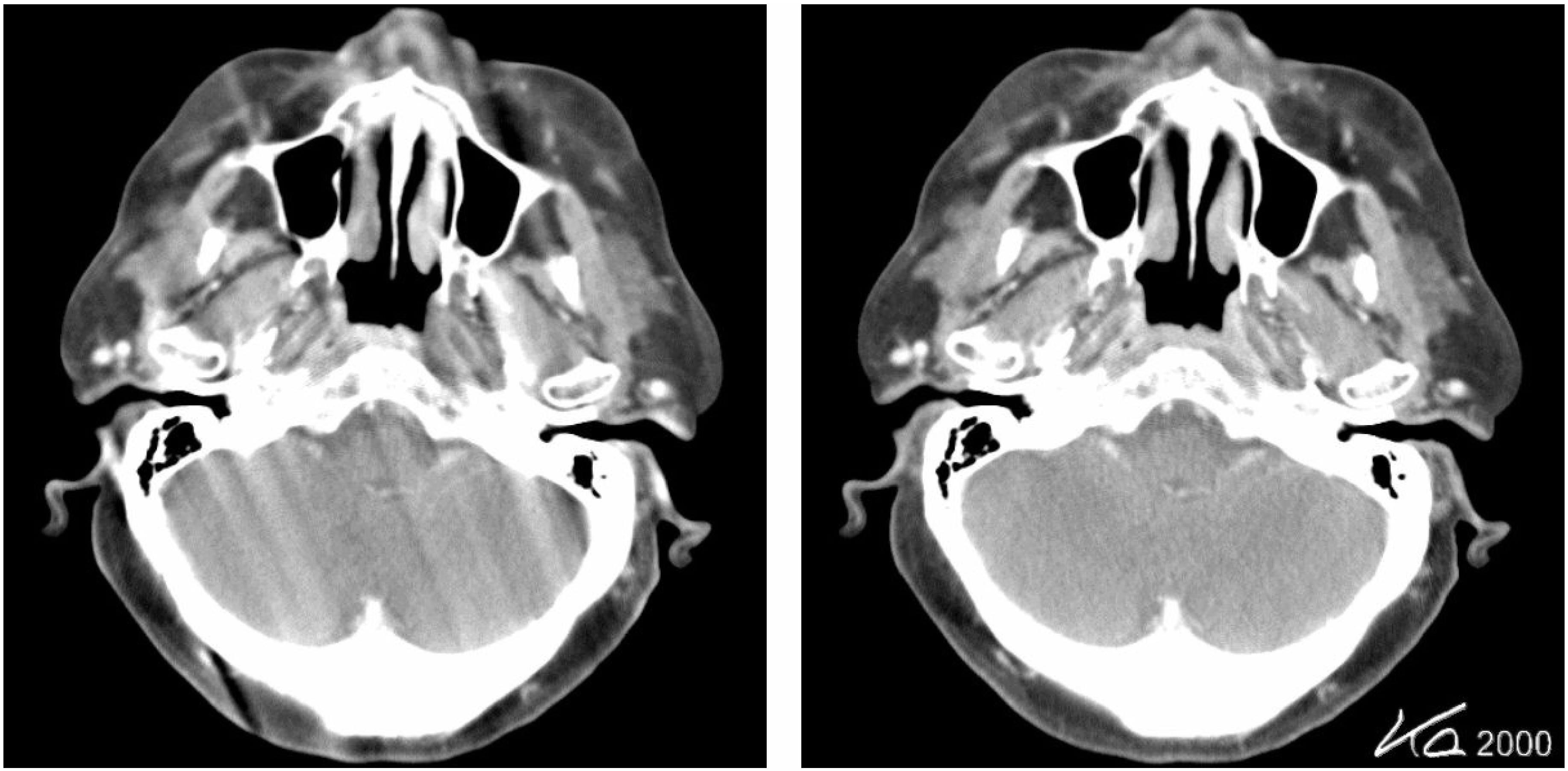

a) without interpolation

b) with interpolation

data acquisition with spiraling CT

	conventional CT	**spiraling CT**
acquisition	n Scans each over 360° at positions z_1 - z_n	1 Scan over $n \cdot 360°$ at positions z_1 - z_n
pre-processing	data correction	data correction
intermediate steps	--	z-interpolation
image reconstruction	convolution and back projection	convolution and back projection
result	n images from fixed positions z_1 - z_n	>n images at arbitrary positions z_1 - z_n

data acquisition with spiraling multi-slice CT

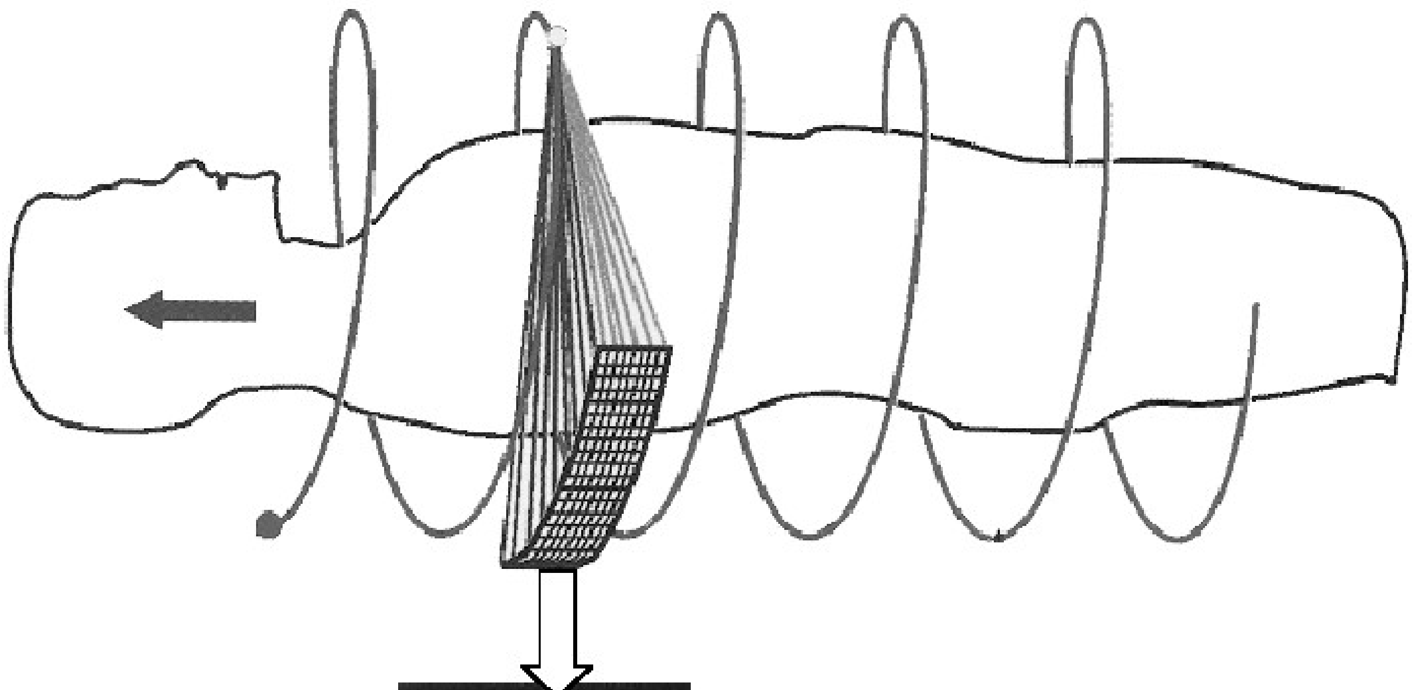

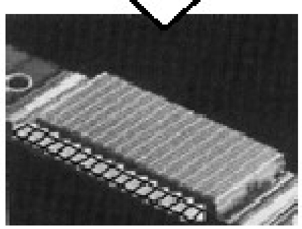

Willi A. Kalender Inst. f. Med. Phys. Universität Erlangen

data acquisition with spiraling multi-slice CT

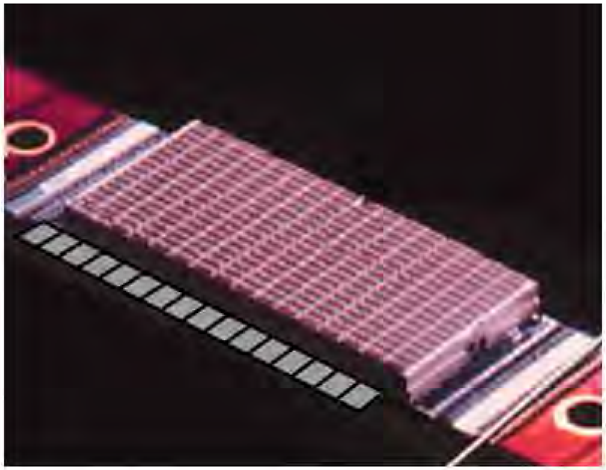

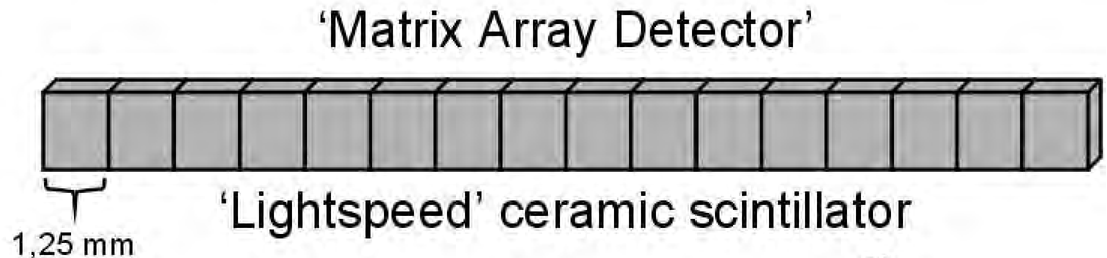

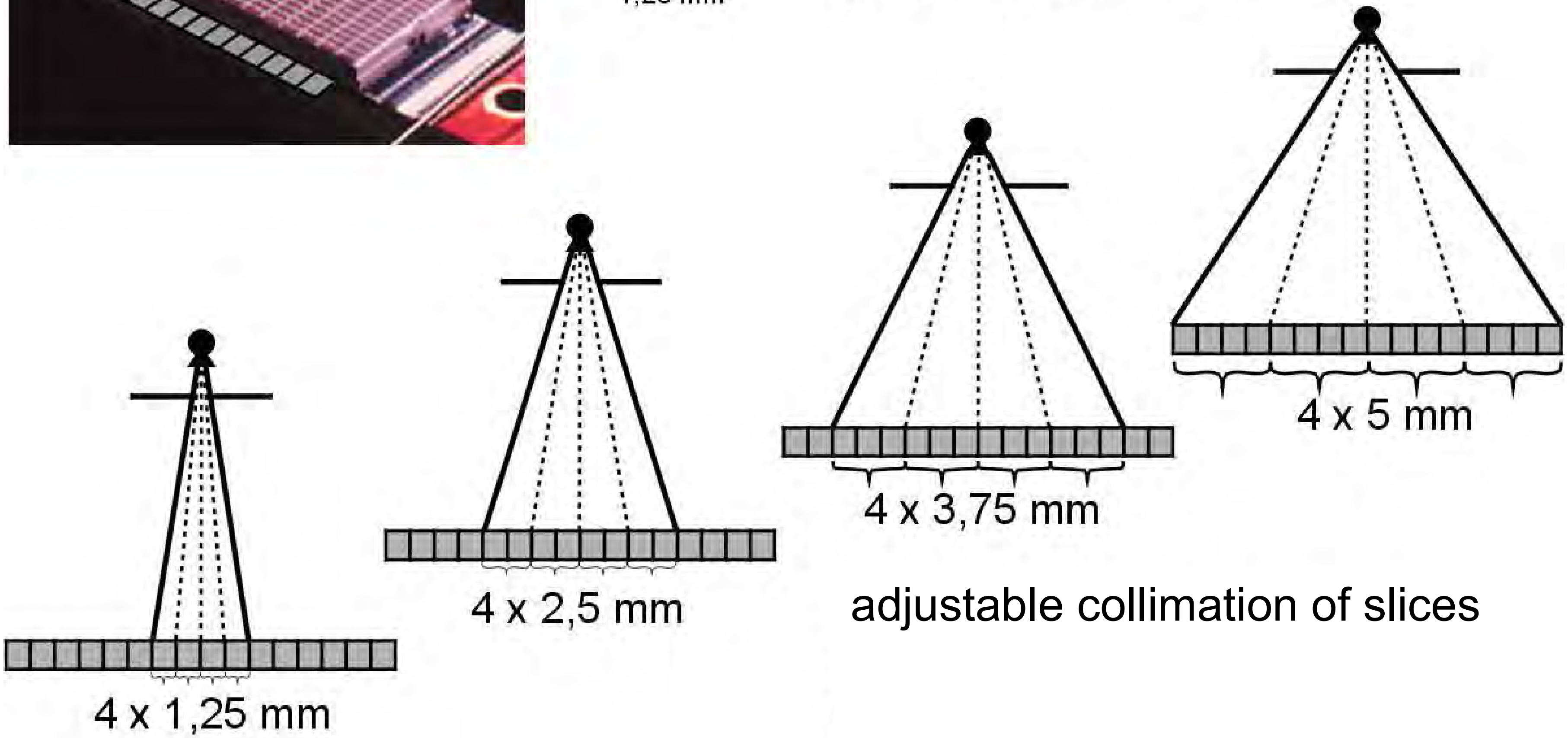

adjustable collimation of slices

data acquisition with spiraling multi-slice CT

‘Adaptive Array Detector’

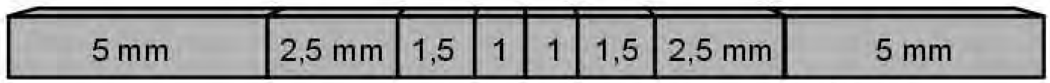

‘Ultrafast” ceramic scintillator (UFC)

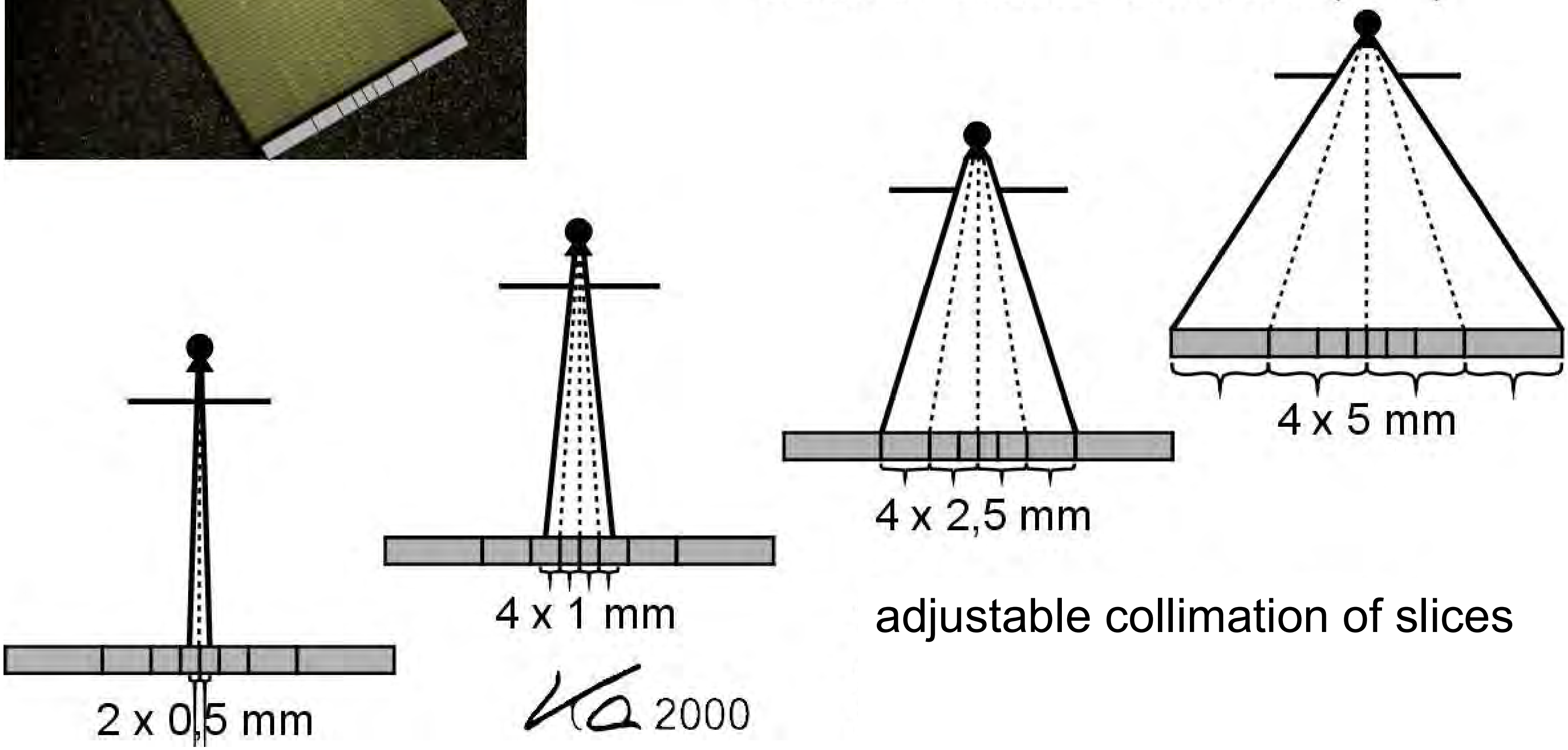

adjustable collimation of slices

data acquisition with spiraling multi-slice CT
impact of effective slice thickness

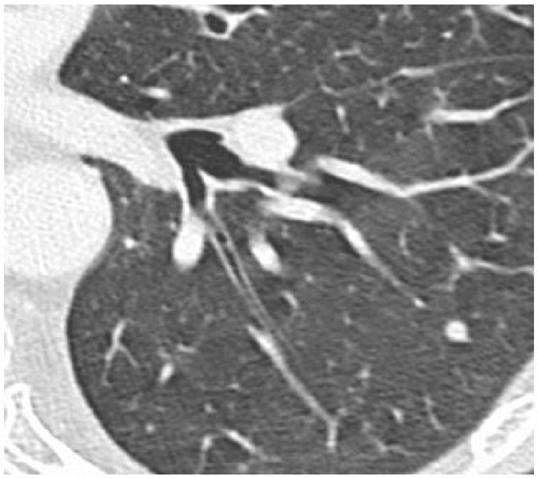
1,25 mm

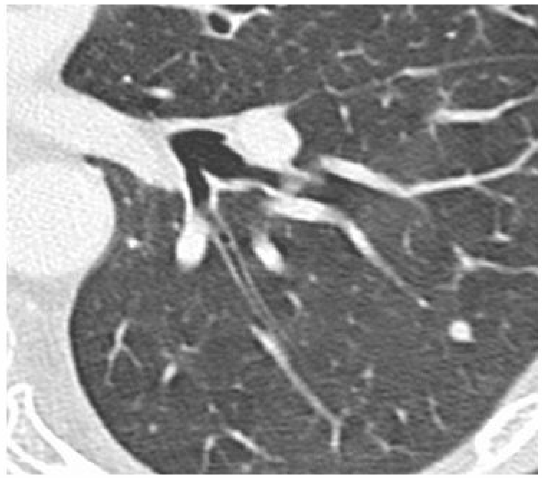
1,5 mm

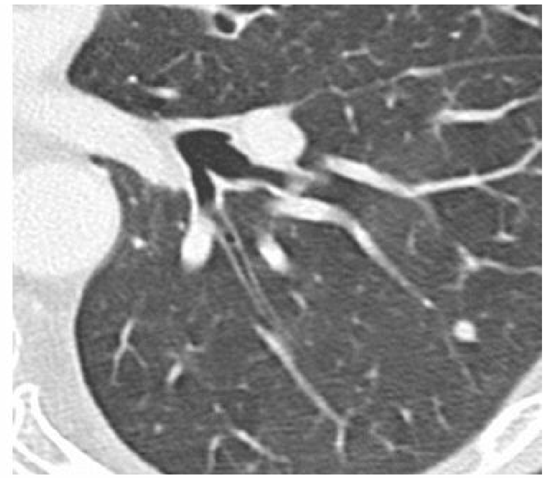
2,0 mm

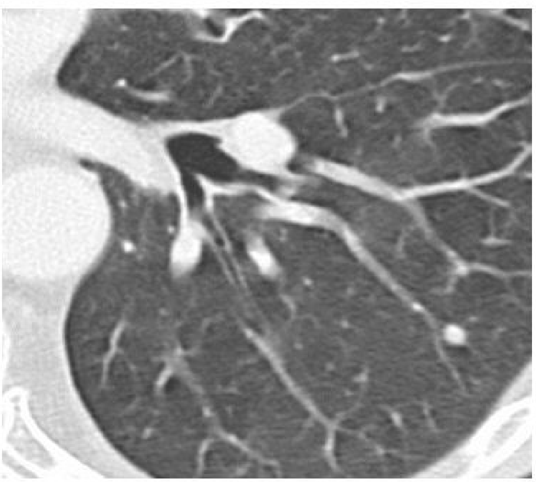
3,0 mm

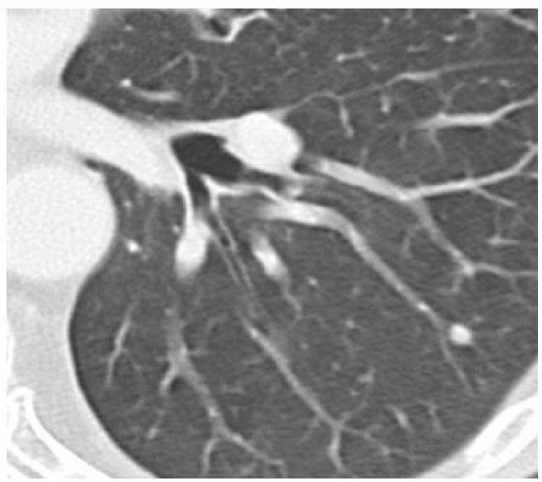
4,0 mm

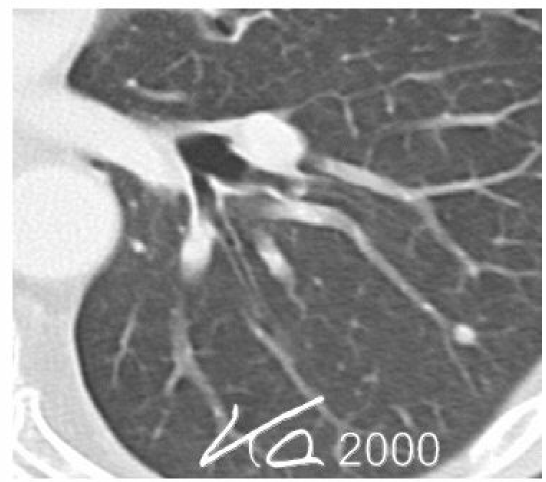

5,0 mm

alternative concepts for data acquisition: electron beam CT

aim: shorten scan time
idea: scanning without mechanical movements (tube, detector)

ansatz: generate electron beam, acceleration and focusing onto anode (ring-like target that encompasses the patient)

advantage: 50 -100 ms scanning time @ slice thickness 1.5 mm

disadvantage: expensive, bad image quality, limited use (e.g. arteries, bypass), rare

alternative concepts for data acquisition: electron beam CT

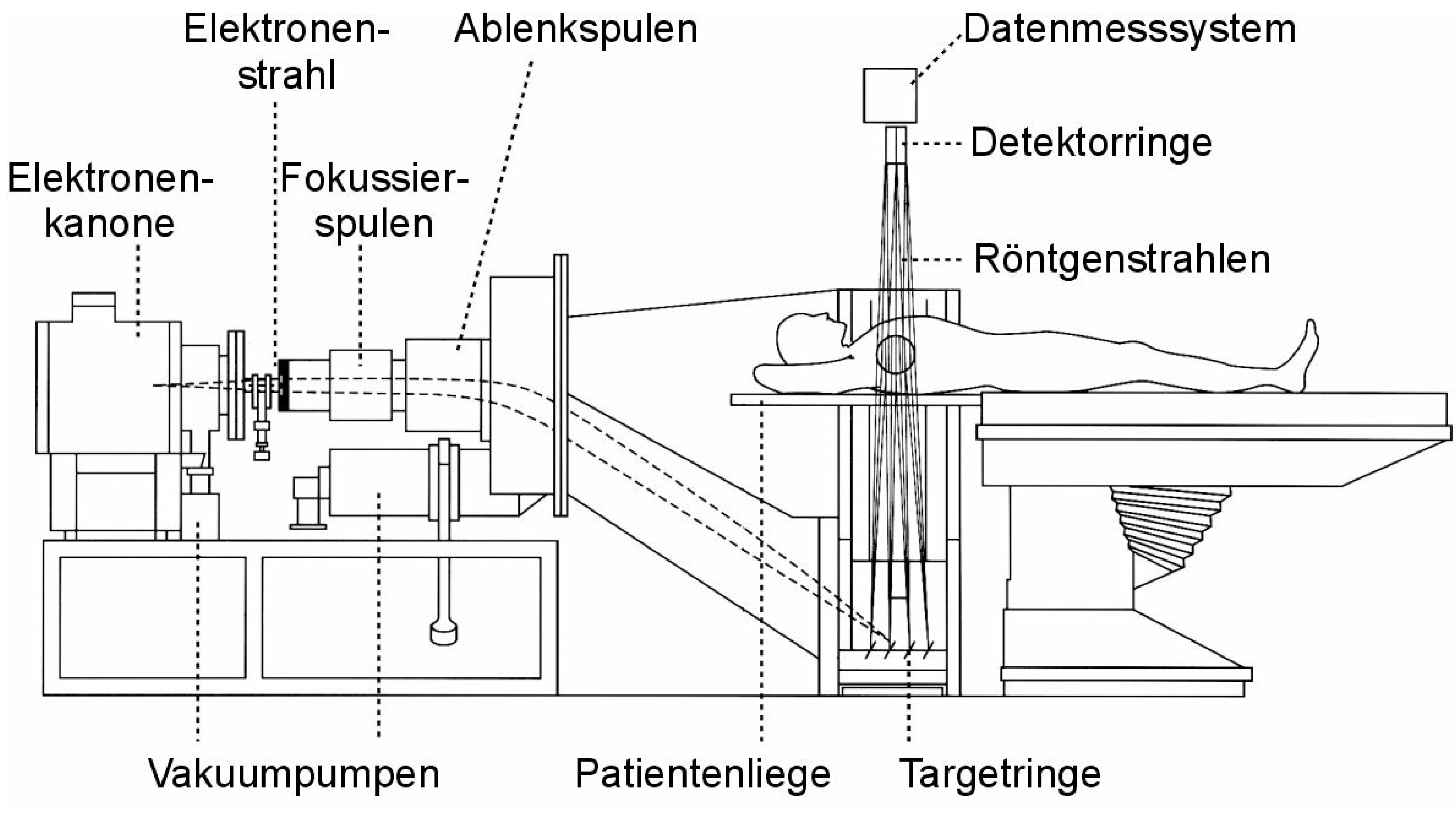

alternative concepts for data acquisition: electron beam CT

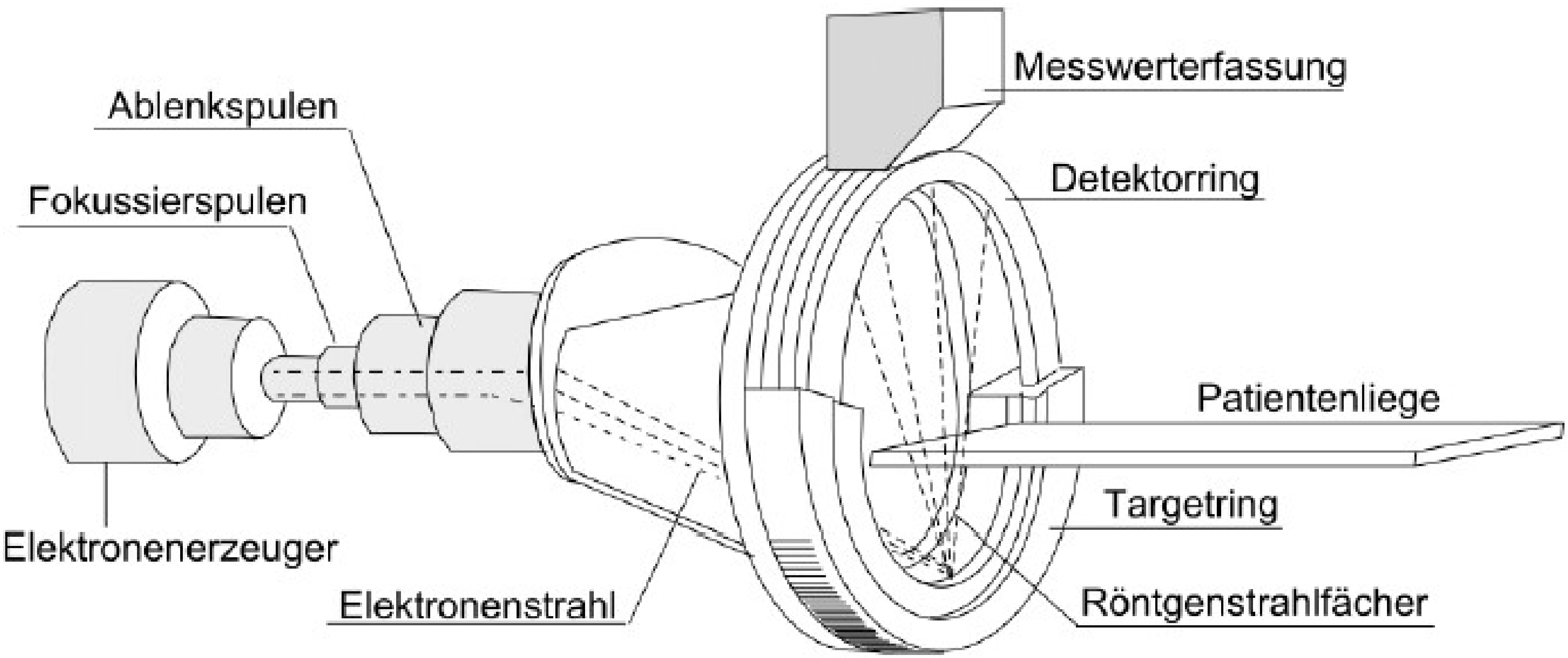

development of CT performance characteristics

	1972	1980	1990	2000
min. scan time	300 s	5-10 s	1-2 s	0,3-1 s
data/360° scan	57,6 kB	1 MB	2 MB	4x2 MB
data/spiraling scan	-	-	24-48 MB	200-500 MB
image matrix	80x80	256x256	512x512	512x512
power	2 kW	10 kW	40 kW	60 kW
slice thickness	13 mm	2-10 mm	1-10 mm	0,5 - 5 mm
spatial resolution	3 Lp/cm	8-12 Lp/cm	10-15 Lp/cm	12-25 Lp/cm
contrast resolution	5 mm(50 mGy)	3 mm (30 mGy)	3 mm (30 mGy)	3 mm (30 mGy)

apparent stagnation of contrast resolution due to early use of efficient detector systems

x-ray computed tomography (CT)

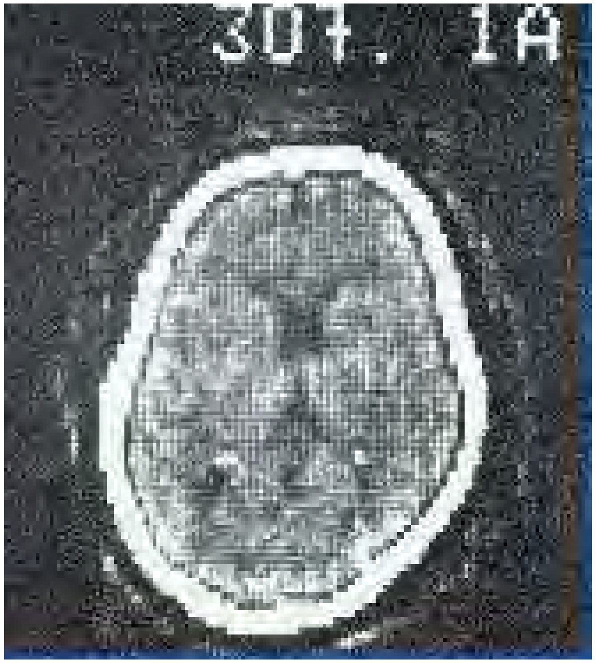

1972
rotation in 4 min
slice thickness: 8-13 mm
~10 cm in >30 min

2001
rotation in 0.5 s
slice thickness: 1 mm
1 m in 1 min

system components

x-ray computed tomography (CT)

system components
gantry

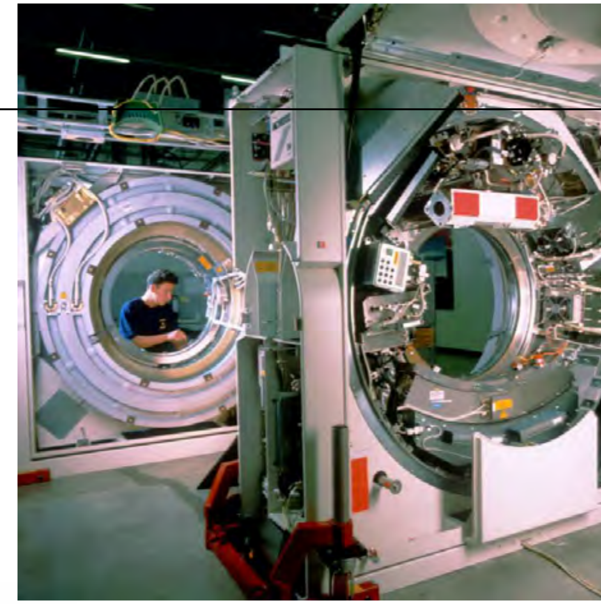

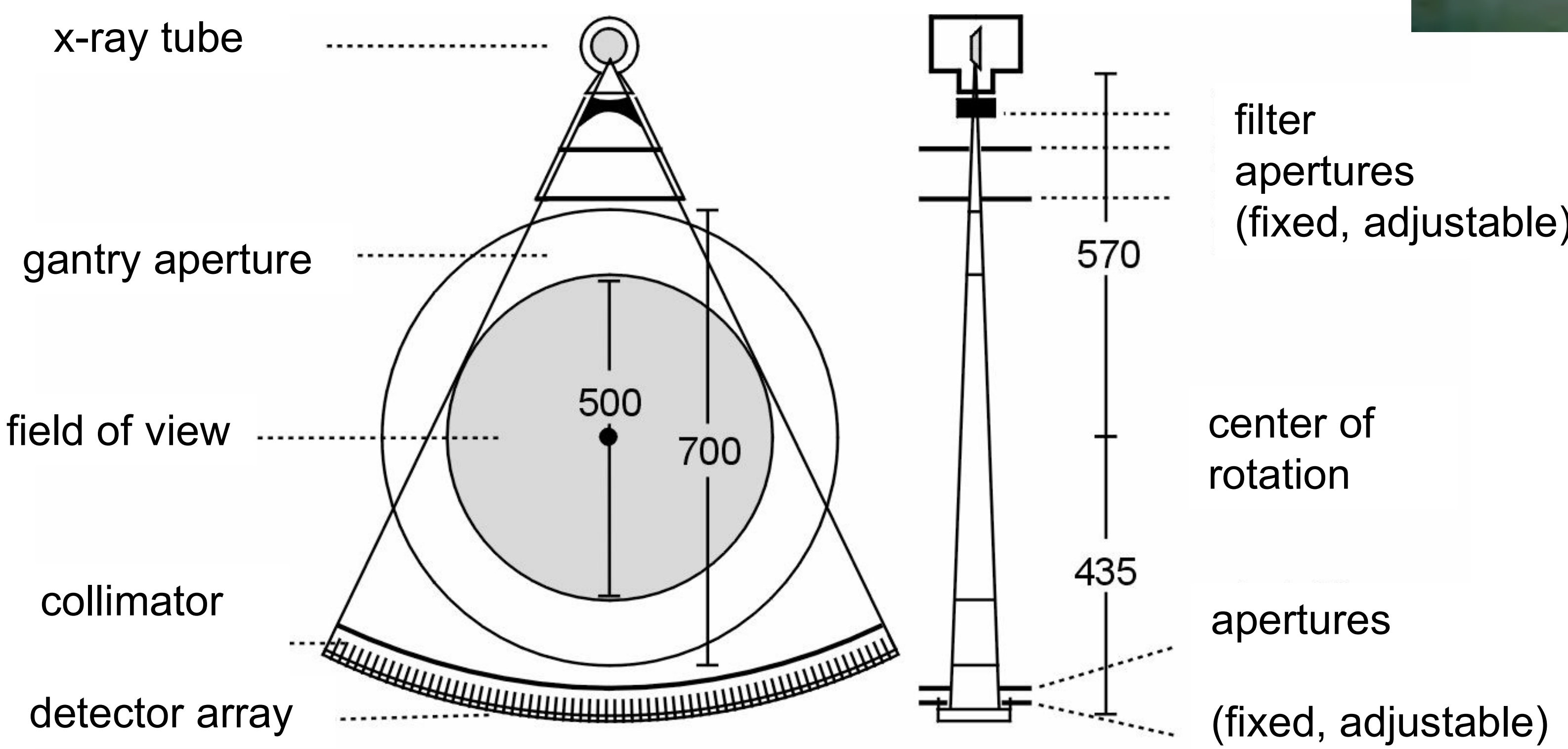

system components **gantry**

total weight: 400 - 1000 kg
weight x-ray tube: ~ 100 kg

rotations: 1-2 per s

estimation of centrifugal force:

distance tube – center of rotation:	~ 600 mm
rotation time:	0.5 s / turn

$\Rightarrow$ acceleration: 9.6 g = 9.6 N/kg

$\Rightarrow$ centrifugal force acting on mounting: ~ 10.000 N

system components **x-ray tube**

characteristics:

- typical power values: 20 - 60 kW @tube voltage 80 - 140 kV

- size of focus: 0.5 – 2.0 mm
  application dependent:
  e.g.: small focus: thin slices, high resolution

- heat storage capacity of anode
- scan duration

x-ray computed tomography (CT)

system components

x-ray tube

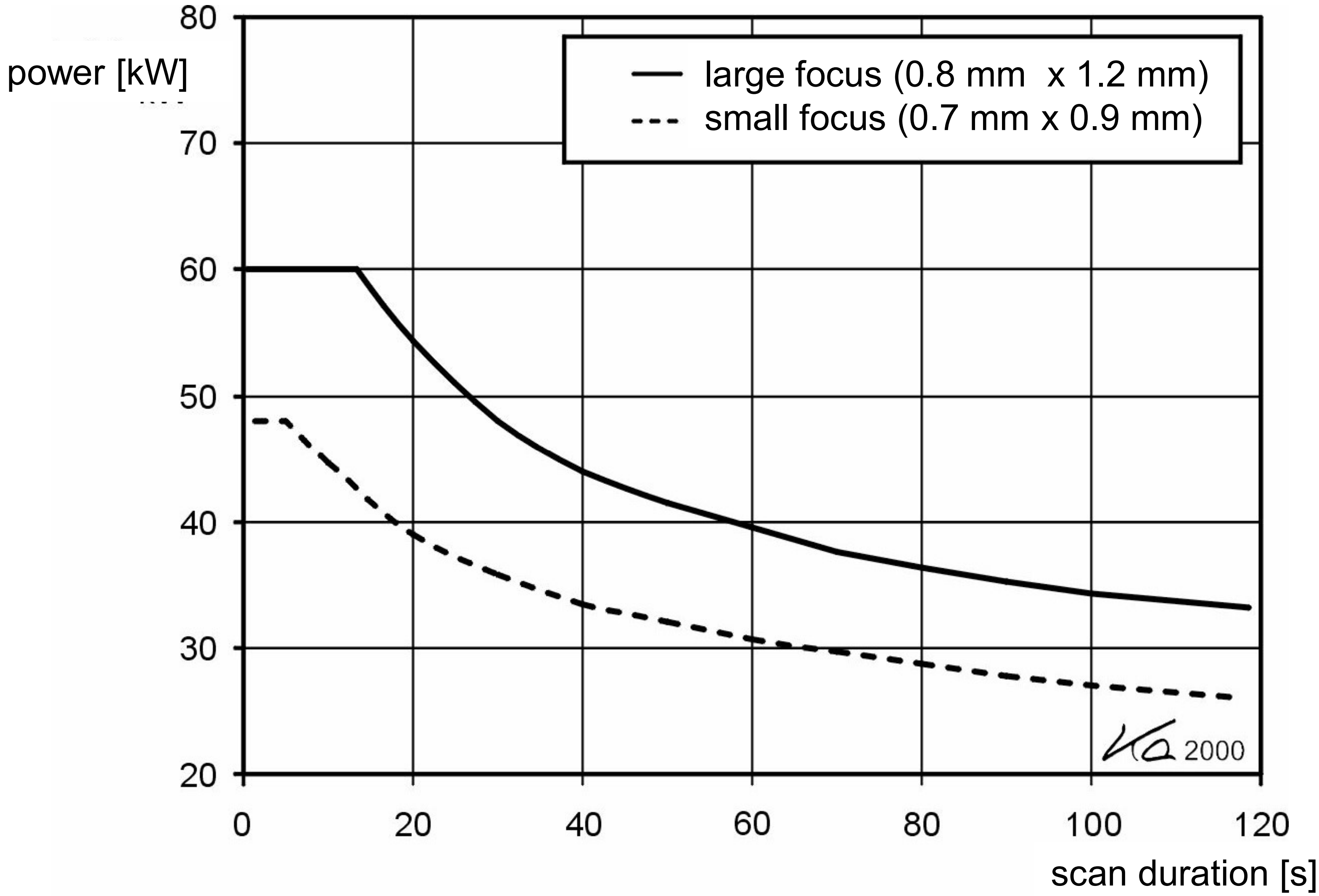

x-ray computed tomography (CT)

system components **filter, apertures, collimation**

- filtering x-ray energy spectrum
- definition of slice
- shielding of detector against scattering
- radiation protection

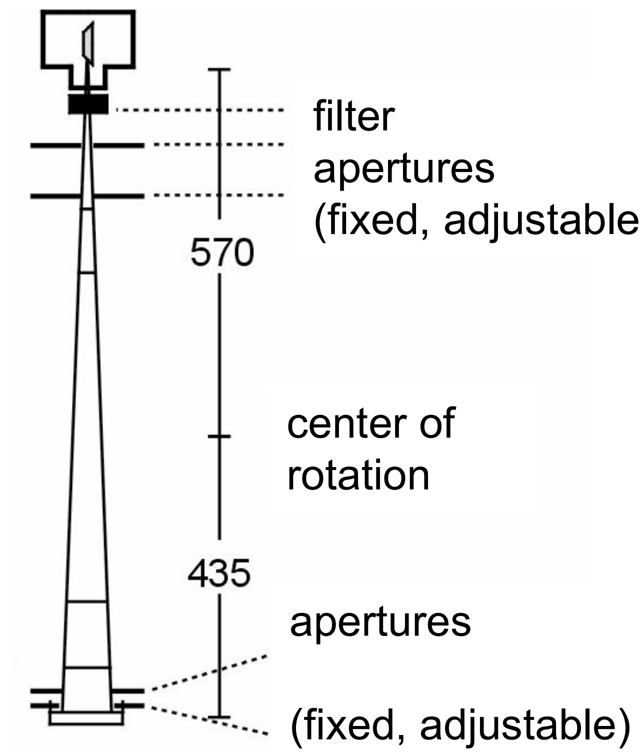

x-ray computed tomography (CT)

system components **detectors**

xenon high-pressure ionization chamber

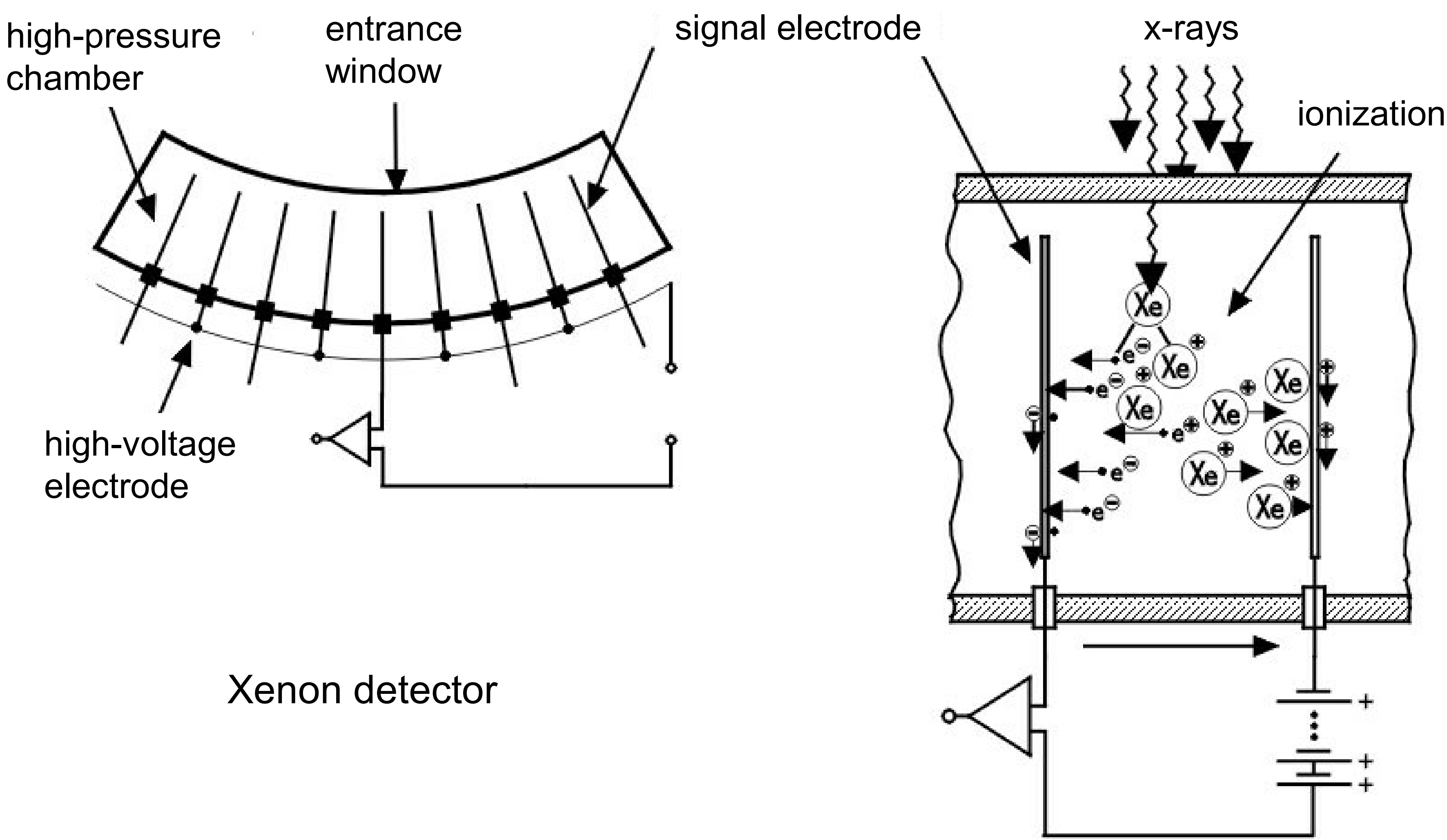

Xenon detector

system components — detectors

solid-state scintillation detector

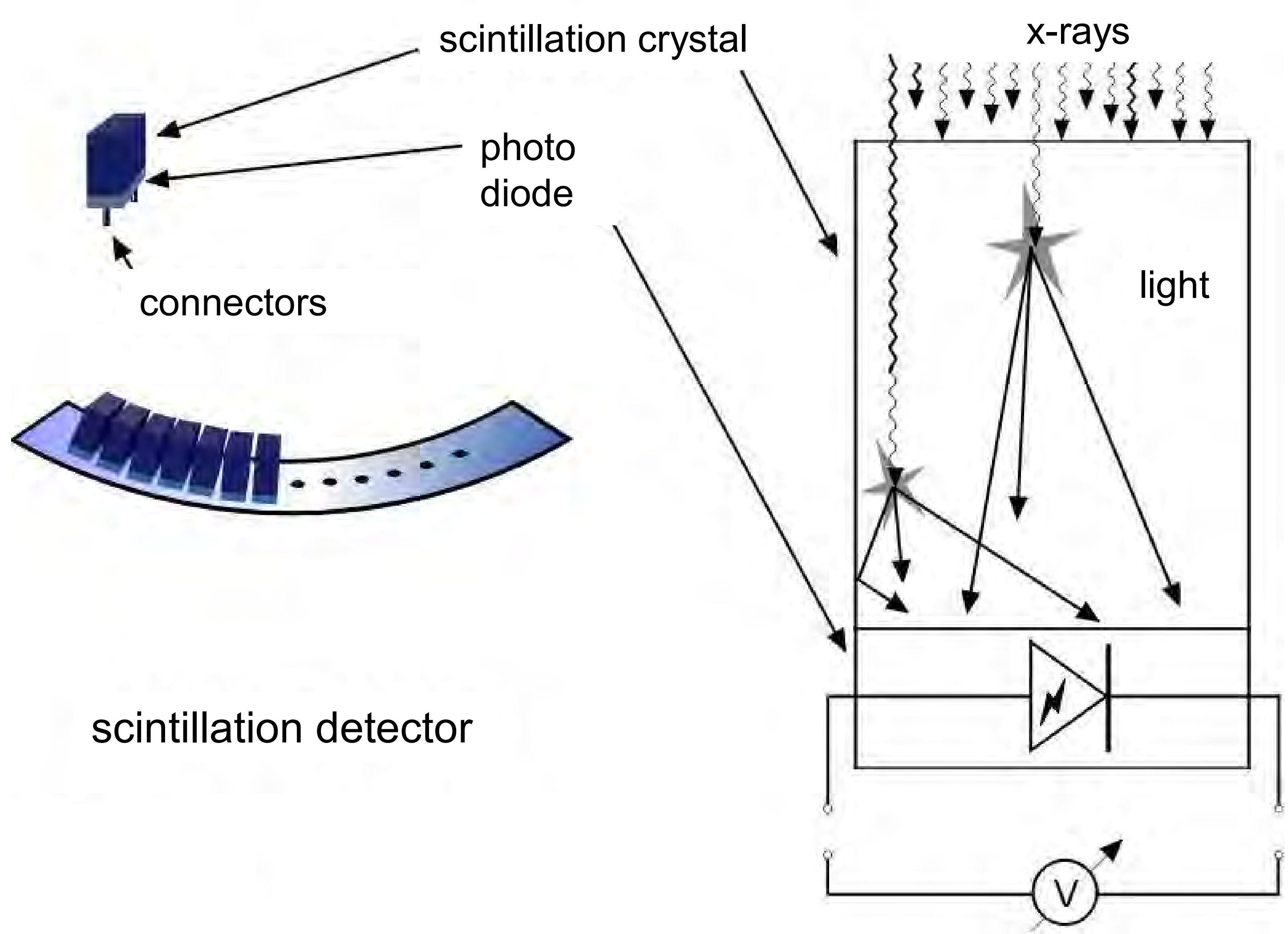

x-ray computed tomography (CT)

system components

detection sensitivity of detectors

	20 cm H_2O	20 cm H_2O + 2 cm bone	40 cm H_2O + 4 cm bone
detector			
		120 kV	
Xenon (10 bar, 3cm)	42.8%	39.2%	32.9%
Xenon (25 bar, 6cm)	73,8%	74.0%	72.7%
Gadolinium-oxysulfide (1.4 mm)	89.9%	88.1%	84.5%
		140 kV	
Xenon (10 bar, 3cm)	38.4%	34.3%	27,1%
Xenon (25 bar, 6cm)	71.0%	70.3%	67.0%
Gadolinium-oxysulfide (1.4 mm)	85.3%	83.0%	78.2%

x-ray computed tomography (CT)

system components

decay behavior of detectors

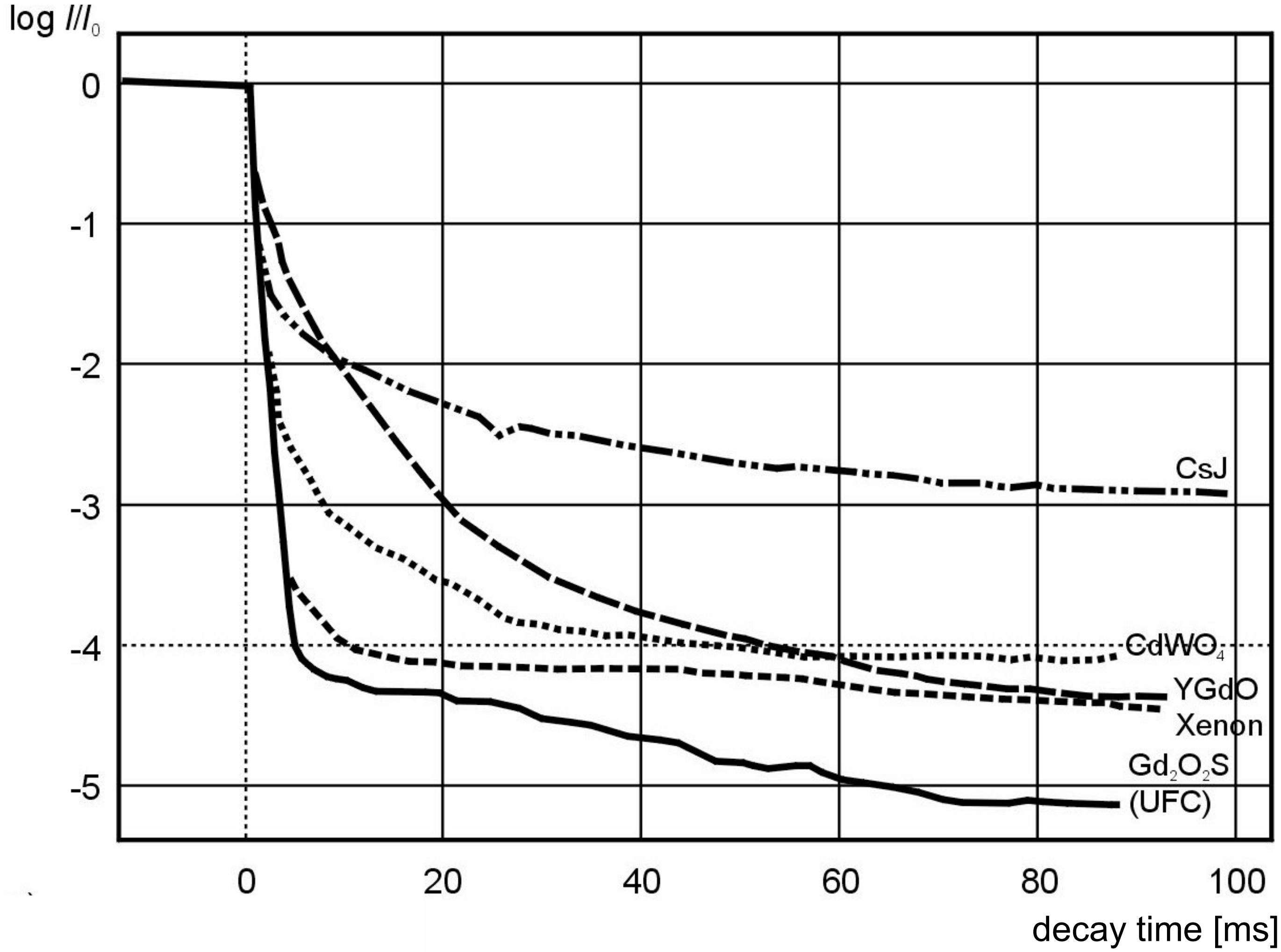

decay behavior can be approximated by two exponentials

UFC: ultra fast ceramic
decay time: 10^{-6} s

short x-ray pulse at T=0

x-ray computed tomography (CT)

system components **decay behavior of detectors**

τ = 0.0 ms τ = 1.0 ms τ = 2.5 ms

a too long decay time τ (afterglow) can deteriorate spatial resolution and image quality!

system components — detectors and sampling theorem

D = size of detector; Δs=center-to-center distance between detectors

signal at detector array

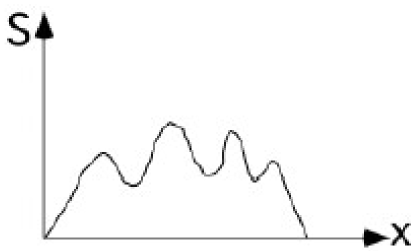

convolution with rectangular function

multiplication in Fourier domain with:

$$\frac{\sin(\pi \cdot D \cdot w)}{\pi \cdot D \cdot w}$$

sensitivity profile of detectors

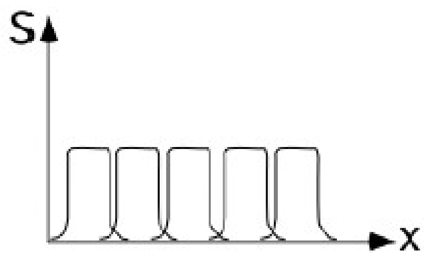

max. frequency: $\pi \cdot D \cdot w_{max} = \pi \Rightarrow w_{max} = \frac{1}{D}$

sampling theorem requires: $\Delta s \le \frac{1}{2w_{max}} = \frac{D}{2}$

aliasing !

system components **detectors and sampling theorem**

solution: “bouncing” focus (cf. 3. generation CT scanner)
$\rightarrow$ sampling with half the width of detector

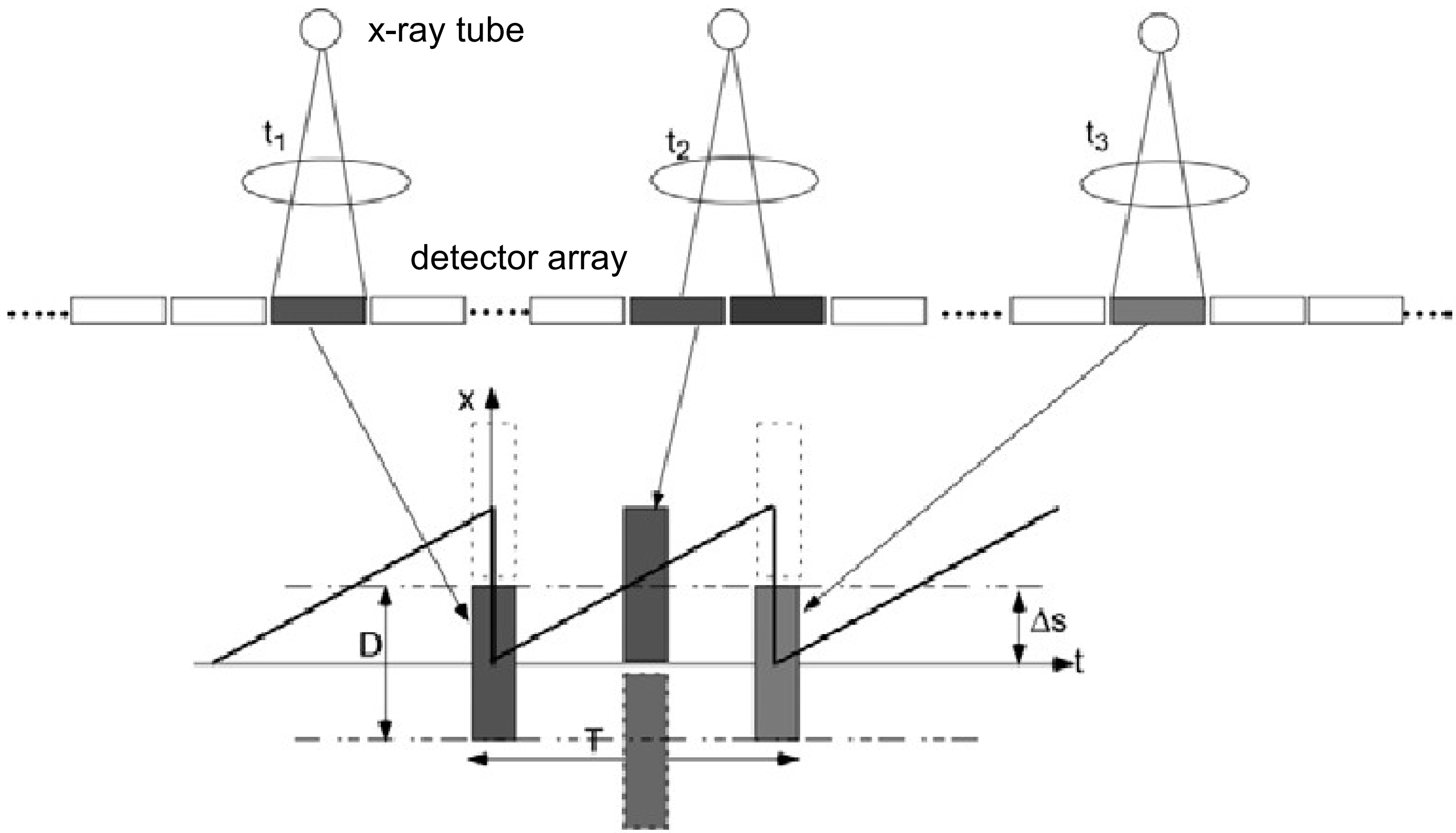

resolution of CT (I)

criterion: modulation transfer function (MTF)

derivation of MTF for CT (restriction to center of scanner):

uncertainties:
(1) deviation of x-ray beam from ideal needle-like beam
(2) reconstruction algorithm

$$\Rightarrow \qquad \boldsymbol{MTF_{CT} = MTF_{beam} \cdot MTF_{algorithm}}$$

resolution of CT (II)

trajectories of x-rays in scanner and definition of some geometric quantities

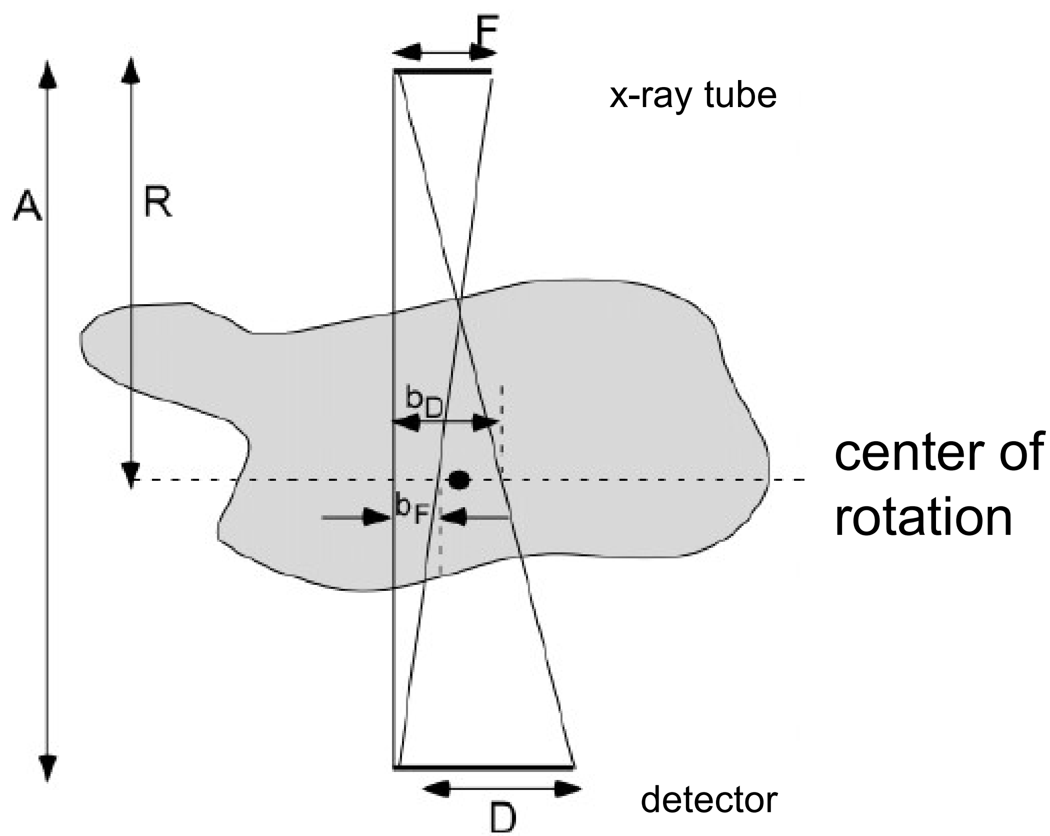

A = distance tube - detector

R = distance tube - center of rotation

F = size of focus in tube

D = size of detector

$b_F = F \cdot \frac{A-R}{A}$ effective size of focus in center

$b_D = D \cdot \frac{R}{A}$ effective size of detector in center

resolution of CT (III) $\quad$ MTF$_{beam}$

- assumption 1: point-like detector; extended focus of x-ray tube

⇒ point spread function = rectangular function with width b_F

⇒ associated MTF in Fourier domain = |sin(u)/u|

- assumption 2: point-like focus of x-ray tube, extended detector

⇒ point spread function = rectangular function with width b_D

⇒ associated MTF in Fourier domain = |sin(u)/u|

(with cylindrical coordinates $u=w\cdot\cos\Theta$ und $v=w\cdot\sin\Theta$ in Fourier domain)

⇒ $$MTF_{beam}(w) = \left|\frac{\sin(\pi \cdot b_F \cdot w)}{\pi \cdot b_F \cdot w}\right| \cdot \left|\frac{\sin(\pi \cdot b_D \cdot w)}{\pi \cdot b_D \cdot w}\right|$$

resolution of CT (III) — MTF_{beam}

point spread function

modulation transfer function

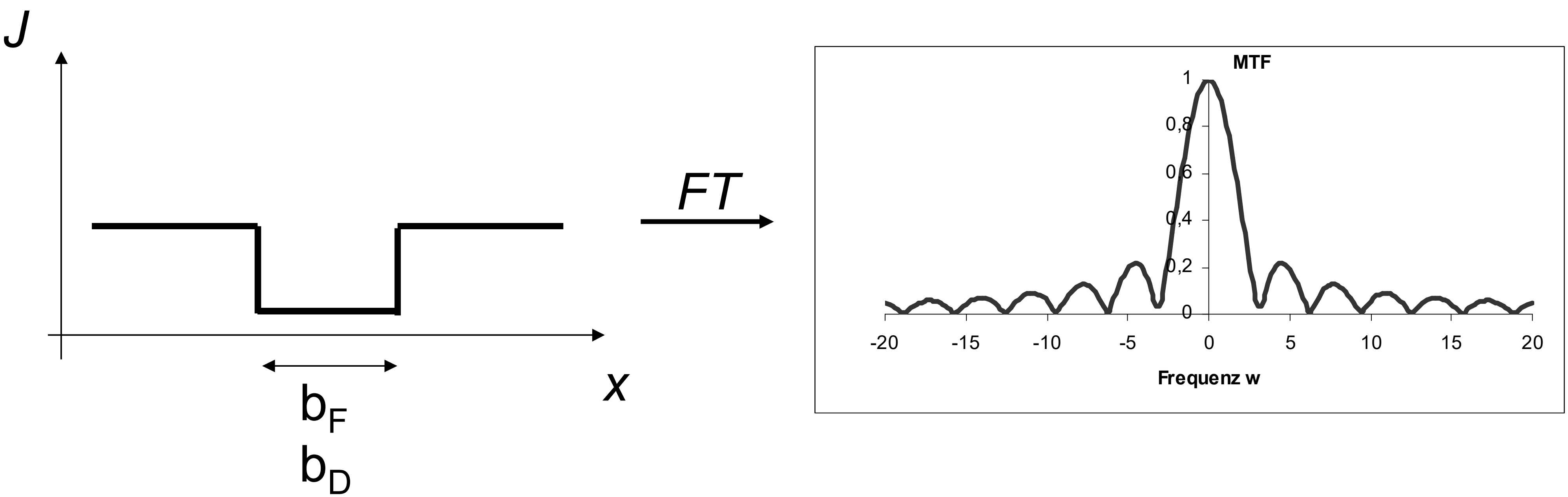

either extended focus in tube (width b_F)
or extended detector (width b_D)

resolution of CT (III) MTF_{beam}

MTF_{beam} is the better the smaller b_F **<u>and</u>** b_D

if patient is lying in the center of scanner, we have with theorem of intersecting lines:

$b_F = 1/2 \cdot F$ and $b_D = 1/2 \cdot D$

example:

size of focus and detector: 1 mm

$\Rightarrow$ resolution: 0.5 mm (typical value !)

resolution of CT (IV) **$\mathbf{MTF_{algorithm}}$**

assumption: image reconstruction with filtered back projection
$\Rightarrow$ influencing factors:

(1) H(w) = filter function = FT of convolution kernel
(application-dependent)

(2) G(w) = FT of interpolation function

$$G(w) = \left(\frac{\sin(\pi \cdot \Delta s \cdot w)}{\pi \cdot \Delta s \cdot w} \right)^2$$

Δs = center-to-center distance between detectors

coarse-grained sampling $\rightarrow$ additional interpolation $\rightarrow$ bad resolution

resolution of CT (V)

$$MTF_{CT}(w) = \left|\frac{\sin(\pi \cdot b_F \cdot w)}{\pi \cdot b_F \cdot w}\right| \cdot \left|\frac{\sin(\pi \cdot b_D \cdot w)}{\pi \cdot b_D \cdot w}\right| \cdot \left|\frac{\sin(\pi \cdot \Delta s \cdot w)}{\pi \cdot \Delta s \cdot w}\right|^2 \cdot \frac{|H(w)|}{|w|}$$

consider frequency w, where MTF is reduced to 50 % :

CT	up to 1.2 lp/mm (~ 0.5 mm)
x-ray image amplifier	up to 5 lp/mm (~ 0.1 mm)
x-ray film	up to 10 lp/mm (~ 0.05 mm)

CT has inferior resolution than other x-ray-based techniques
BUT: CT provides tomographic images!

noise and CT

noise sources in CT

noisy data (detected quanta)

↓ ← recording

noisy projections

↓ ← reconstruction algorithm

pixel noise

x-ray computed tomography (CT)

noise and CT

noisy data

consider number N of quanta in detector: $N_\Theta(s) = N_0 \cdot e^{-\int \mu(x,y)dl}$

where N_0 = detected quanta/detector without patient
and $N_\theta(s)$ = detected quanta/detector with patient
(projection angle Θ; site of detector s)

for the projections, we have:

$$p_\Theta(s) = \ln \frac{N_0}{N_\Theta(s)} = \ln N_0 - \ln N_\Theta(s)$$

number of detected quanta is Poisson distributed:

$$N_\Theta(s) = \overline{N}_\Theta(s) \pm \sqrt{\overline{N}_\Theta(s)}$$

noise and CT

$\Rightarrow$

$$\ln N_{\Theta}(s) = \ln\left\{\overline{N}_{\Theta}(s) \pm \sqrt{\overline{N}_{\Theta}(s)}\right\} = \ln\left\{\overline{N}_{\Theta}(s)\left(1 \pm \frac{\sqrt{\overline{N}_{\Theta}(s)}}{\overline{N}_{\Theta}(s)}\right)\right\}$$

$$= \ln\left\{\overline{N}_{\Theta}(s)\left(1 \pm \frac{\sqrt{\overline{N}_{\Theta}(s)}}{\overline{N}_{\Theta}(s)}\right)\right\} \approx \ln \overline{N}_{\Theta}(s) \pm \frac{1}{\sqrt{\overline{N}_{\Theta}(s)}}$$

with $\frac{1}{\sqrt{\overline{N}_{\Theta}(s)}} << 1$

noise and CT

$\Rightarrow$ ***noisy projections***

assumption: number of quanta N_0 (without patient) can be estimated with arbitrary precision

$$p_\Theta(s) = \ln N_0 - \ln N_\Theta(s)$$
$$= \ln N_0 - \ln \overline{N}_\Theta(s) \pm \frac{1}{\sqrt{\overline{N}_\Theta(s)}}$$
$$= \overline{p}_\Theta(s) \pm \frac{1}{\sqrt{\overline{N}_\Theta(s)}}$$

$$\Rightarrow \sigma_P^2 = \frac{1}{\overline{N}_\Theta(s)}$$

variance of projections

noise and CT

influence of *noisy projections on pixel noise*

assume cylinder with homogeneous μ in center of scanner

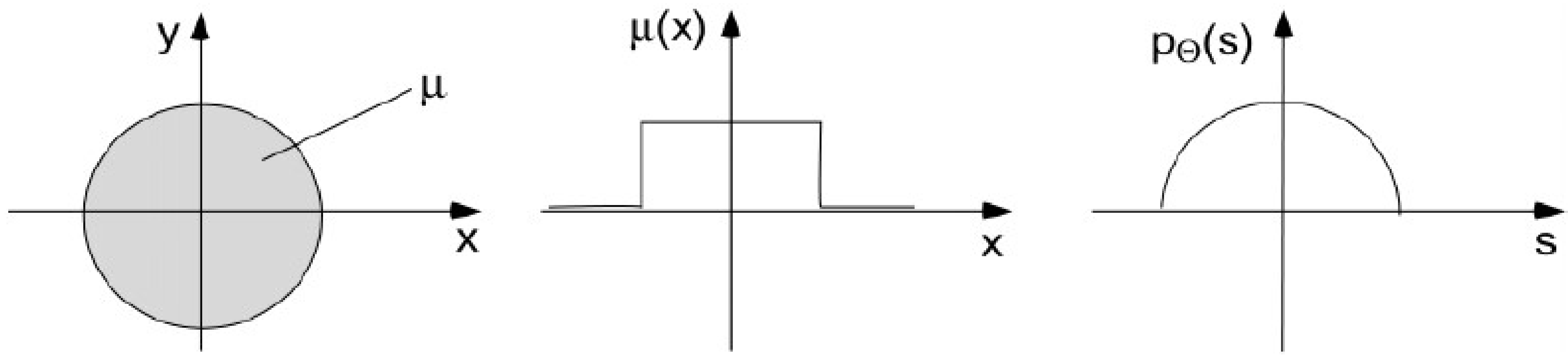

projections are equal for all angles Θ.

now consider pixel noise at x=y=0 ($p_\Theta(s)$ are flat)

noise and CT

pixel noise

with

$$\widetilde{p}_{\Theta}(n \cdot \Delta s) = \Delta s \cdot \sum_{k=-K}^{+K} p_{\Theta}(n \cdot \Delta s - k \cdot \Delta s) \cdot h(k \cdot \Delta s)$$

and

$$f(x,y) = \frac{\pi}{M} \sum_{i=1}^{M} \widetilde{p}_{\Theta}(x \cos \Theta_i + y \sin \Theta_i)$$

we have:

$$f(0,0) = \frac{\pi}{M} \cdot \Delta s \cdot \sum_{k=-K}^{+K} p_{\Theta}(0) \cdot h(k \cdot \Delta s)$$

cf. image reconstruction with filtered back projection *analog and digital filtering*

Δs = center-to-center distance between detectors
M = number of projections
h = filter function

with flat projections:
all data to the left and right of s = 0 equal $p_{\Theta}(0)$ in the range -K ... +K

noise and CT

pixel noise

projections p_Θ are statistically independent

and distributed around the mean $\bar{p}_\Theta(0)$

$$p_\Theta(0) = \bar{p}_\Theta(0) \pm \frac{1}{\sqrt{\overline{\overline{N}}}} \quad \text{where } \overline{N} = \overline{N}_\Theta(0)$$

with error propagation :

if $E(A) = A \pm a$ und $E(B) = B \pm b$ ($E(\bullet)$ = expected value)

$$\Rightarrow E(A+B) = A + B \pm \sqrt{a^2 + b^2}$$

$$\Rightarrow f(0,0) = \overline{f(0,0)} \pm \frac{\pi}{M} \cdot \Delta s \cdot \sqrt{\sum_{\Theta_i} \sum_{k=-K}^{+K} \frac{h^2(k \cdot \Delta s)}{\overline{\overline{N}}}}$$

noise and CT

pixel noise

$\overline{N}$ is constant; sum over all Θ_i

$$\Rightarrow \sigma^2_{Pixel} = \left(\frac{\pi}{M}\cdot\Delta s\right)^2 \cdot M \cdot \frac{1}{\overline{\overline{N}}} \sum_{k=-K}^{+K} h^2(k\cdot\Delta s)$$

with Parseval's theorem, we have:

$$\Rightarrow \sigma^2_{pixel} = \frac{\pi^2\cdot\Delta s}{M}\cdot\frac{1}{\overline{\overline{N}}} \int_{-\omega_{\max}}^{+\omega_{\max}} \left|H(\omega)\right|^2 d\omega$$

Δs = center-to-center distance detectors

M = number of projections

$\overline{N}$ = mean count rate

$H(\omega)$ = filter function for filtered back projection

noise and CT

pixel noise is the smallest, if

- ***center-to-center distance between detectors Δs is small***
- ***number of projections M is high***
- ***number of quanta per recording site is high***

and

- ***area under squared filter function H(ω) is small***

BUT:

MTF is deteriorated by the same token !

artifacts

- patient movements
- failure of recording electronics
- metal implants
- violation of limits of field of view
- partial volume artifacts
- beam hardening
- scattering

x-ray computed tomography (CT)

artifacts **patient movements**

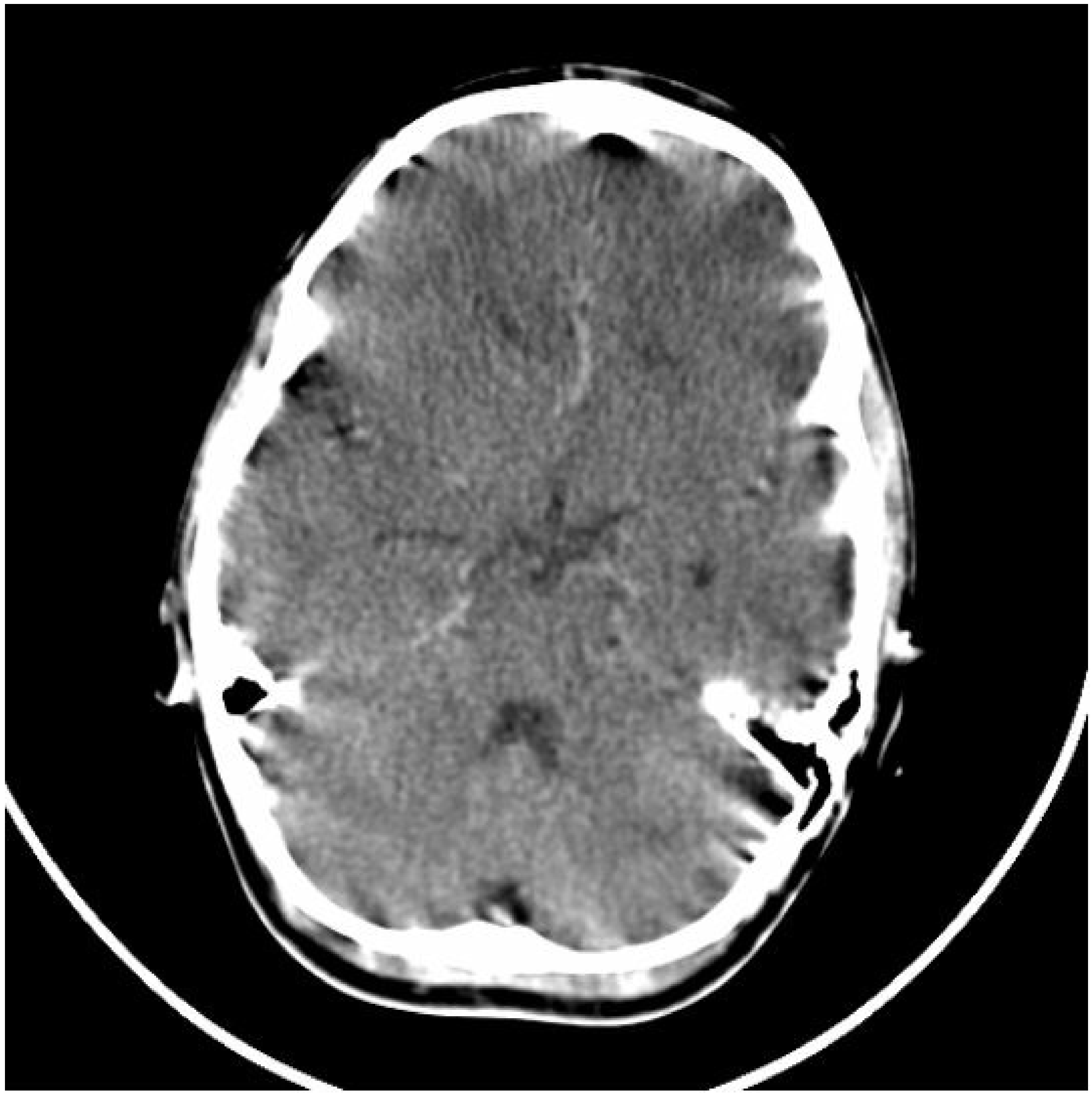

x-ray computed tomography (CT)

artifacts **patient movements**

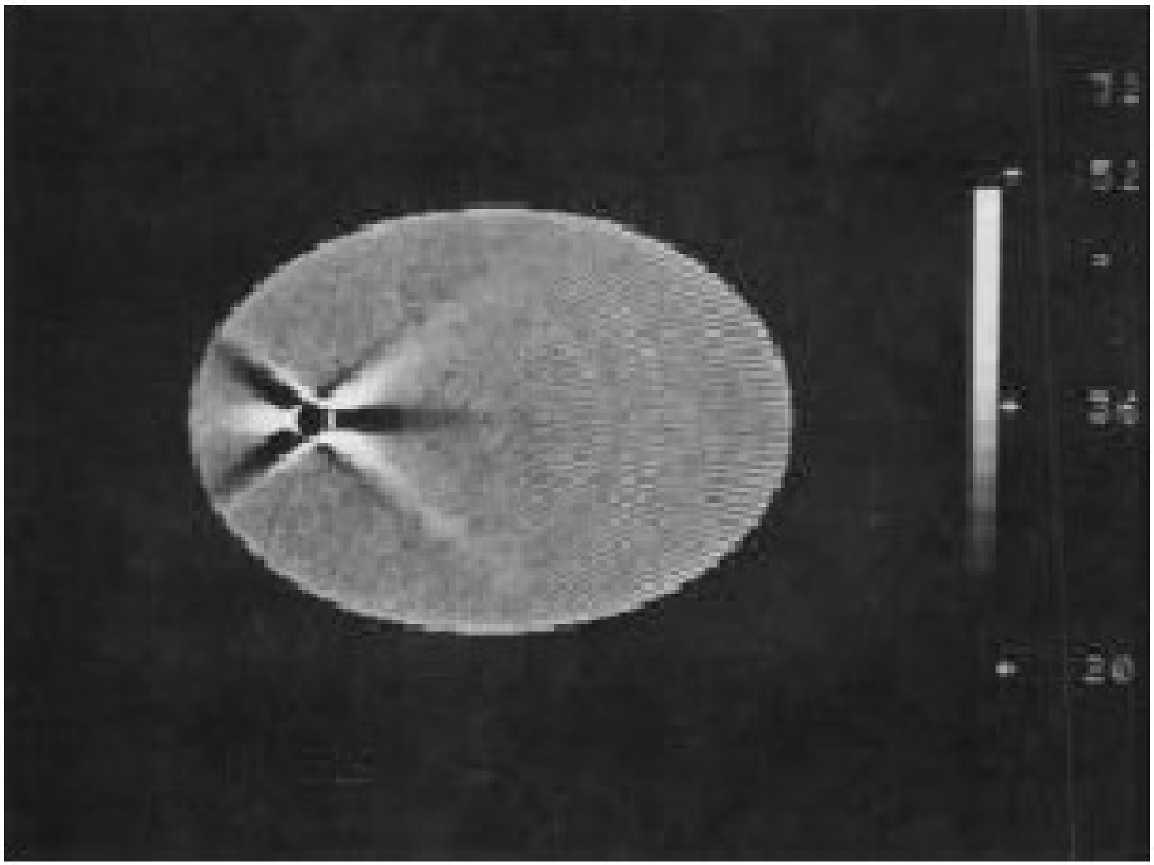

interference structure induced by movement

x-ray computed tomography (CT)

artifacts **patient movements**

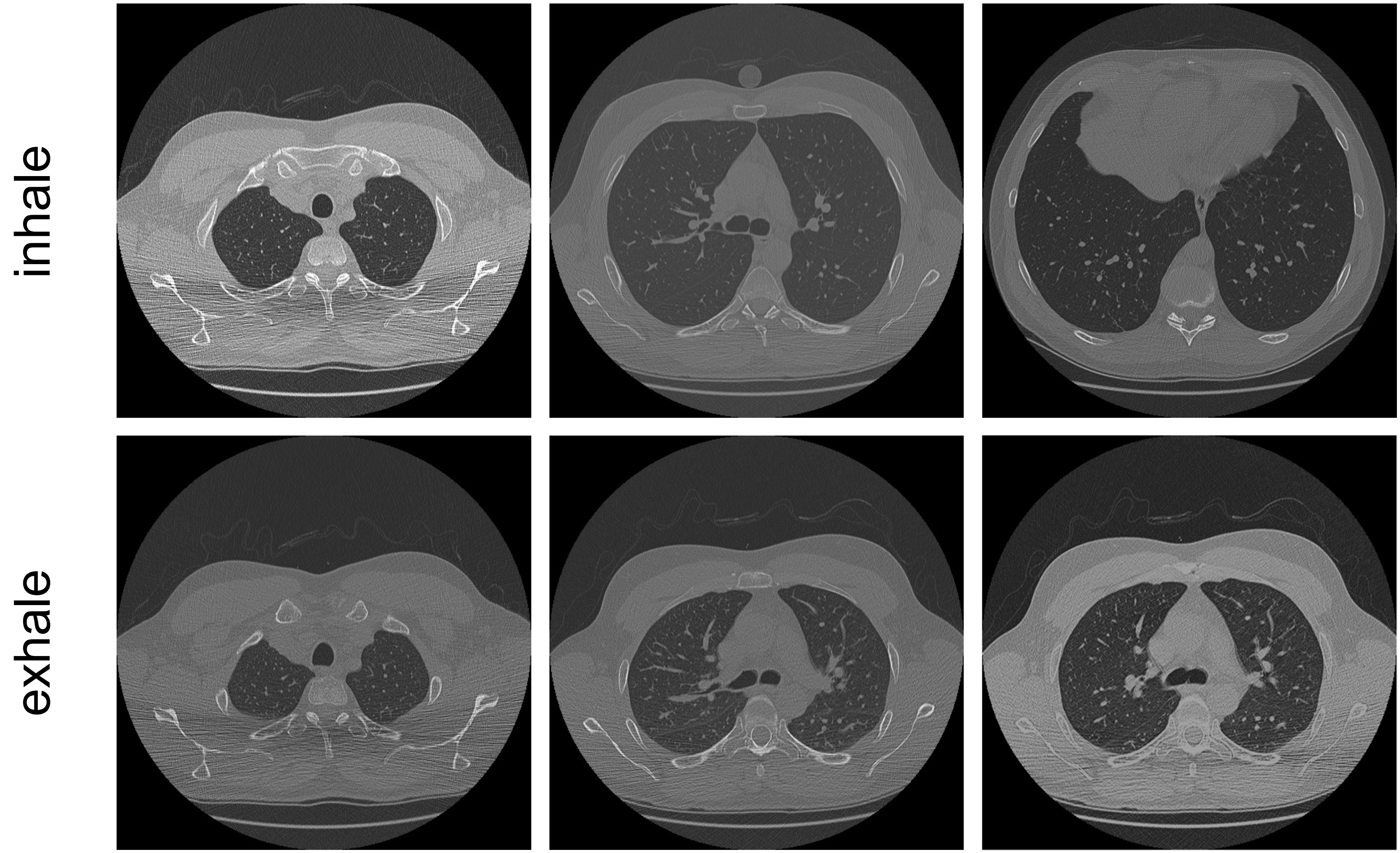

x-ray computed tomography (CT)

artifacts **failure of recording electronics**

x-ray computed tomography (CT)

artifacts **metal implants**

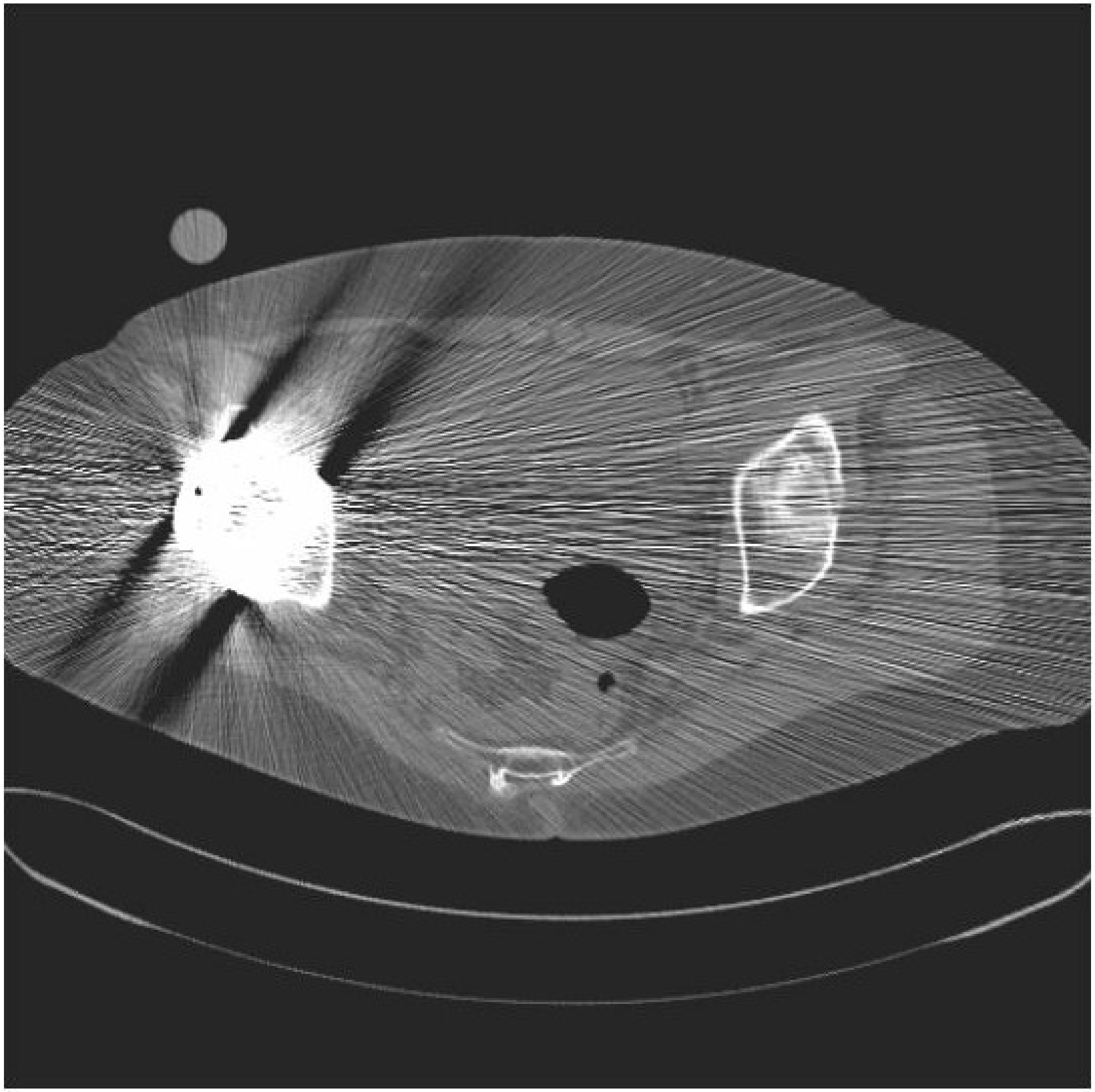

tooth: gold filling

artifacts **violation of limits of field of view**

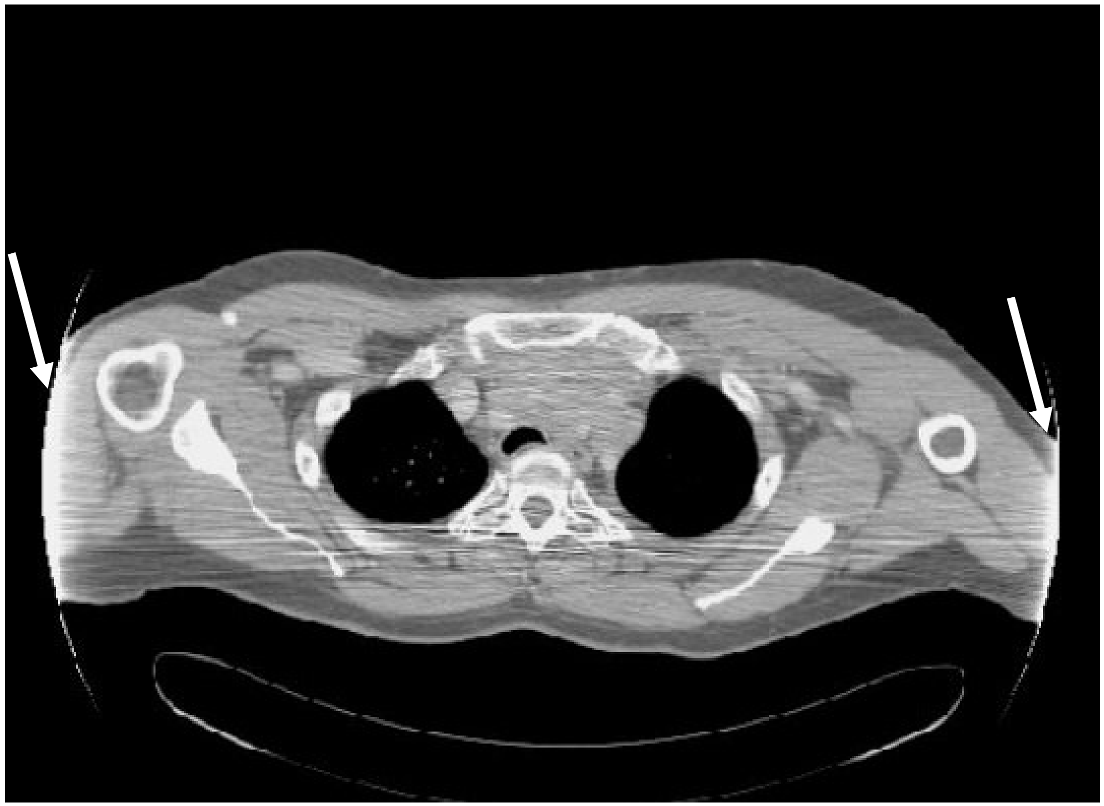

artifacts

partial volume artifacts

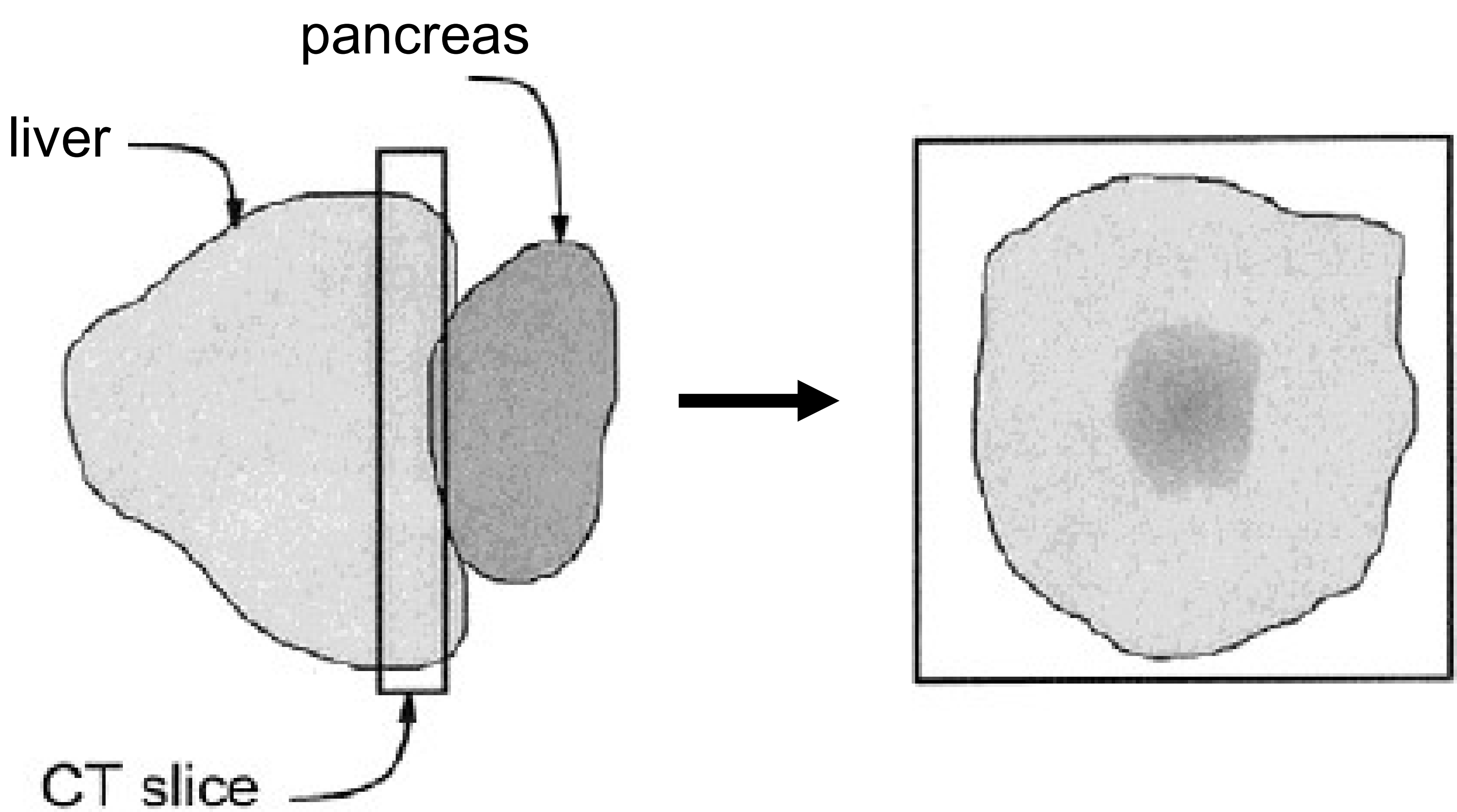

artifacts **partial volume artifacts**

consider two areas with strongly differing μ captured in a single pixel

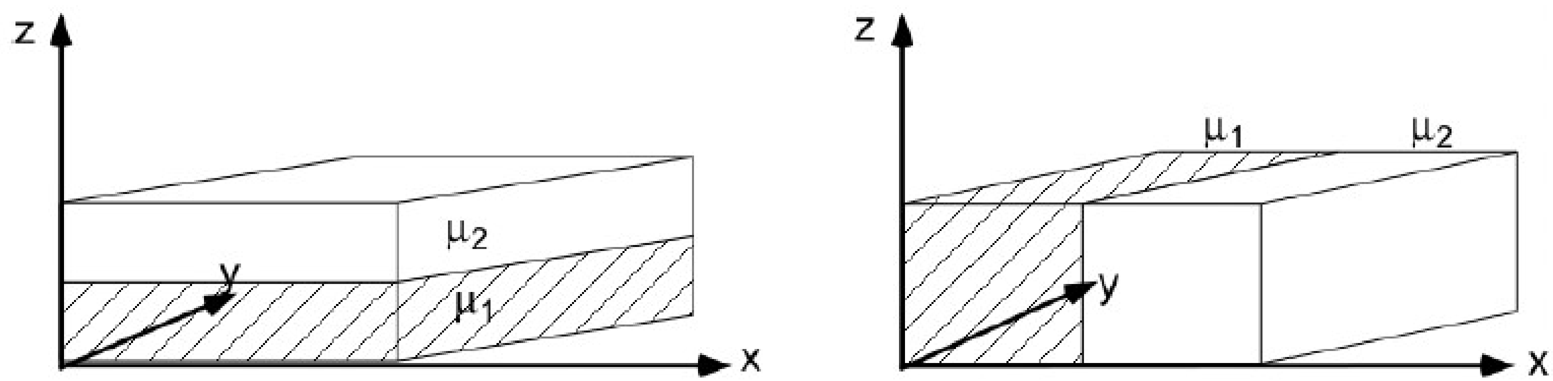

artifacts **partial volume artifacts**

areas with strongly differing μ captured in a single pixel

case A:

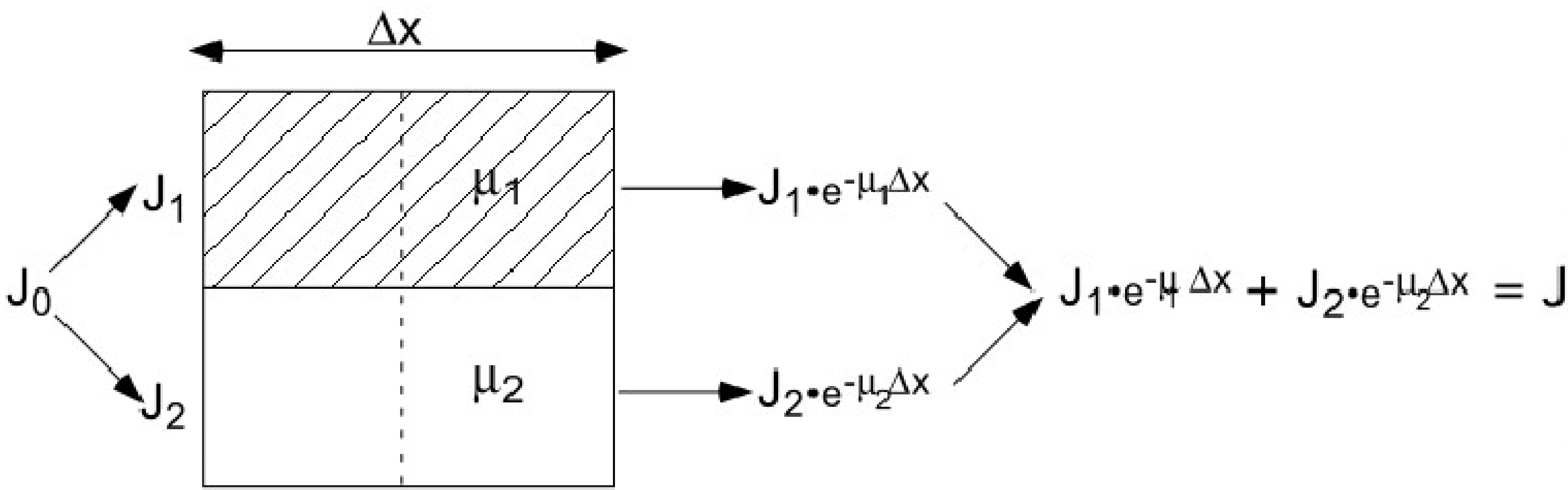

artifacts **partial volume artifacts**

areas with strongly differing μ captured in a single pixel

case B:

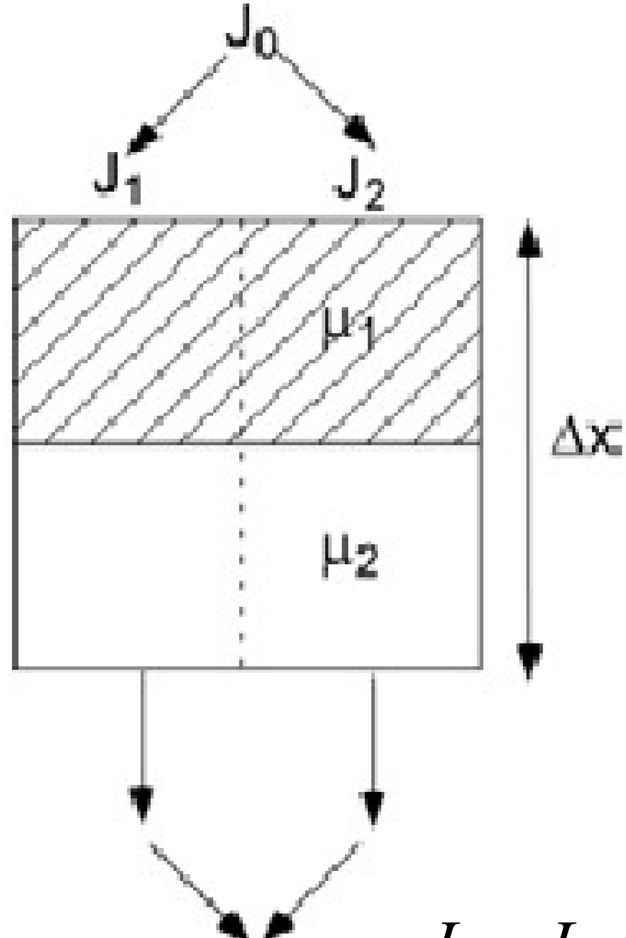

$$J = J_0 e^{-\mu_1 \frac{\Delta x}{2} - \mu_2 \frac{\Delta x}{2}}$$

artifacts **partial volume artifacts**

consider x-ray intensity at detector site

case A: $J = J_1 e^{-\mu_1 \Delta x} + J_2 e^{-\mu_2 \Delta x}$

case B: $J = J_0 e^{-\mu_1 \frac{\Delta x}{2} - \mu_2 \frac{\Delta x}{2}}$

in general, we do NOT have: $\overline{\mu} = \ln \frac{J_0}{J}$

even worse: mean μ-values from different projections do NOT match

result: banding

prevention: thin slices, higher sampling

artifacts **partial volume artifacts**

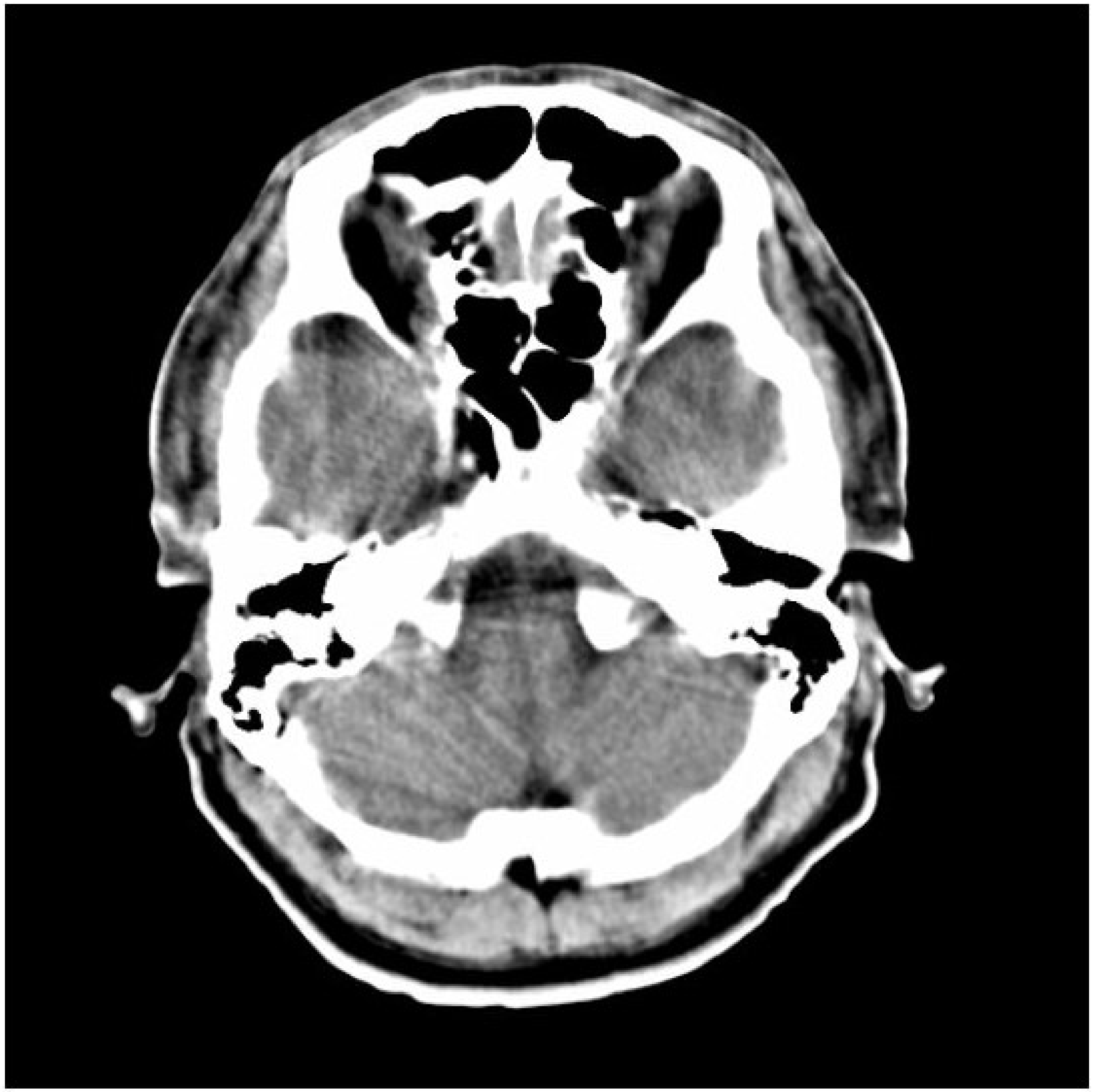

x-ray computed tomography (CT)

artifacts **beam hardening**

recap:
- μ depends on x-ray energy
- x-ray tube provides broad-band energy spectrum

absorption:
- "soft" low-energetic radiation is strongly absorbed
- "hard" high-energetic radiation remains

$\Rightarrow$ ***beam hardening***

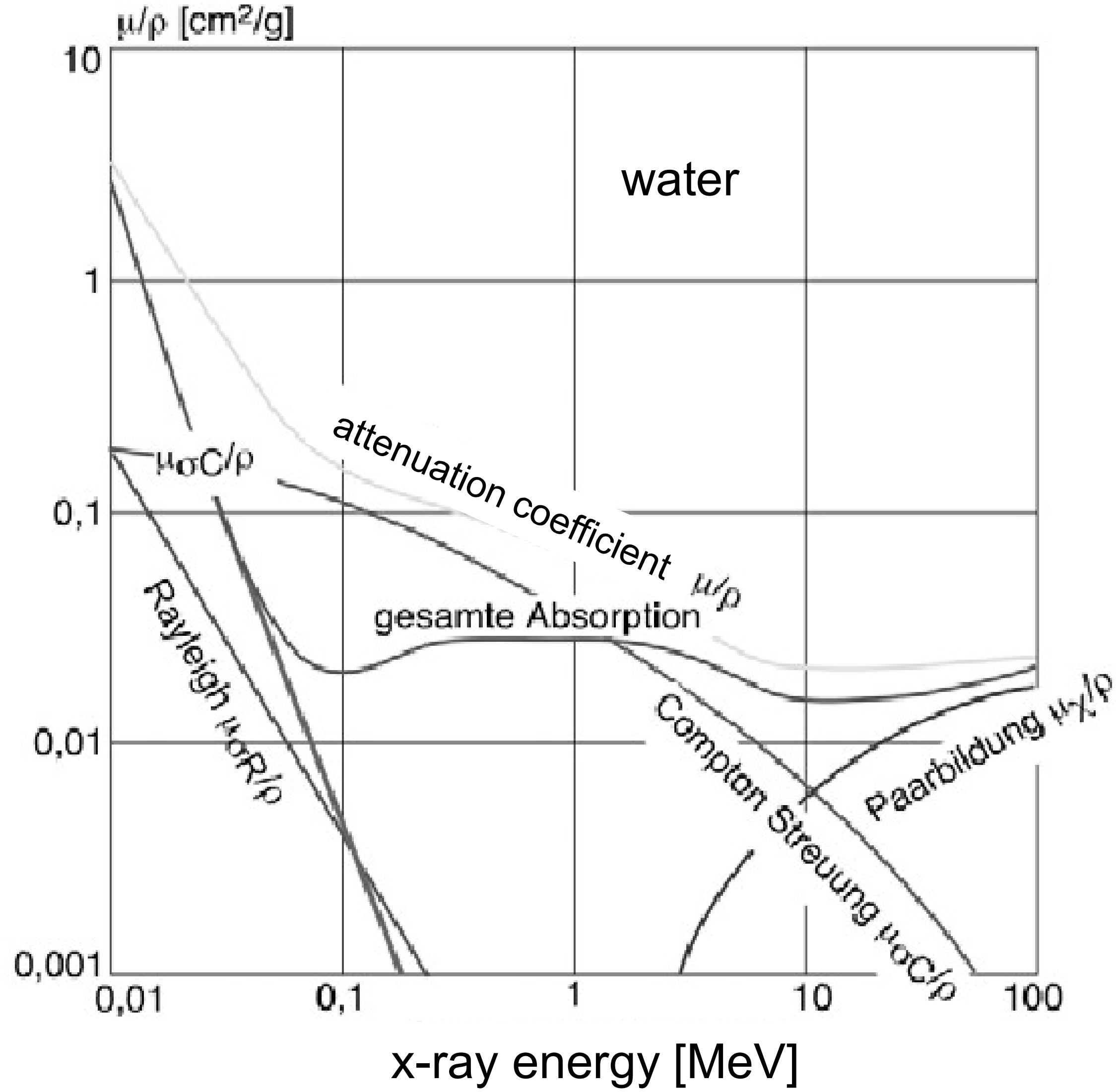

artifacts **beam hardening**

effective radiation power of x-ray tube (polychromatic radiation):

$$J_0 = \underbrace{\int_{E_{\min}}^{E_{\max}} \frac{dJ_0(E)}{dE}}_{\text{power in energy interval } dE} dE$$

power in
energy interval dE

total radiation power passed through the body:

$$J = \int_{E_{\min}}^{E_{\max}} \frac{dJ_0(E)}{dE} \cdot e^{-\int \mu(x,y,E)\,d\ell} dE$$

x-ray computed tomography (CT)

artifacts **beam hardening**

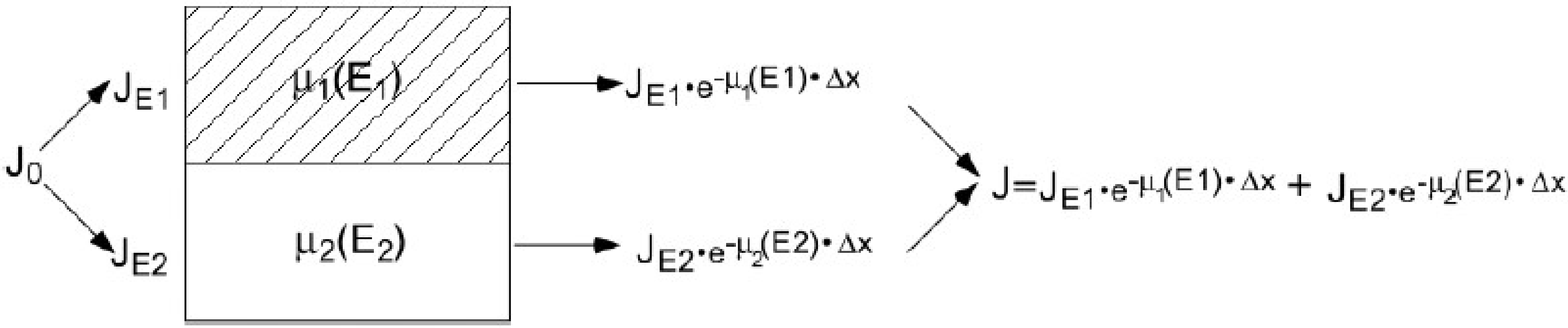

in general, we do NOT have: $\bar{\mu} = \ln \frac{J_0}{J}$

effect: banding (as with partial volume artifacts)

avoidance: - higher-energetic radiation (flat μ(E)-dependence)
- filtering of low-energetic part of energy spectrum (e.g. copper)

artifacts **beam hardening**

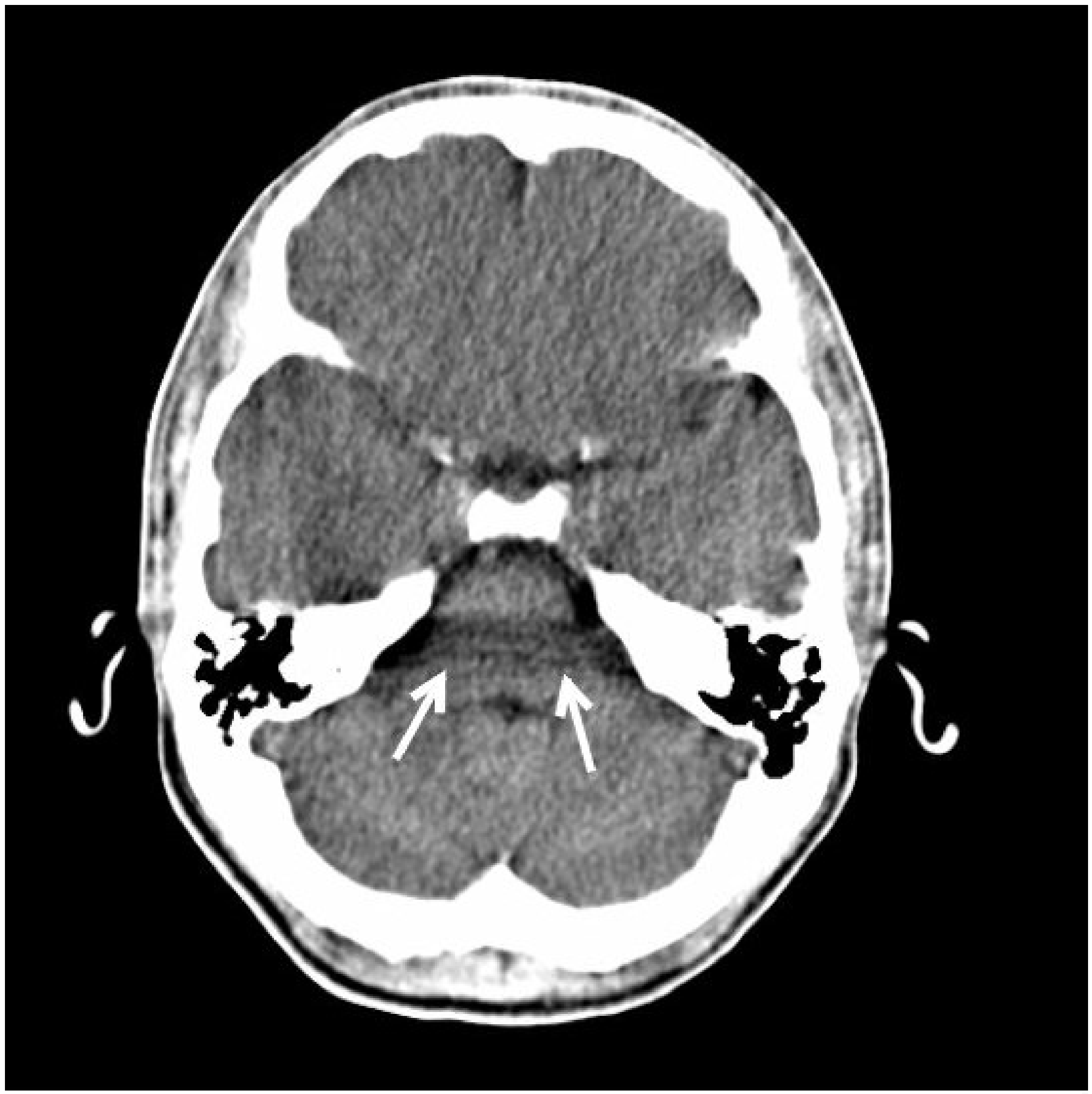

artifacts **scattering**

- Compton scattering leads to an uniform increase of radiation power

- inconsistent data (for reconstruction)

- remedy:
  3. generation scanner: raster
  4. generation scanner: subtraction using additional detectors

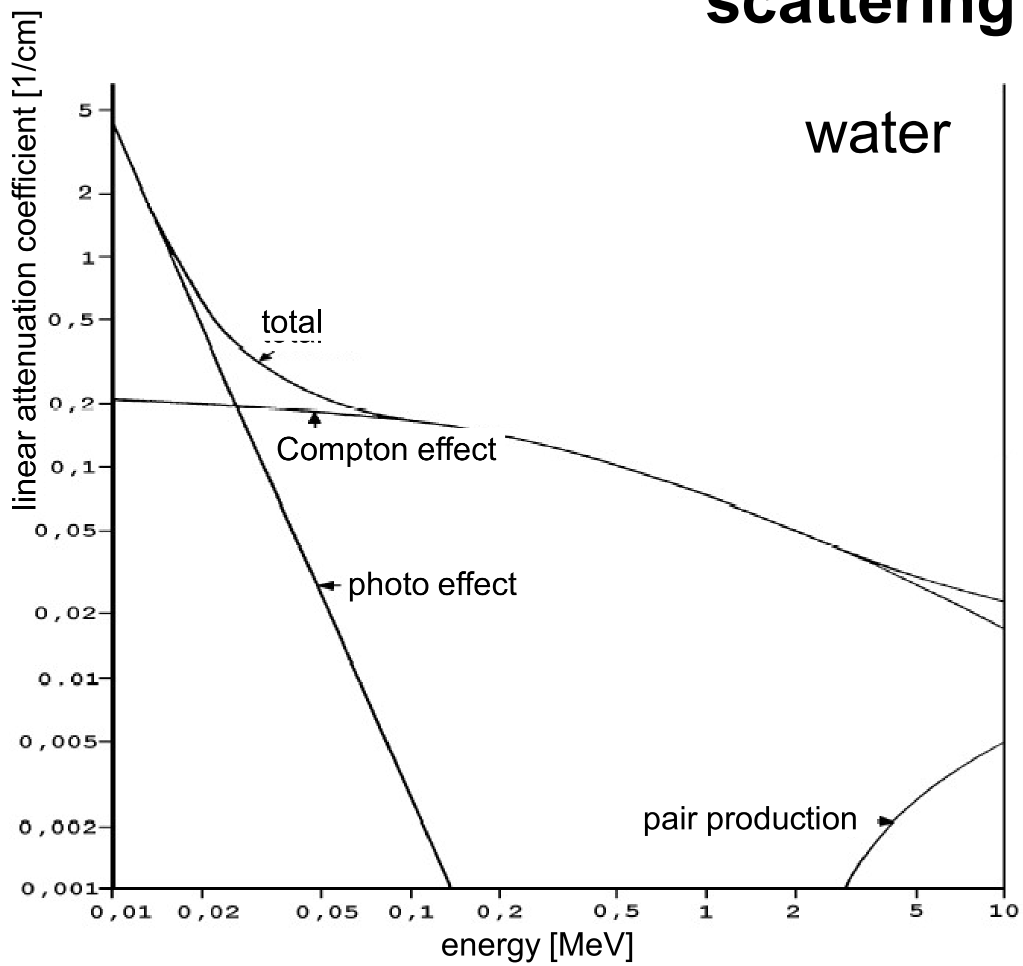

artifacts **scattering**

scattering can lead to false data for back projection, depending on relative orientation of detector to absorber

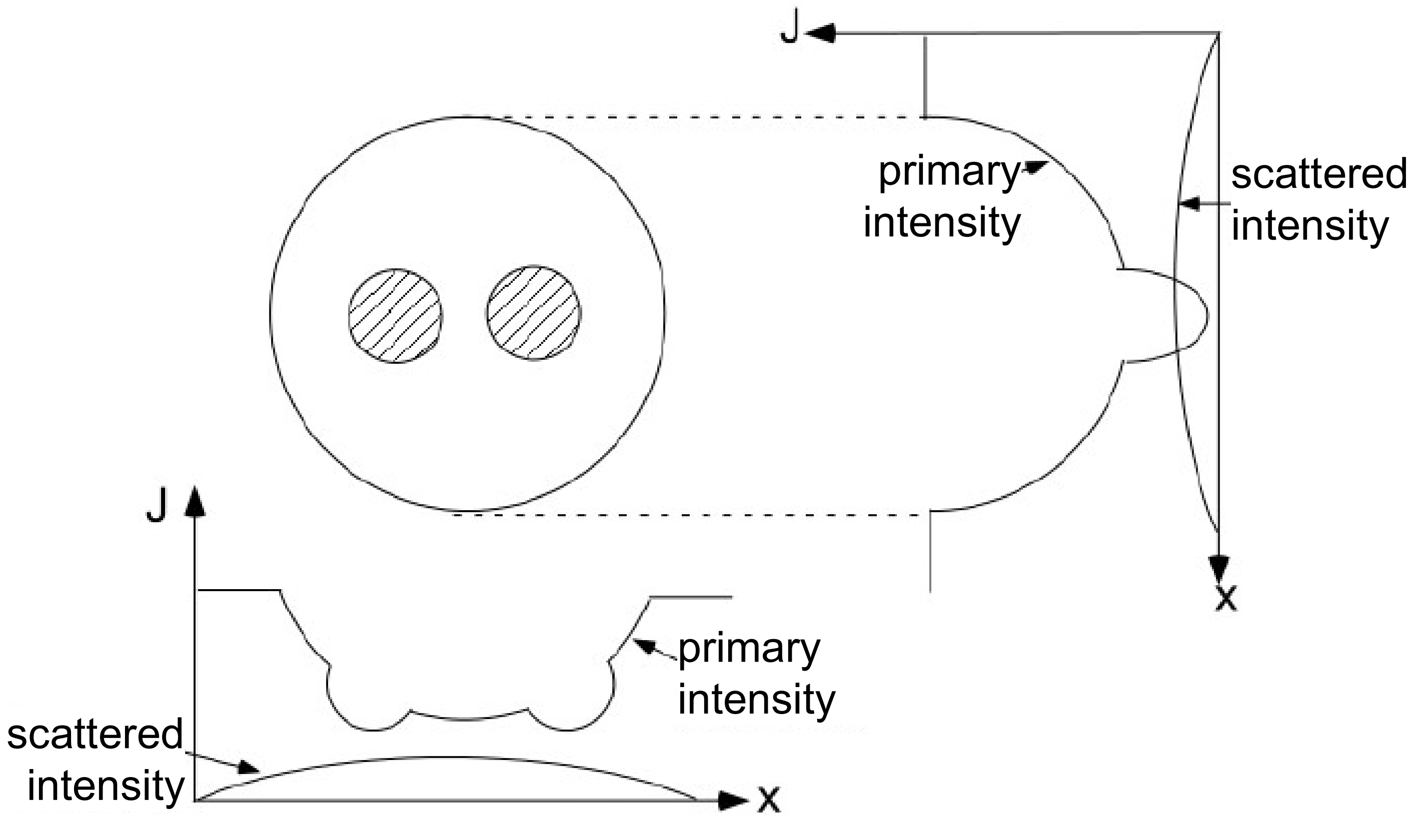

x-ray computed tomography (CT)

areas of application

Trauma	Unfalldiagnostik im gesamten Körper
Kopf-Hals	Akutes nicht-traumatisches neurologisches Defizit (Blutung, Infarkt)
Spinalkanal	Spinales Trauma
HNO	Mittelohr, Innenohr, Schädelbasis, Trauma der Schädelbasis, Kranio-faziales Skelett und Nasennebenhöhlen, Hypopharynx, Larynx, Tumor
Augenheikunde	Intra-Okulärer Fremdkörper, Ductus nasolacrimalis
Thoraxorgane	Thoraxwand: Tumor, Pleura: Entzündungen, Tumor, Lunge: Lungenstruktur, Pulmonale Läsionen, Nekrose, Verkalkungen, Tumorausdehnung und Infiltration, Interstitielle Pneumonie, Bronchiektasen, Hiläre Raumforderung, Lungenmetastasen, Zentrales Tracheobronchiales System, Gefäßmalformation, Sequestration, Mediastinum: Raumforderung (angeboren/entzündlich/Neoplastisch) Lokalisation, Ausdehnung, Ätiologie, Tumor-Staging
Herz-Kreislauf-System	Aorta Thoracalis: Dissektion, Aneurysma
Bewegungs-apparat	Knochen: Biopsie, Hüftgelenk: Dissektat, Frakturen, Orthopädische Operationsplannung
Gastroenterologie	Pankreas: Endokrin, akute Pankreatitis, Verdauungstrakt: Tumor-Staging

broad applicability

x-ray computed tomography (CT)

special applications:

- bone density measurement (quantitative CT)
  osteoporosis treatment and monitoring
- lung density measurement (xenon inhalation)
- 3D planning (tumor irradiation / surgery)
- virtual endoscopy („fly through“)
  colonoscopy (fistula, intestinal polyp, tumor)
  bronchoscopy (fistula, ruptures)
  angioscopy (aneurysm, plaque diagnostics)
- tissue perfusion measurement (contrast agents)
- real time CT
- cardio CT (EKG triggered)

x-ray computed tomography (CT)

areas of application **visualization**

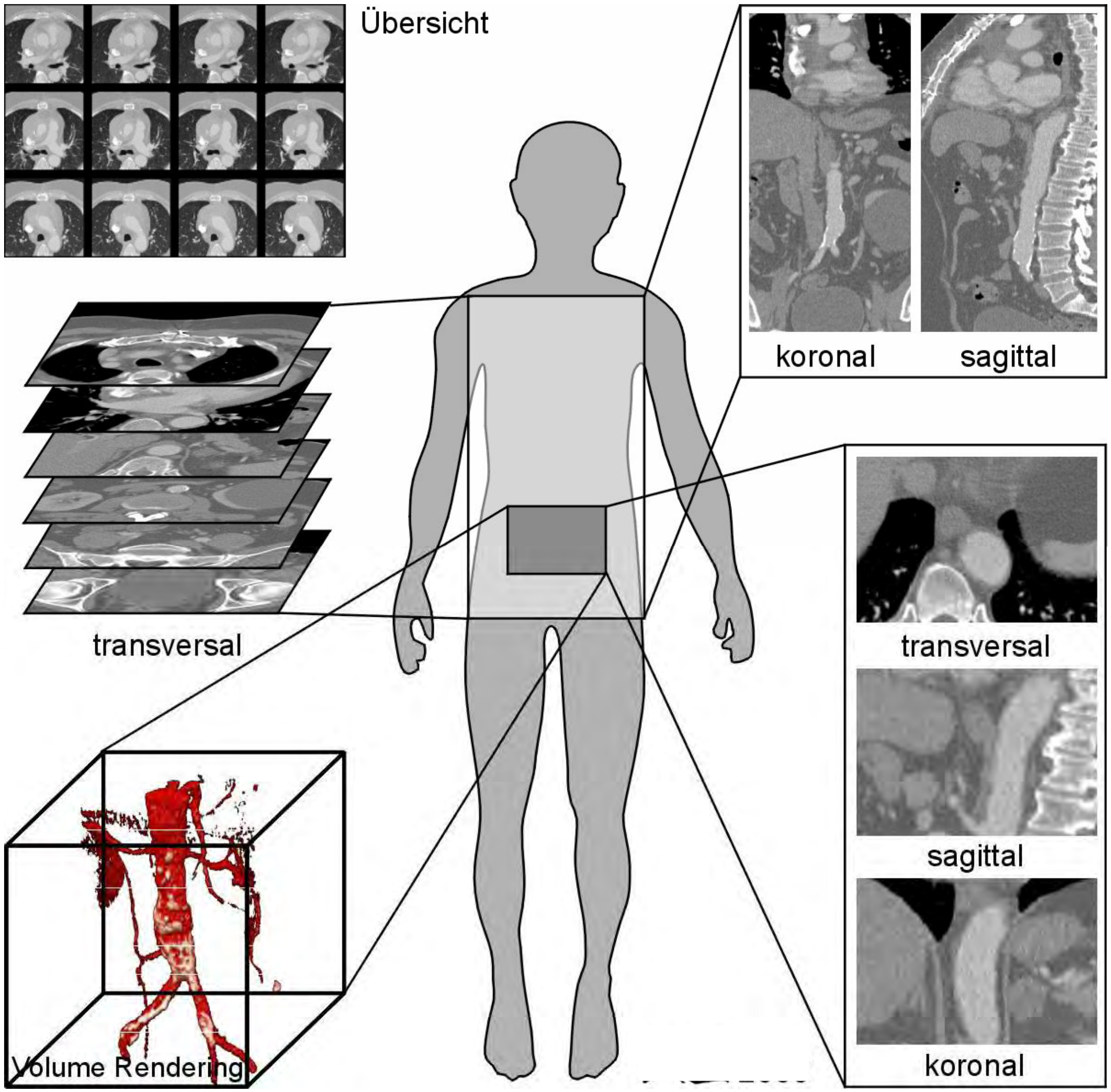

x-ray computed tomography (CT)

areas of application **3D visualization**

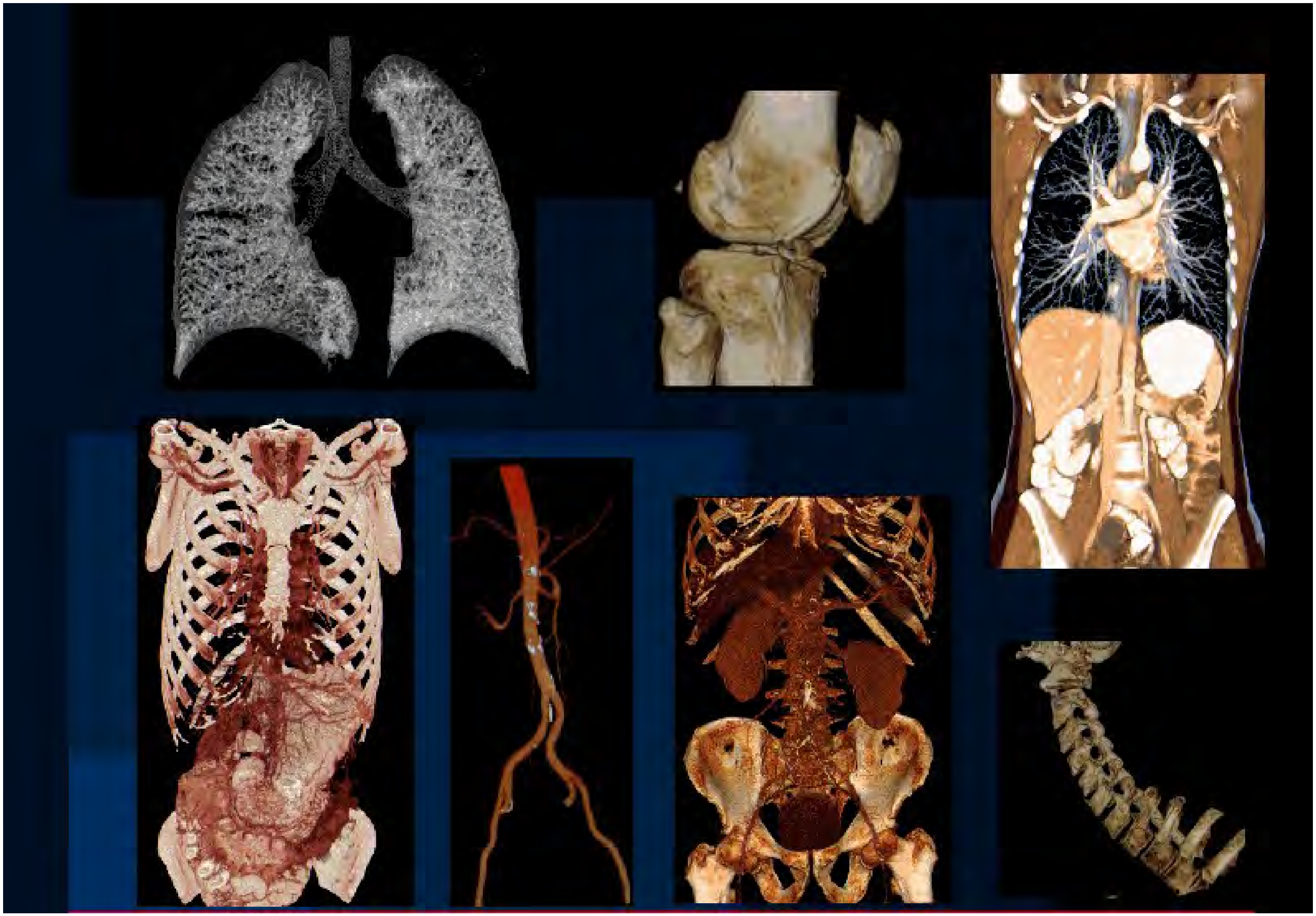

x-ray computed tomography (CT)

areas of application

3D visualization

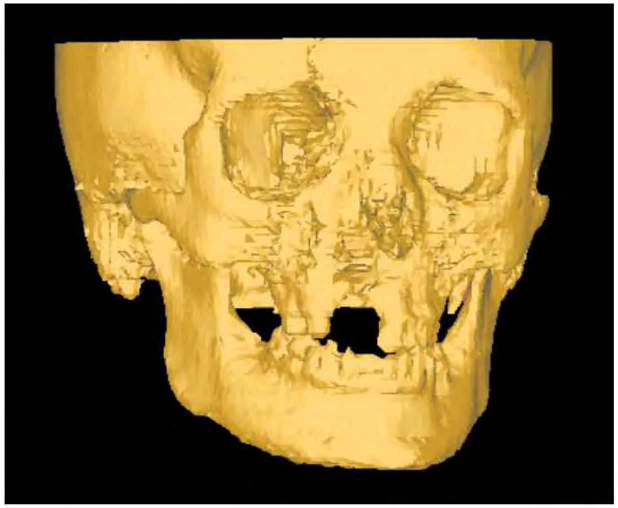

a)

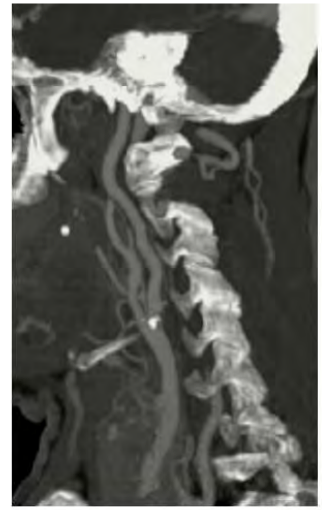

b)

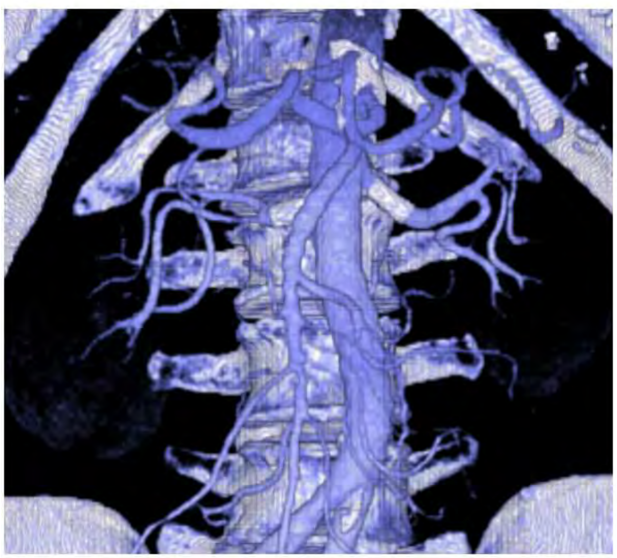

c)

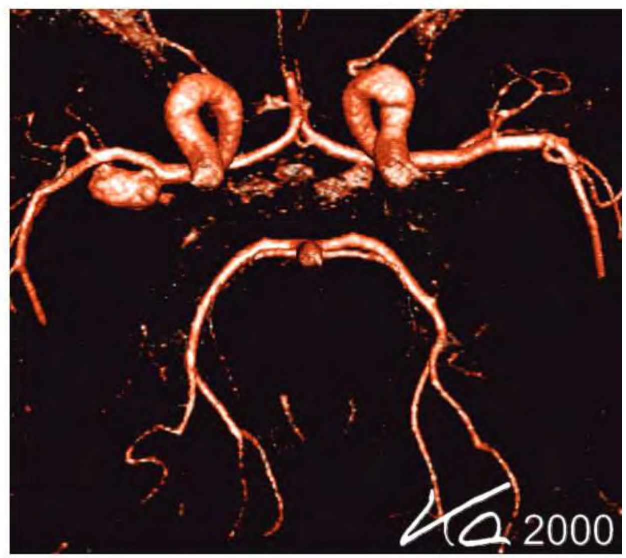

d)

x-ray computed tomography (CT)

areas of application

3D visualization

areas of application **3D visualization**

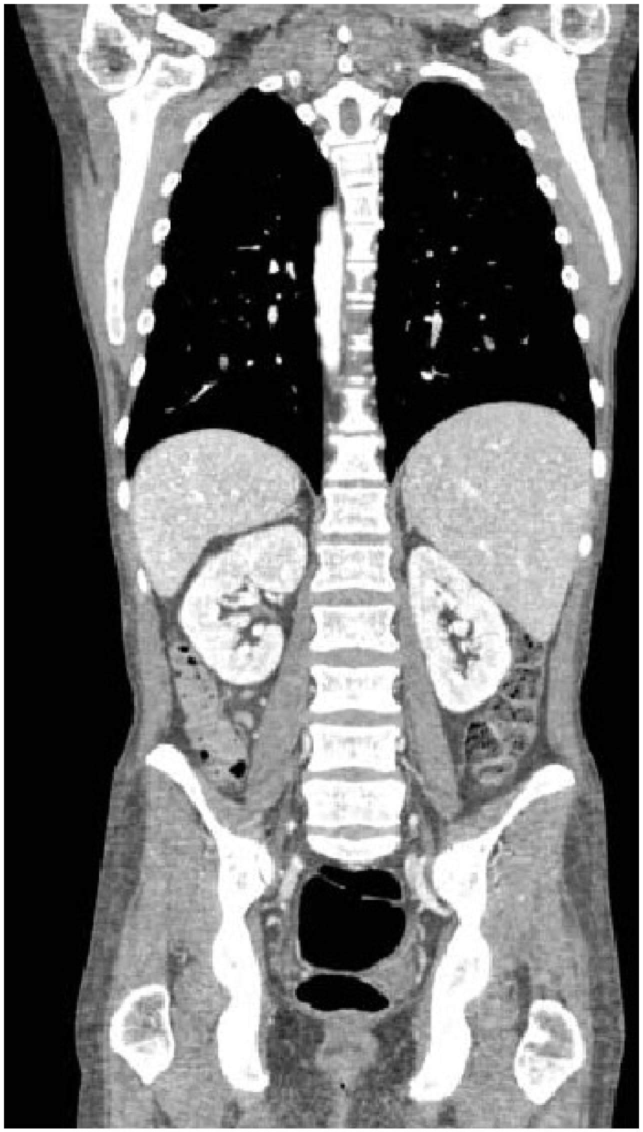

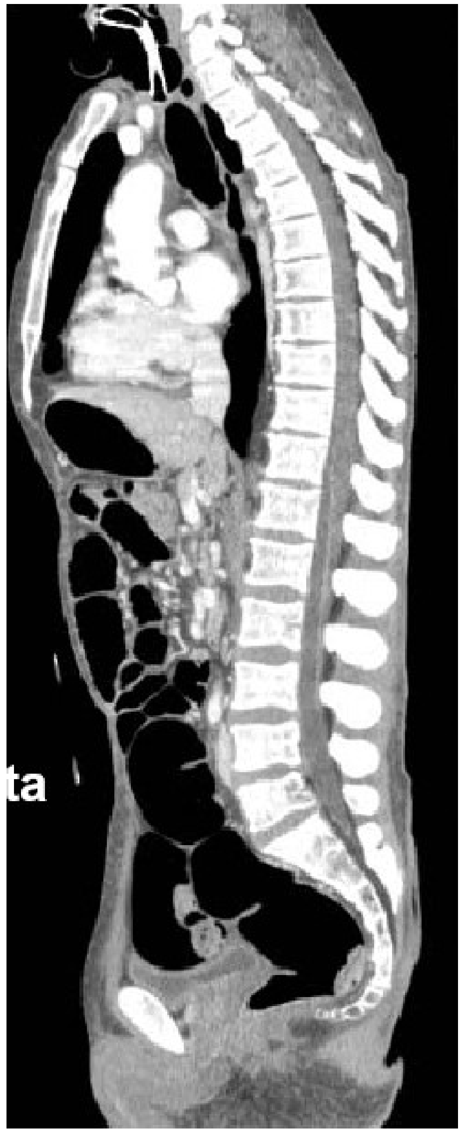

multi-slice CT:

-16 detectors
- rotation time: 0.5 s
- resolution: 16 x 0.75 mm
- advance: 25 mm/s
- 70 cm in 28 s

- raw data: 1.4 GB
  1400 images

x-ray computed tomography (CT)

areas of application **3D visualization**

areas of application **angiography**

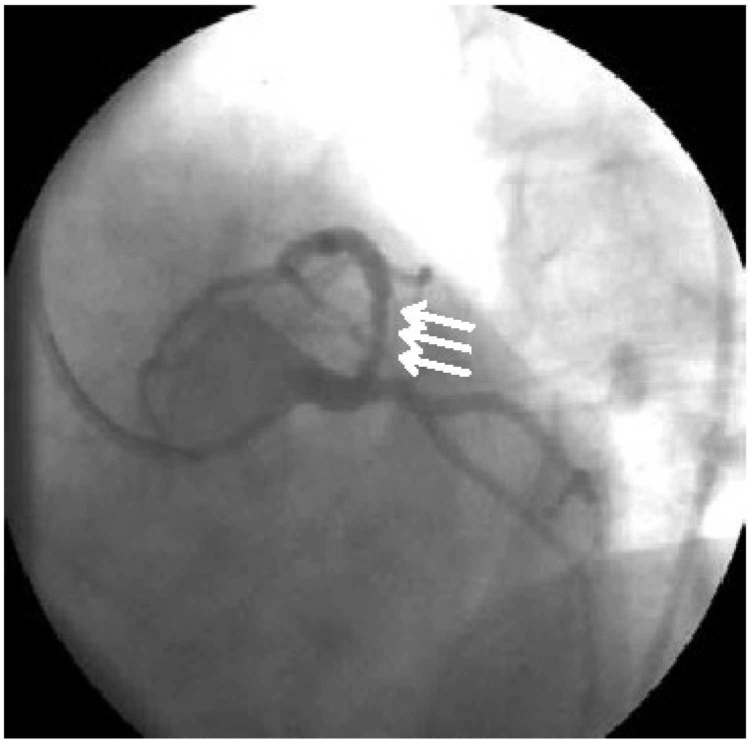

conventional angiography

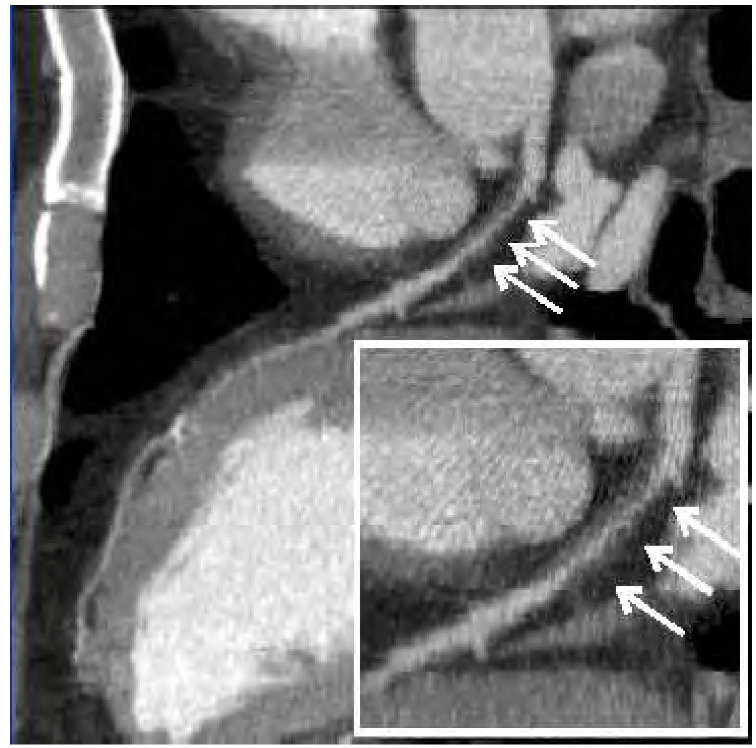

CT angiography

x-ray computed tomography (CT)

special applications

visualization of volumes

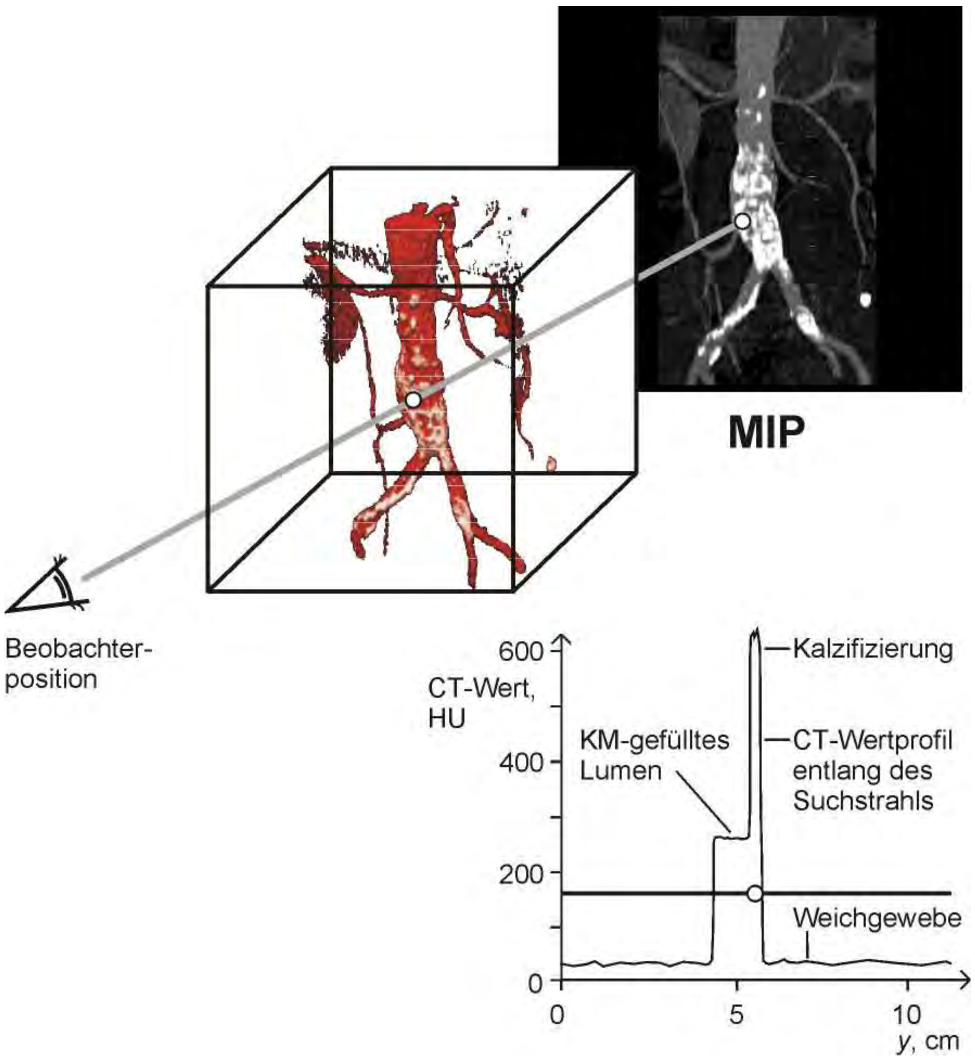

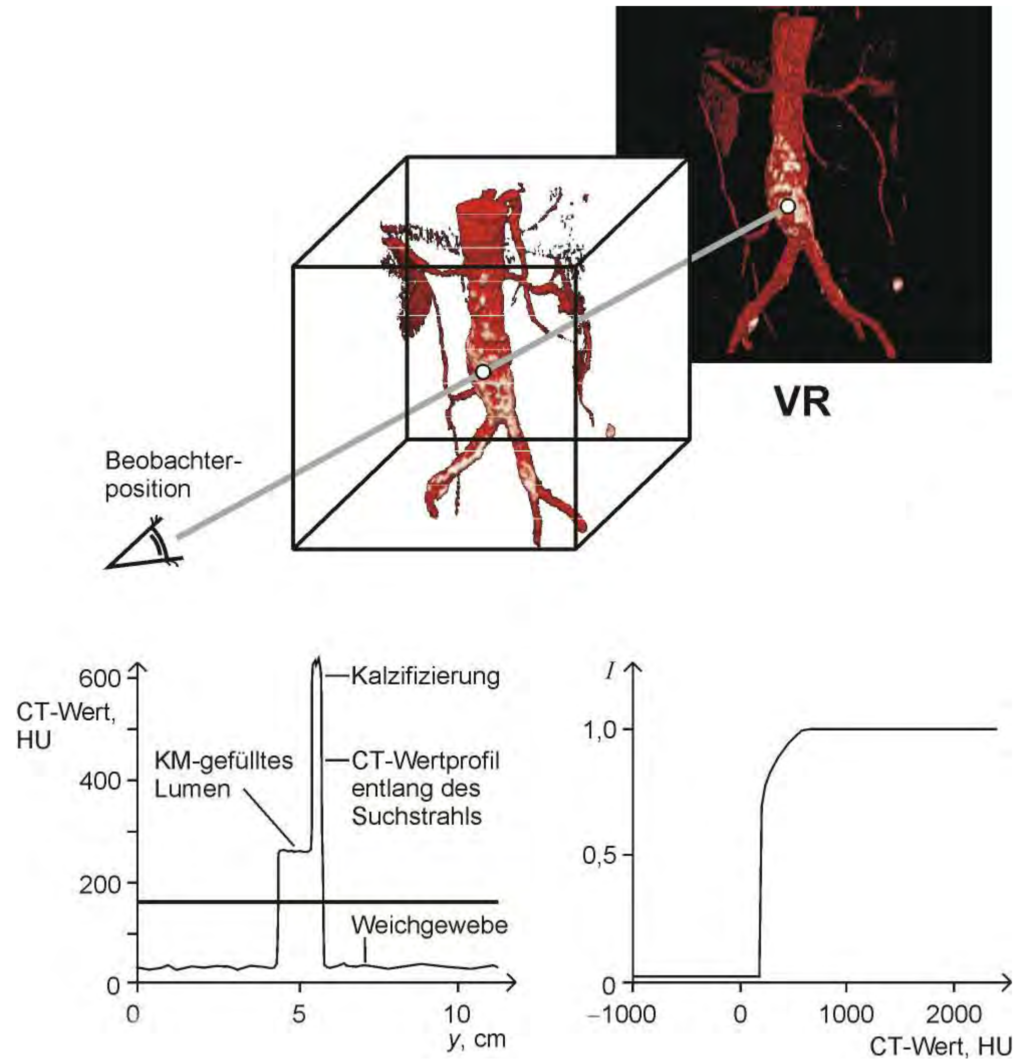

x-ray computed tomography (CT)

special applications **virtual endoscopy**

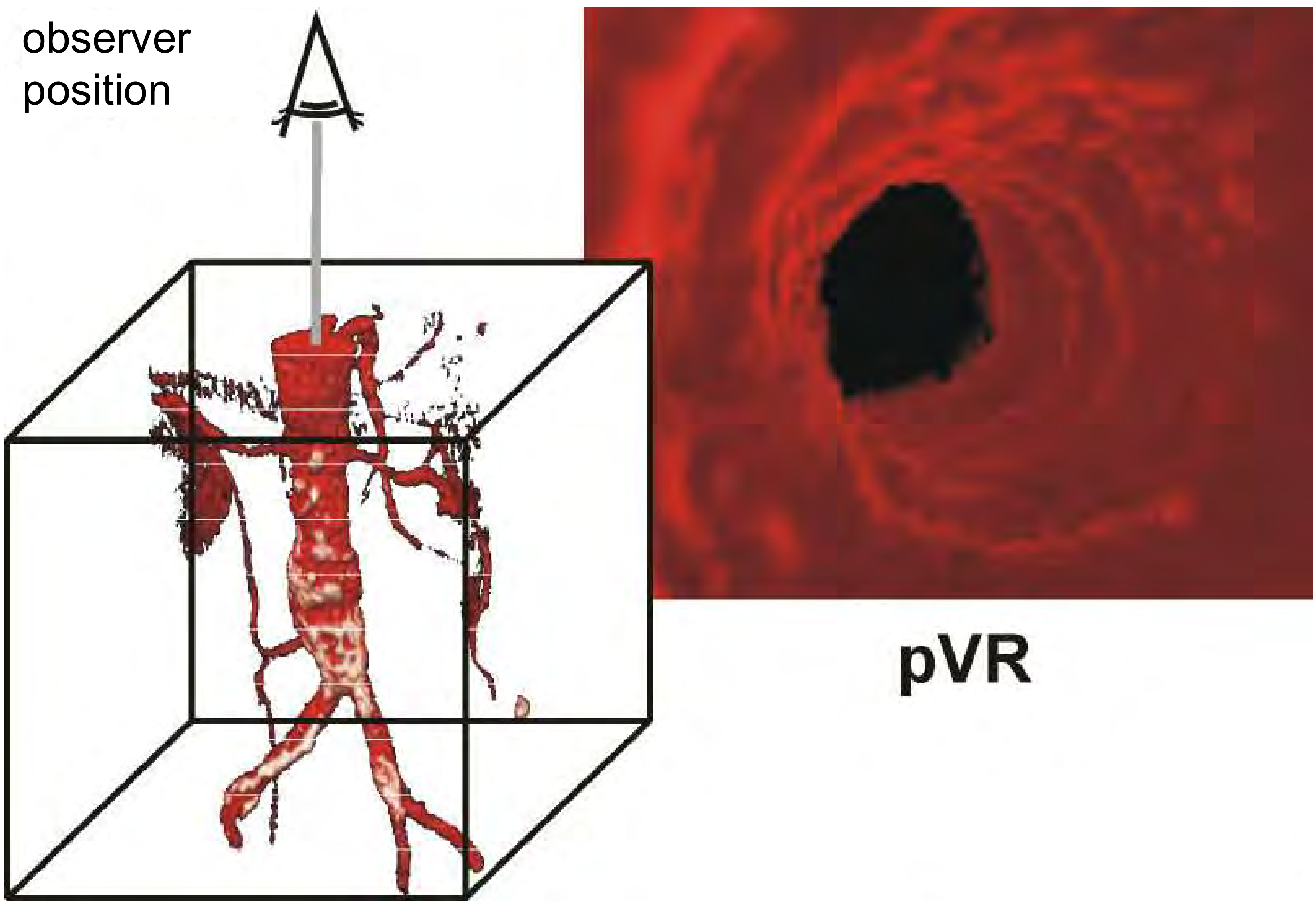

x-ray computed tomography (CT)

special applications

dynamic CT

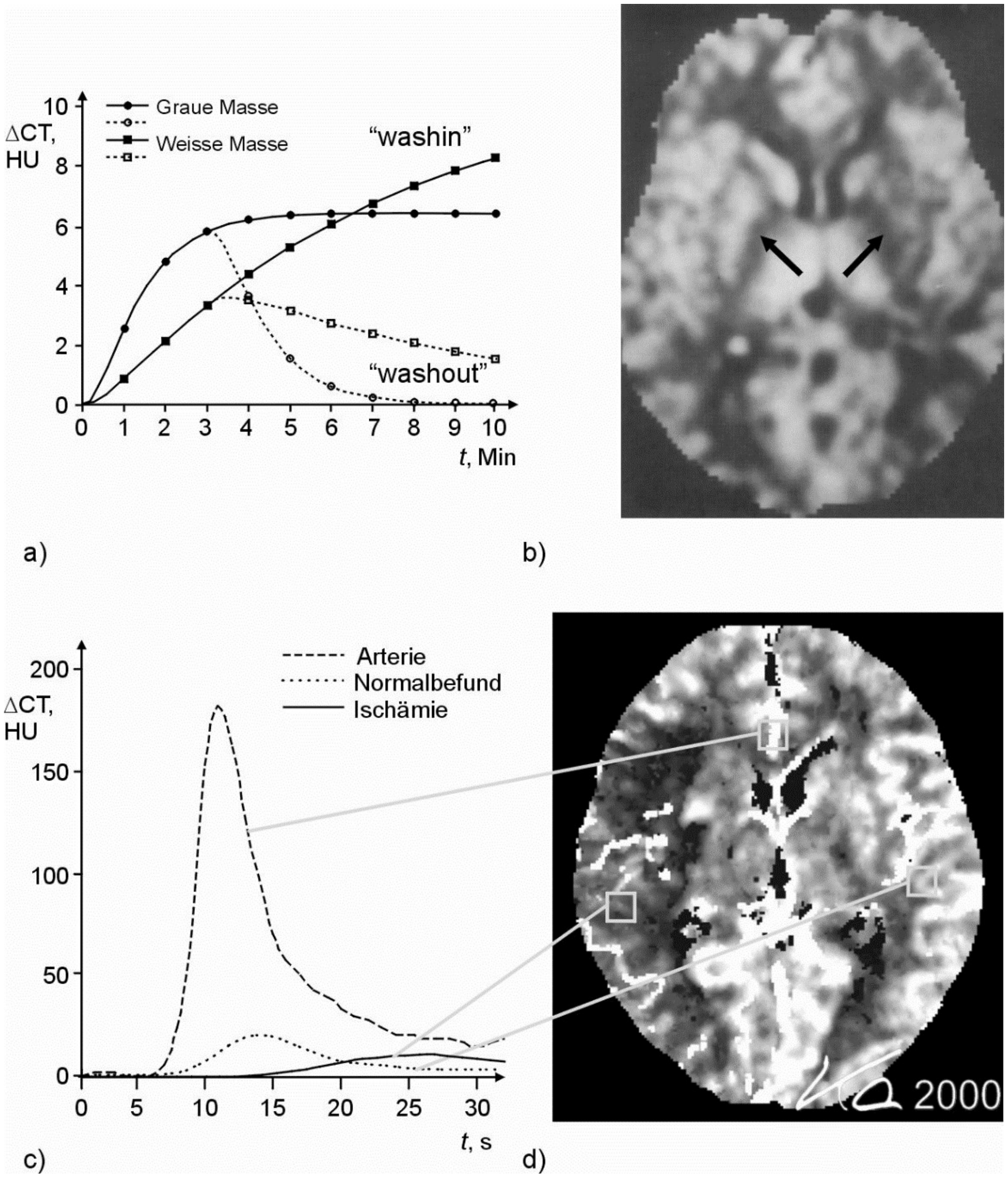

recording of
brain tissue perfusion

with xenon inhalation
(minute range) (a+b)

with contrast agent
(second range) (c+d)

special applications **CT-controlled biopsy**

a)

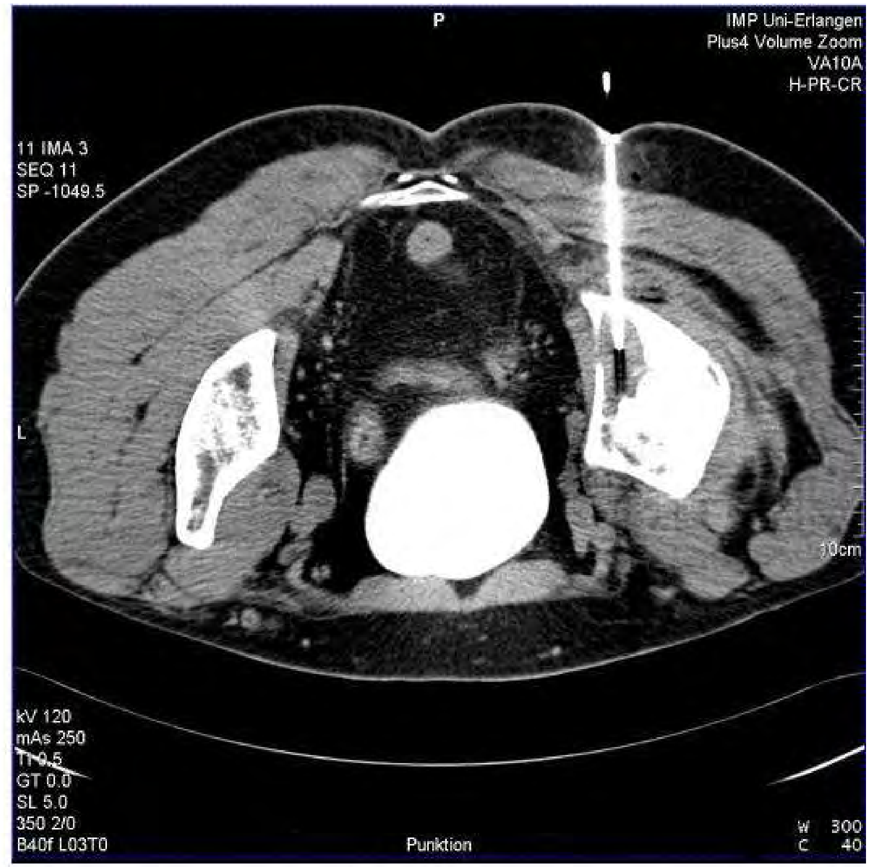

b)

x-ray computed tomography (CT)

special applications **quantitative CT**

bone density measurement (lumbar spine)

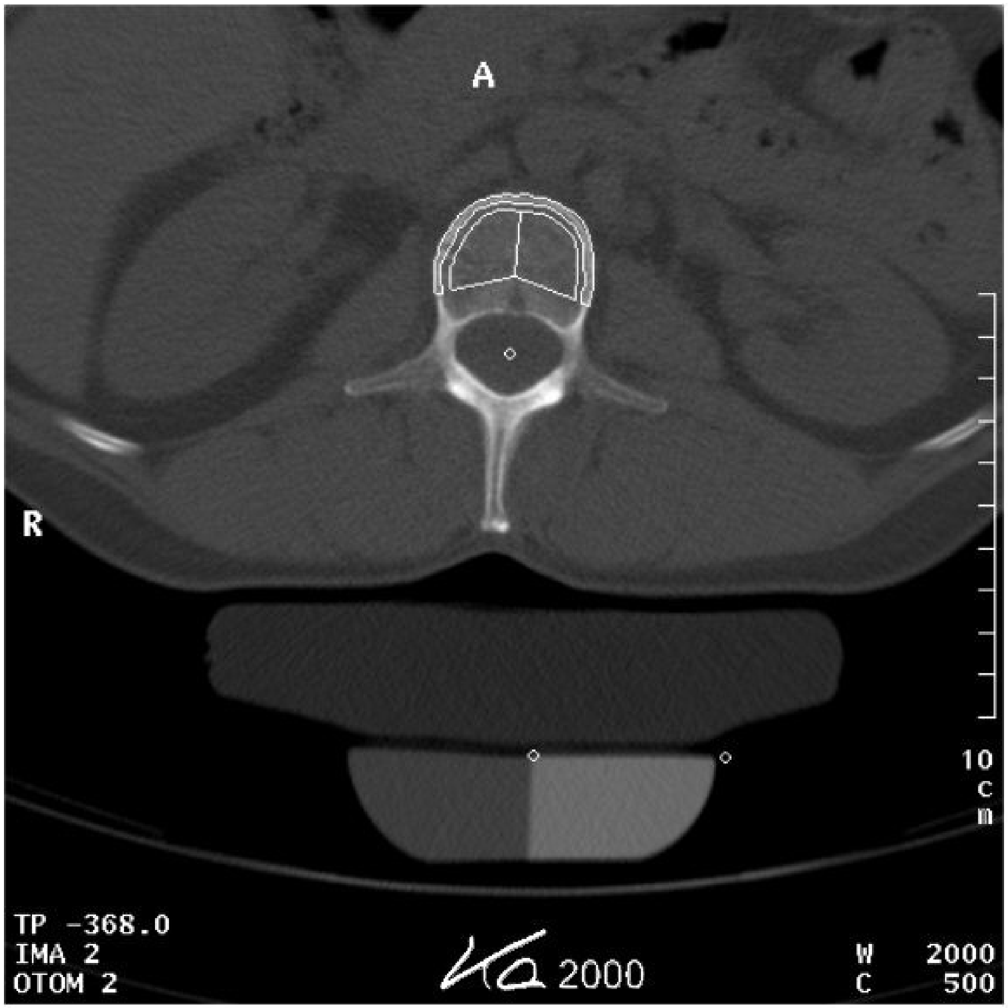

a)

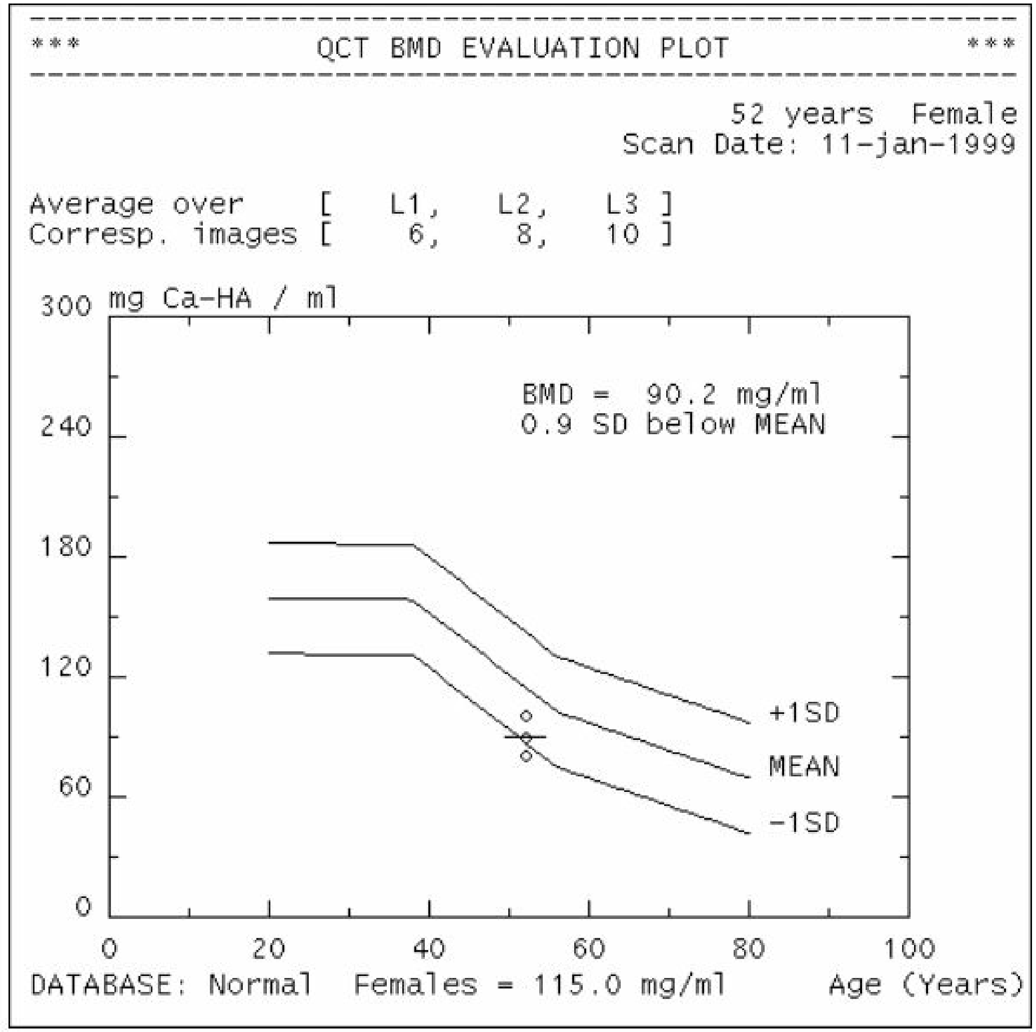

b)

comparison projection radiography / CT

		Röntgen	CT
imaging of	bones	+++	+++
	soft tissue	-/+	-
	vessels	++	++
	functions	-	-
	volumes	-	++
real time		fluoroscopy only	+
image quality		excellent	good
psychic burden		low	medium
somatic burden		high	high
examination time [min]		10	25
costs/examination [€]		ca. 40	ca.100